IFNγ AT THE FRONTLINE OF TUBERCULOSIS CONTROL: INVESTIGATING THE DYNAMIC RESPONSES TO IFNγ IN DISTINCT MACROPHAGE POPULATIONS

By

Laurisa M. Ankley

A DISSERTATION

Submitted to
Michigan State University
in partial fulfillment of the requirements
for the degree of

Microbiology and Molecular Genetics—Doctor of Philosophy

2023

ABSTRACT

Tuberculosis (TB) is a major public health concern, affecting millions of people worldwide. Current *Mycobacterium tuberculosis* (*Mtb*) treatment strategies have many limitations including long treatment duration, drug toxicity, emergence of drug-resistant strains, and inadequate efficacy. One new strategy to eradicate *Mtb* is the use of host directed therapy; however, we must first gain a better understanding of how the host responds to *Mtb* infection. Understanding that IFNγ is critical for *Mtb* control, we used IFNγ to dissect macrophage responses. Here, we used a CRISPR Cas9 screen to broadly understand genes necessary for IFNγ-dependent MHCII expression. MHCII drives T-cell activation needed for pathogen clearance. Additionally, we took advantage of a new alveolar macrophage model, known as FLAMs, that was optimized by our lab, to better understand AM IFNγ-responses. Our findings reveal that IFNγ robustly activates both macrophage types; however, the profile of activated IFNγ-stimulated genes varies significantly. Notably, FLAMs show limited activation of costimulatory markers essential for T cell activation upon IFNγ stimulation alone. However, with the inhibition of GSK3α/β, a well-conserved multifunctional kinase, FLAMs express a high amount of co-stimulatory molecules, particularly CD40. We also discovered that TNF and IFNβ contribute to the increase in costimulatory molecules during GSK3α/β inhibition and IFNγ stimulation. Together, these data suggest that AMs' capacity to respond to IFNγ is restricted in a GSK3α/β dependent manner and that IFNγ responses differ across distinct macrophage populations.

I dedicate this dissertation to anyone that still has even a little bit of ‘save the world’ left in them, including me.

ACKNOWLEDGEMENTS

First, I want to thank my PI, Andrew Olive. Almost every time Andrew has introduced me for a talk, since day one, he has made sure to include that I really took a chance joining his lab as his first graduate student. But to be honest, he took a big chance on me too. Thank you, Andrew, for taking that chance. After five years, I can still stay that the best academic decision I made in grad school was joining your lab. It has really been a privilege to be a part of so many lab firsts and experience the growth of the lab from the first culture to the first R01. My time at MSU would not have been the same without my lab mates, especially Sean and Haleigh. Sean, you've always been the person to hold it together when the lows of graduate school are really testing the rest of us and the first person to provide a reality check when we start heading down a rabbit hole of unnecessary worry. The wild "what if…" debates that you've prompted are some of my favorite and most memorable conversations that we've had in the lab. Haleigh, as you know, a lot of life happens while we're in graduate school and I want to thank you for always being there to listen. You've been there for me during some of my toughest moments and I can't thank you enough for that. I respect that you're able to just feel your feels, and if this has made you cry, gotcha haha.

I also couldn't have accomplished this without the guidance of my committee: Dr. Sean Crosson, Dr. Peggy Petroff, Dr. Dohun Pyeon, and Dr. Cheryl Rockwell. Thank you for the feedback throughout the years that has shaped this final work. You have always showed up to our meetings with an excitement for my research that helped me leave our sessions with an extra boost of motivation. Also, a big thank you to Roseann. The work you put in to keep all of us graduate students on the right track doesn't go unnoticed. Jake Weir, you have been the biggest advocate for GRIT and our mission. I cannot thank you enough for that. The care that you have

for BMS recruiting is so admirable and I appreciate the extra work that you do to help students be successful.

As an undergrad, Drs. Andrea Castillo and Robin O'Quinn from Eastern Washington University gave me the opportunity to simply have fun and research my own questions without the pressure of publications or prestige. That was an experience that I am so grateful for and has since allowed me to use that same curiosity to drive novel solutions to old problems surrounding topics away from the bench. Dr. Christina and Cynthia with the EWU McNair Scholar's program spent countless hours helping me and my cohort to prepare for graduate school and the application process. Their motivation to help students succeed is something that I have carried with me and hope to provide for others.

Since leaving WA and coming to East Lansing, I have found many friends that are more like family. Particularly those that we endearingly call the Pam Fam. Pam, Joe, Tatum, Kaela, Kyla, Shey, and Teagan (Rossie and Oscar too) I'll never be able to explain the value that I put on our family becoming part of yours. A lot of my favorite moments over the past several years have been shared with all of you and I couldn't be more grateful. Kaylee, you were the friend I did not see coming. Professionally—you've pushed me to set bigger goals, drive plans towards them, and have celebrated the wins right there with me when they happen. Personally—we do a really great job keeping each other humble and I wouldn't have it any other way. I look forward to forever driving each other towards our goals or crazy, either way I wouldn't have it any other way.

Next, I'd like to thank my mom, my brother, and my dad. Mom—I truly believe that you went through your hard so that my hard could be this degree. This accomplishment is something that will impact all of us and without the foundation of love, motivation, and support that you

built; this wouldn't have been possible. You have always reassured me that I am capable of hard things and have been a listening ear whenever I've needed it. Jake—thank you for being my best friend. You've taught me things that a degree never could. Whenever I have been in a complete lull with my research you always have fun projects, ideas, or topics to debate that remind me why I wanted to do this in the first place. Dad—Thank you for showing up for me and sharing the excitement of all my wins.

Lastly, I want to acknowledge my little family. Our pets, Remi and Eleanor, that have provided the chaos, humor, and joy that has really been a relief on my craziest days. Jenna, you have been there through it all and I really do not have the words to express how grateful I am for that. Thank you for going on this wild ride with me. This degree was for us and like everything else we really did this together and I am so happy that we did.

TABLE OF CONTENTS

CHAPTER 1: How IFNg orchestrates host defense strategies against Mycobacterium tuberculosis

GLOBAL IMPACT OF MTB

Mycobacterium tuberculosis (*Mtb*), the causative agent of Tuberculosis (TB), is one of the most devastating infectious diseases worldwide. An estimated 25% of the global population has been infected by TB at some point in their lives [1]. Most of those infected do not progress to a disease state and some even clear the infection completely. In 2021 alone, there were 10.6 million people around the world reported to have active TB disease and an estimated 1.6 million deaths caused by the disease [2].

TB has been a prominent societal burden for millennia and causes the highest burden on poor individuals in low to middle-income countries and among other marginalized populations. Geographical and financial burden often prevent individuals from early diagnoses that lead to increased transmission of disease and delayed treatment [3]. The costs associated with TB illness and treatment can be catastrophic to families and cause further impoverishment [4]. Overall poverty has been connected to an increased risk of TB infection, developing active TB disease, delayed diagnosis[3], poor adherence to TB treatment plans, and TB fatality[5]. [6]

Treatments currently available to combat *Mtb* infections include the drugs: Isoniazid [7], Rifampin [8,9], Ethambutol [10,11], and Pyrazinamide [12]. These drugs are used in combination over several months and cause major side effects [13–18]. They have been used for more than 60 years leading to both multidrug resistant strains of tuberculosis and extensively drug-resistant tuberculosis [19–23]. When patients are infected with resistant strains, they are treated with a combination of second-line defense drugs that often take even more time and additional trial and error to determine the right combination treatment. In addition to developing resistance, *Mtb* has rapidly evolved strategies to evade immune responses within the host.

The only tuberculosis vaccine licensed for global use at this time, and for the last century, is the Bacillus Calmette-Guérin (BCG) vaccine. Despite the vaccine's failure to protect against pulmonary TB, it continues to be the most widely used TB preventative treatment [24]. BCG causes a host response that activates inflammatory cells like CD4+ and CD8+ T-cells which leads to the production of protective cytokines like IFNγ, TNFα, IL-2, and IL-17. Experimentally, these responses show protective effects against *Mtb*, but when initiated by the BCG vaccine they are not enough to control infection [24]. Better vaccines and host-directed therapies are needed to minimize the global burden of TB that has impacted lives since ancient times. By understanding protective host responses to *Mtb* infection we can begin to develop host directed strategies that combat the sophisticated infection tactics of *Mtb*.

HOST IMMUNE RESPONSE TO MTB

Individually, the adaptive and innate immune responses are not enough to eradicate *Mtb* infection. The two systems must carefully orchestrate their defense strategies to combat the sophisticated tactics of *Mtb*. First the innate immune system minimizes bacterial burden and spread, then after several weeks the adaptive immune response specifically targets *Mtb* infected cells for eradication. Upon infection, alveolar macrophages (AMs) are the first contact for *Mtb* [25]. AMs are the lung occupying resident macrophage. Resident macrophages are tissue specific and are important for maintaining tissue homeostasis and responding to tissue damage or infection. AMs phagocytose *Mtb* but maintain a relatively low activation state and have low migratory potential that ultimately favor *Mtb* survival[26]. These characteristics cause a lag in the activation of an adaptive immune response making AMs an ideal niche for *Mtb* intracellular survival [25,27]. There are several receptors on the surface of the AM that recognize *Mtb* including toll-like receptors [28–30], collectins [31,32], and c-type lectins [33]. Each receptor activates a different

network of receptor-mediated signaling pathways that cause distinct gene expression profiles of the infected macrophage. This suggests that even upon recognition of *Mtb*, there is already variability in how the infected macrophage will respond and how it will elicit an immune response.

Once *Mtb* is engulfed, AMs in both mice and humans produce nitric oxide[34–36] and reactive oxygen species[37], both of which are antimycobacterial effectors that should be able to clear the infection. However, *Mtb* detoxifies the nitrogen and oxygen radicals evading this clearance attempt [38–40]. When *Mtb* establishes a proper niche within the cell, it replicates sufficiently to the point of cellular burst [41]. This burst then releases the bacteria from the infected cell where they can then infect neighboring cells and progress the infection.

After approximately six weeks in humans[42,43] and 2 weeks in mice [44], the adaptive immune response is initiated. This delay is unique to *Mtb* and has not been observed in other lung infections [45]. This suggests that *Mtb* actively takes advantage of the low activation state and low trafficking potential of AMs to avoid activation of the adaptive immune response. Eventually, the *Mtb* infected AMs move from the alveoli to the interstitial space [25]. Once *Mtb* infected AMs are in the interstitial space, inflammatory macrophages (IMs) are recruited to the area and become infected with *Mtb* [27]. Recruited macrophages are directed to the site of infection during an immune response and provide a more robust response to infection. IMs express MHCII and costimulatory markers including CD40, CD80, and CD86 [46–48]. They produce pro inflammatory cytokines including IL-1α, IL-1β, and TNFα that are important for pathogen control [49]. They are also very responsive to cytokines, particularly IFNγ [50]. Activation of IMs triggers robust inflammation that ultimately initiates the hosts adaptive response. *Mtb* antigens are trafficked to the draining lymph nodes where they activate *Mtb*-specific T-cells [27]. T-cells

have proven to be critical for the control of *Mtb* infection in human, non-human primate, and murine models. When T-cells are depleted individuals become highly susceptible to *Mtb* infection. [51–54]. T-cells require three distinct signals to be activated during *Mtb* infection [55]. The first is recognition of the pathogen derived peptides that are loaded onto the major histocompatibility complex class II on the surface of macrophages (MHCII) by antigen specific T-cell receptors (TCRs). The second signal is the binding of costimulation molecules including CD80, CD86, and CD40 on the surface of the macrophage to their corresponding ligand on the T-cell. How the T-cell binds each costimulatory molecule can alter its function, having a direct effect on *Mtb* control [48]. The third signal is driven by cytokines like IFNγ, TNFα, and IL-2 that enhance T-cell activation. Deficient Th1 cytokine production, especially IFNγ, is a well-established risk factor for *Mtb* infection and disease progression. In this dissertation, I will focus on the mechanisms of IFNγ, a cytokine produced by activated CD4+ T-cells that orchestrates the macrophage activation required to limit TB disease progression.

IFNγ AND MTB INFECTION

IFNγ plays an important role in the control of several pathogens including *Salmonella* [56], *Listeria* [57], and *Mycobacteria* species [58]. IFNγ is produced by T-cells in response to *Mtb* infection and is quantified to test for infection. An Interferon Gamma Release Assay (IGRA) is a blood test that exploits the strong T-cell response to *Mtb* to detect even latent TB infection [59]. This release of IFNγ by T-cells during *Mtb* infection is crucial for disease control [58]. Studies have shown that by knocking out genes needed for IFNγ production mice succumb to disease faster and have a higher bacterial burden of *Mtb* [58,60]. Approximately 1 out of 50,000 people have a condition called Mycobacterial susceptibility to mycobacterial disease (MSMD) which is caused by genetic mutations in genes that are needed to produce or respond to IFNγ [61]. There are nine

specific genes (*IFNGR1, IFNGR2, STAT1, IL12B, IL12RB1, ISG15*, and *IRF8*) that when mutated cause this condition, all of which are involved in IFNγ-dependent immunity [62–73]. These individuals are predisposed to disease caused by the BCG vaccine, mycobacteria, and other intra-macrophagic pathogens. Given the severe results of these mutations, IFNγ seems to be one of, if not the most important T-cell derived effector molecule for protection against *Mtb* infection.

The regulation of IFNγ is controlled positively and negatively by several factors, making its control of the immune system highly specific and tightly regulated. IFNγ is released from Natural Killer (NK) cells, NK T-cells, CD4+ T-cells, and CD8+ T-cells. One of the most important regulators of IFNγ is T-bet, the T-cell specific T-box transcription factor[74]. T-bet is considered the final check point for signaling pathways to activate IFNγ expression or to block it. T-bet has a broad role in chromatin structure and can enhance or suppress IFNγ gene expression both directly or indirectly. NFAT, nuclear factor of activated T-cell, binding sites are located upstream of the IFNγ transcription start site and have been shown to be required for maximum activity of the IFNγ promoter in T-cells [75,76]. Activating promoter 1, AP-1, is also linked to enhancing NFAT proteins through the formation of transcription factor complexes including c-Jun, CREB, and ATF-2 [77]. While it is important to activate IFNγ via positive regulators, too much IFNγ can be problematic and lead to autoimmune responses and tissue damage. Negative regulators are also in place to control this important balance. PPARγ links to Prox1 in T-cells to inhibit the expression of IFNγ [78]. PPARγ has also been reported to inhibit IFNγ by antagonizing transcription factors AP-1, STAT, and NFκβ [79]. However, when IFNγ is expressed, it in turn limits PPARγ by increasing STAT1 expression creating a regulatory cycle to balance expression of both PPARγ and IFNγ [80]. Activated TGFβ binds to T-bet causing IFNγ suppression by

limiting T-bet activity [81,82]. Gata3 in T-cells also restricts access to the promoter regions of both T-bet and IFNγ, preventing IFNγ expression [83]. Additionally, IFNγ is largely regulated by cell activation from cell surface receptor signaling. Il-2, Il-12, Il-15, Il-18, and Il-27 all induce IFNγ expression [84]. IFNγ also causes a feed-forward loop; when it is released by CD4+ T cells macrophages become activated which in turn leads to the release of additional IFNγ. Broadly it is important to acknowledge the complexity of IFNγ regulation and its implications in the host immune response. There is much more work to do to fully understand the regulation of IFNγ and by understanding it, we can use this cytokine as a target for host directed therapies during infection and disease.

IFNγ-dependent macrophage activation occurs when IFNγ binds to the IFNγ receptor (IFNGR) on the surface of macrophages causing a confirmational change in the receptor. This activates autophosphorylation and activation of Jak2 followed by activation of Jak1. Jak1 phosphorylates functionally important tyrosine residues on the IFNGR1 chain to form two docking sites for latent STAT1. STAT1 is then activated leading to the transcription of target genes including Ciita, a transcriptional coactivator of MHC genes.[85] From IFNγ binding IFNGR to STAT1 activation this process takes less than one minute. After activation, many of the exact IFNγ-dependent factors that control *Mtb* are unclear. The generation of oxygen and nitrogen radicals by IFNγ has been shown to limit *Mtb* replication in macrophages ex vivo but is only mildly antimicrobial in vivo [86–88]. GBPs that are induced by IFNγ disrupt the intracellular niche required for many intracellular pathogens, but do not protect against *Mtb* [89]. IFNγ-dependent GTPases, like Irgm1, have been reported to target the *Mtb* containing vacuole to limit growth, however recent evidence questions if Irgm1 is targeting the phagosome [90,91]. Together these findings demonstrate that IFNγ-dependent mechanisms, while crucial, are not enough alone to

clear *Mtb* infection. This suggests that *Mtb* is using sophisticated evasion tactics to skew or avoid such defenses.

The outcome of IFNγ-dependent pathway control and *Mtb* disease outcome is not as simple as IFNγ being on or off. IFNγ is tightly regulated at several levels and has many mechanisms that contribute to *Mtb* control. Researchers have tried to increase the protective effects of IFNγ by driving IFNγ production. In mice, driving IFNγ production during *Mtb* infection results in premature death rates comparable to mice that lack T-cells altogether [92]. Given the effects of MSMD and several IFNγ KO studies, we understand the importance of IFNγ in *Mtb* control. However, given the complicated regulation of IFNγ and its dependent downstream pathways, more research needs to be done to use IFNγ as a target for future therapeutics.

MTB EVASION STRATEGIES RELATED TO IFNγ REGULATED PATHWAYS

Mtb has evolved sophisticated evasion tactics that challenge nearly every step of host defense, including those involved in and regulated by IFNγ. IFNγ provides protection from TB disease progression but does not full eradicate the pathogen. This suggests that *Mtb* has additional, undiscovered, evasion tactics that are IFNγ specific. Guanylate binding proteins (GBPs) are an important host defense protein that is effective at clearing many intracellular pathogens including *Mycobacterium bovis* BCG, but not *Mtb* [89]. These differences are explained by the lack of the ESX1 secretion system in *M. bovis* BCG, suggesting an important role of ESX1 in GBP specific evasion by *Mtb* [89]. The 19-kDa lipoprotein of *Mtb* limits IFNγ-dependent activation of class II transactivator (Ciita) that regulates MHCII antigen presentation [93]. *Mtb* specifically targets TLR2-induced MAPK signaling causing hypoacetylation of the histone at CIITA pIV, thus suppressing its function [94]. The 19-kDa lipoprotein also inhibits IFNγ-

dependent HLA-DR, an MHCII surface receptor [95]. *Mtb* also inhibits how macrophages respond to IFNγ by inducing other cytokines like IL-6, which inhibits Th1 differentiation and activates the suppressor of cytokine signaling (SOCS) [96]. SOCS also limits STAT1 phosphorylation causing limited antigen presentation [97]. The production of IFNγ is also affected by *Mtb*. PD1 and Tim3 are upregulated on *Mtb*-specific T-cells which reduces the production of IL-2, TNFα, and IFNγ [98,99]. Even though these defense strategies should work to limit or even eradicate *Mtb*, we still are not quite sure which specific IFNγ mechanisms are the most effective at *Mtb* restriction or why these mechanisms are not enough. We hypothesize that there are additional unknown mechanisms of regulation and evasion.

HOST DIRECTED STRATEGIES

Together it is clear, that a better understanding of IFNγ pathways is needed to understand its mechanisms in controling *Mtb* and disease progression. Using advanced CRISPR tools to study IFNγ on a global scale, we aim to identify novel IFNγ regulatory pathways that contribute to infection control. Given that simply driving more IFNγ is not an effective approach to increasing IFNγ protection[92], we must gain an understanding of how each specific IFNγ-dependent protective mechanism works individually and as a system to identify appropriate therapeutic targets. Using host directed therapies to target such IFNγ-dependent mechanisms, has the potential to effectively combat TB. Current TB drug treatments have been used for the past 60 years and have caused a massive evolution of multidrug resistant and extensively drug resistant strains, making treatment difficult. Recent treatment development initiatives have shifted towards the development of host directed therapies that target host responses to infection rather than the pathogen. The mission now is to determine which host responses are reasonable targets to balance resistance, pathogen reduction of elimination, and tolerance, reduction of host damage

caused by the pathogen, to the infection. Given the proven importance of IFNγ in *Mtb* control, we hypothesize that IFNγ regulation or IFNγ-dependent pathways are a reasonable option. Some studies have attempted to use exogenous IFNγ to treat TB with varied results. One study reported that giving MDR-TB patients aerosolized IFNγ (500ug, three times a week for a month) resulted in radiological improvements [100]. Another found that giving IFNγ at two million IU, three times a week for 6 months had no effect [101]. A clinical study that gave recombinant IFNγ treatments in combination with standard drug treatments found that the IFNγ suppressed proinflammatory cytokines that can lead to tissue damage including IL-1β, Il-6, and IL-8 [102]. One study observed increased CD4+ lymphocyte responses and increase *Mtb* clearance in sputum during IFNγ supplementation given at 200μg, there times a week for 4 months [102]. There is clearly much work left to do to tap into the potential of IFNγ directed host therapies, but together this work shows that IFNγ can be used to alter infection outcome. The high variation with exogenous IFNγ, also suggests that by specifically targeting these pathways in the host perhaps we could tap into a more consistent method for treatment. In this dissertation, I work to further define the IFNγ-dependent regulation of macrophage activated CD4+ T-cell responses to better understand *Mtb* control and identify potential therapeutic targets in the host. In Chapter 2, we identify several novel regulators of MHCII, focusing mainly on Med16, a subunit of the mediator complex important for transcription, and GSK3β, a multifunctional kinase, both of which are highly conserved across all eukaryotes. Next in Chapter 3, we characterize the role of IFNγ and GSK3-dependent IFNγ signaling in both resident (FLAM) and recruited macrophages (iBMDMs)—reporting several distinctions and similarities between the two cell types. In Chapter 4, we investigate how TGFβ controls AM function and overall inflammation and TLR2 specific

responses—uncovering an unexpected connection between TGFβ, TLR2, and type I IFN responses. Together these chapters provide a better understanding of macrophage immune responses relevant to *Mtb* infection.

REFERENCES

1. Houben, R. M. G. J. & Dodd, P. J. The Global Burden of Latent Tuberculosis Infection: A Re-estimation Using Mathematical Modelling. *PLoS Med* **13**, (2016).

2. WHO. *Global Tuberculosis Report 2022*. http://apps.who.int/bookorders. (2022).

3. Storla, D. G., Yimer, S. & Bjune, G. A. A systematic review of delay in the diagnosis and treatment of tuberculosis. *BMC Public Health* vol. 8 Preprint at https://doi.org/10.1186/1471-2458-8-15 (2008).

4. Tanimura, T., Jaramillo, E., Weil, D., Raviglione, M. & Lönnroth, K. Financial burden for tuberculosis patients in low- And middle-income countries: A systematic review. *European Respiratory Journal* vol. 43 1763–1775 Preprint at https://doi.org/10.1183/09031936.00193413 (2014).

5. Waitt, C. J. & Squire, S. B. A systematic review of risk factors for death in adults during and after tuberculosis treatment. *International Journal of Tuberculosis and Lung Disease* vol. 15 871–885 Preprint at https://doi.org/10.5588/ijtld.10.0352 (2011).

6. Lönnroth, K., Jaramillo, E., Williams, B. G., Dye, C. & Raviglione, M. Drivers of tuberculosis epidemics: The role of risk factors and social determinants. *Soc Sci Med* **68**, 2240–2246 (2009).

7. Robitzek, E. & Selikoff, I. Hydrazine derivatives of isonicotinic acid in the treatment of active progressive caseous-pneumonic tuberculosis: a preliminary report. *Am Rev Tuberc* (1952).

8. Batten, J. Rifampicin in treatment of experimental tuberculosis in mice. *Tubercle* **50**, 294–8 (1969).

9. Furesz, S., Scotti, R., Pallanza, R. & Mapelli, E. Rifampicin: a new rifamycin. 3. Absorption, distribution, and elimination in man. *Arzneimittelforschung* **17**, 534–7 (1967).

10. THOMAS, J. P., BAUGHN, C. O., WILKINSON, R. G. & SHEPHERD, R. G. A new synthetic compound with antituberculous activity in mice: ethambutol (dextro-2,2'-(ethylenediimino)-di-l-butanol). *Am Rev Respir Dis* **83**, 891–893 (1961).

11. Karlson, A. The in Vitro Activity of Ethambutol (Dextro-2,2′-[Ethylenediimino]-Di-l-Butanol) Against Tubercle Bacilli and Other Microorganisms | American Review of Respiratory Disease. *American Review of Respiratory Disease* 905–906 https://www.atsjournals.org/doi/abs/10.1164/arrd.1961.84.6.905 (1961).

12. Yeager, R. I., Munroe, W. G. C. & Dessau, F. Pyrazinamide (Aldinamide) in the Treatment of Pulmonary Tuberculosis. *American Review of Tuberculosis* 523–546 https://www.atsjournals.org/doi/epdf/10.1164/art.1952.65.5.523?role=tab (1952).

13. Jindani, A. *et al.* A randomised Phase II trial to evaluate the toxicity of high-dose rifampicin to treat pulmonary tuberculosis. *International Journal of Tuberculosis and Lung Disease* **20**, 832–838 (2016).

14. 738 Daily ethambutol regimens and ocular toxicity in adults Ocular toxicity Time of Dose Duration Routine No of (No of toxicity Regimens (mglkg).

15. Goldman, A. L. & Braman, S. S. Isoniazid: A Review with Emphasis on Adverse Effects.

16. Tostmann, A. *et al.* Isoniazid and its toxic metabolite hydrazine induce in vitro pyrazinamide toxicity. *Int J Antimicrob Agents* **31**, 577–580 (2008).

17. Girling, D. J. The hepatic toxicity of antituberculosis regimens containing isoniazid, rifampicin and pyrazinamide. *Tubercle* **59**, 13–32 (1977).

18. Singh, M. *et al.* Studies on toxicity of antitubercular drugs namely isoniazid, rifampicin, and pyrazinamide in an in vitro model of HepG2 cell line. *Medicinal Chemistry Research* **20**, 1611–1615 (2011).

19. Somoskovi, A., Parsons, L. M. & Salfinger, M. The molecular basis of resistance to isoniazid, rifampin, and pyrazinamide in Mycobacterium tuberculosis. *Respir Res* **2**, 164 (2001).

20. Barry, C. E., Slayden, R. A. & Mdluli, K. Mechanisms of isoniazid resistance in Mycobacterium tuberculosis. *Drug Resistance Updates* **1**, 128–134 (1998).

21. Raynaud, C. *et al.* Mechanisms of pyrazinamide resistance in mycobacteria : importance of lack of uptake in addition to lack of pyrazinamidase activity. *Microbiology (N Y)* **145**, 367 (1999).

22. Telenti, A. *et al.* Detection of rifampicin-resistance mutations in Mycobacterium tuberculosis. *The Lancet* 647–651 (1993).

23. Sreevatsan, S. *et al.* Ethambutol resistance in Mycobacterium tuberculosis: critical role of embB mutations. *Antimicrob Agents Chemother* **41**, 1677–1681 (1997).

24. Dockrell, H. M. & Smith, S. G. What have we learnt about BCG vaccination in the last 20 years? *Frontiers in Immunology* vol. 8 Preprint at https://doi.org/10.3389/fimmu.2017.01134 (2017).

25. Cohen, S. B. *et al.* Alveolar Macrophages Provide an Early Mycobacterium tuberculosis Niche and Initiate Dissemination. *Cell Host Microbe* **24**, 439-446.e4 (2018).

26. Leemans, J. C. *et al.* Depletion of Alveolar Macrophages Exerts Protective Effects in Pulmonary Tuberculosis in Mice. *The Journal of Immunology* **166**, 4604–4611 (2001).

27. Wolf, A. J. *et al.* Initiation of the adaptive immune response to Mycobacterium tuberculosis depends on antigen production in the local lymph node, not the lungs. *Journal of Experimental Medicine* **205**, 105–115 (2008).

28. Means, T. K. *et al.* Human Toll-Like Receptors Mediate Cellular Activation by Mycobacterium tuberculosis . *The Journal of Immunology* **163**, 3920–3927 (1999).

29. Abel, B. *et al.* Toll-Like Receptor 4 Expression Is Required to Control Chronic Mycobacterium tuberculosis Infection in Mice . *The Journal of Immunology* **169**, 3155–3162 (2002).

30. Drage, M. G. *et al.* TLR2 and its co-receptors determine responses of macrophages and dendritic cells to lipoproteins of Mycobacterium tuberculosis. *Cell Immunol* **258**, 29–37 (2009).

31. Ferguson, J. S., Voelker, D. R., McCormack, F. X. & Schlesinger, L. S. Surfactant Protein D Binds to Mycobacterium tuberculosis Bacilli and Lipoarabinomannan via Carbohydrate-Lectin Interactions Resulting in Reduced Phagocytosis of the Bacteria by Macrophages1 . *The Journal of Immunology* **163**, 312–321 (1999).

32. Pasula, R. *et al. Surfactant Protein A (SP-A) Mediates Attachment of Mycobacterium tuberculosis to Murine Alveolar Macrophages tein A (SP-A) mediates attachment of Mycobacterium tuberculosis to murine alveolar macrophages*. *Am. J. Respir. Cell Mol. Biol* vol. 17 (1997).

33. Goyal, S., Klassert, T. E. & Slevogt, H. C-type lectin receptors in tuberculosis: what we know. *Medical Microbiology and Immunology* vol. 205 513–535 Preprint at https://doi.org/10.1007/s00430-016-0470-1 (2016).

34. Susan Nicholson, B. *et al.* Inducible Nitric Oxide Synthase in Pulmonary Alveolar Macrophages from Patients with Tuberculosis.

35. Chan, J., Xing, Y., Magliozzo, R. S. & Bloom, B. R. Killing of Virulent Mycobacterium tuberculosis by Reactive Nitrogen Intermediates Produced by Activated Murine Macrophages.

36. Denis, M. Interferon-gamma-treated murine macrophages inhibit growth of tubercle bacilli via the generation of reactive nitrogen intermediates. *Cell Immunol* **132**, 150–157 (1991).

37. Lovey, A. *et al.* Early alveolar macrophage response and IL-1R-dependent T cell priming determine transmissibility of Mycobacterium tuberculosis strains. *Nat Commun* **13**, 884 (2022).

38. Singh, B., Singh, G., Trajkovic, V. & Sharma, P. Intracellular expression of Mycobacterium tuberculosis-specific 10-kDa antigen down-regulates macrophage B7·1 expression and nitric oxide release. *Clin Exp Immunol* **134**, 70–77 (2003).

39. Nambi, S. *et al.* The oxidative stress network of Mycobacterium tuberculosis reveals coordination between radical detoxification systems HHS Public Access. *Cell Host Microbe* **17**, 829–837 (2015).

40. Buter, J. *et al.* Mycobacterium tuberculosis releases an antacid that remodels phagosomes. *Nat Chem Biol* **15**, 889–899 (2019).

41. Repasy, T., Lee, J., Marino, S., Martinez, N. & Kirschner, D. E. Intracellular Bacillary Burden Reflects a Burst Size for Mycobacterium tuberculosis In Vivo. *PLoS Pathog* **9**, 1003190 (2013).

42. POULSEN, A. Some clinical features of tuberculosis. 1. Incubation period. *Acta Tuberc Scand* **24**, 311–46 (1950).

43. WALLGREN, A. The time-table of tuberculosis. *Tubercle* **29**, 245–51 (1948).

44. Chackerian, A. A., Alt, J. M., Perera, T. v, Dascher, C. C. & Behar, S. M. Dissemination of Mycobacterium tuberculosis Is Influenced by Host Factors and Precedes the Initiation of T-Cell Immunity. *Infect Immun* **70**, 4501–4509 (2002).

45. Knudson, C. J., Weiss, K. A., Hartwig, S. M. & Varga, S. M. The Pulmonary Localization of Virus-Specific T Lymphocytes Is Governed by the Tissue Tropism of Infection. (2014) doi:10.1128/JVI.00329-14.

46. Hathcock, K. S., Laszlo, G., Pucillo, C., Linsley, I. P. & Hodes, R. J. Comparative Analysis of B7-1 and B7-2 Costimulatory Ligands: Expression and Function.

47. Clark, E. A. & Ledbettert, J. A. Activation of human B cells mediated through two distinct cell surface differentiation antigens, Bp35 and Bp5O (B lymphocytes/growth/monoclonal antibodies/cell cyde). *Proc. Nati. Acad. Sci. USA* **83**, 4494–4498 (1986).

48. Sia, J. K., Bizzell, E., Madan-Lala, R. & Rengarajan, J. Engaging the CD40-CD40L pathway augments T-helper cell responses and improves control of Mycobacterium tuberculosis infection. (2017) doi:10.1371/journal.ppat.1006530.

49. Arango Duque, G., Descoteaux, A., Lacy, P., Gavrilin, M. A. & Zoe Murray, R. Macrophage cytokines: involvement in immunity and infectious diseases. (2014) doi:10.3389/fimmu.2014.00491.

50. Mosser, D. M. & Edwards, J. P. Exploring the full spectrum of macrophage activation. (2008) doi:10.1038/nri2448.

51. Ling Lin, P. *et al.* CD4 T Cell Depletion Exacerbates Acute Mycobacterium tuberculosis While Reactivation of Latent Infection Is Dependent on Severity of Tissue Depletion in Cynomolgus Macaques. doi:10.1089/aid.2012.0028.

52. Flory, C. M., Hubbard, R. D. & Collins, F. M. Effects of in vivo T lymphocyte subset depletion on mycobacterial infections in mice. *J Leukoc Biol* **51**, 225–229 (1992).

53. Leveton, C. *et al.* T-Cell-Mediated Protection of Mice against Virulent Mycobacterium tuberculosis. *Infect Immun* **57**, 390–395 (1989).

54. Müller, I., Cobbold, S. P., Waldmann, H. & Kaufmann, S. H. Impaired resistance to Mycobacterium tuberculosis infection after selective in vivo depletion of L3T4+ and Lyt-2+ T cells. *Infect Immun* **55**, 2037–2041 (1987).

55. Sckisel, G. D. *et al.* Out-of-Sequence Signal 3 Paralyzes Primary CD4 + T-Cell-Dependent Immunity Article Out-of-Sequence Signal 3 Paralyzes Primary CD4 + T-Cell-Dependent Immunity. (2015) doi:10.1016/j.immuni.2015.06.023.

56. Muotiala, A. & Makela, P. H. *The role of IFN-y in murine Salmonella typhimurium infection*. *Microbial Pathogenesis* vol. 8 (1990).

57. Kernbauer, E. *et al.* Conditional stat1 ablation reveals the importance of interferon signaling for immunity to Listeria monocytogenes infection. *PLoS Pathog* **8**, (2012).

58. Flynn, J. L. *et al. An Essential Role for Interferon Gamma in Resistance to Mycobacterium tuberculosis Infection*. http://rupress.org/jem/article-pdf/178/6/2249/1104362/2249.pdf (1993).

59. Thillai, M., Pollock, K., Pareek, M. & Lalvani, A. Interferon-gamma release assays for tuberculosis: Current and future applications. *Expert Rev Respir Med* **8**, 67–78 (2014).

60. Cooper, A. M. *et al. Disseminated Tuberculosis in Interferon Gamma Gene-disrupted Mice*. (1993).

61. Rosain, J. *et al.* Mendelian susceptibility to mycobacterial disease: 2014–2018 update. *Immunol Cell Biol* (2019) doi:10.1111/imcb.12210.

62. Picard, C., Casanova, J. L. & Puel, A. Infectious diseases in patients with IRAK-4, MyD88, NEMO, or IκBα deficiency. *Clin Microbiol Rev* **24**, 490–497 (2011).

63. Bogunovic, D. *et al.* Mycobacterial disease and impaired IFN-γ immunity in humans with inherited ISG15 deficiency. *Science (1979)* **337**, 1684–1688 (2012).

64. Salem, S., Langlais, D., Blood, F. L.-, Journal, T. & 2014, undefined. Functional characterization of the human dendritic cell immunodeficiency associated with the IRF8K108E mutation. *ashpublications.org*.

65. Boisson-Dupuis, S., Kong, X., … S. O.-C. opinion in & 2012, undefined. Inborn errors of human STAT1: allelic heterogeneity governs the diversity of immunological and infectious phenotypes. *Elsevier*.

66. Filipe-Santos, O., … J. B.-T. J. of & 2006, undefined. X-linked susceptibility to mycobacteria is caused by mutations in NEMO impairing CD40-dependent IL-12 production. *rupress.org*.

67. Hambleton, S. *et al.* IRF8 Mutations and Human Dendritic-Cell Immunodeficiency . *New England Journal of Medicine* **365**, 127–138 (2011).

68. Beaucoudrey, L. de, Samarina, A., Medicine, J. B.- & 2010, undefined. Revisiting human IL-12Rβ1 deficiency: a survey of 141 patients from 30 countries. *ncbi.nlm.nih.gov*.

69. Prando, C., Samarina, A., Medicine, J. B.- & 2013, undefined. Inherited IL-12p40 deficiency: genetic, immunologic, and clinical features of 49 patients from 30 kindreds. *ncbi.nlm.nih.gov*.

70. Bustamante, J., Arias, A., Vogt, G., … C. P.-N. & 2011, undefined. Germline CYBB mutations that selectively affect macrophages in kindreds with X-linked predisposition to tuberculous mycobacterial disease. *nature.com*.

71. Filipe-Santos, O., Bustamante, J., … A. C.-S. in & 2006, undefined. Inborn errors of IL-12/23-and IFN-γ-mediated immunity: molecular, cellular, and clinical features. *Elsevier*.

72. Newport, M. J. A mutation in the interferon-γ-receptor gene and susceptibility to mycobacterial infection. *Pneumologie* **51**, 518 (1997).

73. Jouanguy, E. *et al.* Interferon-γ –Receptor Deficiency in an Infant with Fatal Bacille Calmette–Guérin Infection. *New England Journal of Medicine* **335**, 1956–1962 (1996).

74. Lugo-Villarino, G., Maldonado-López, R., Possemato, R., Peñaranda, C. & Glimcher, L. H. T-bet is required for optimal production of IFN-gamma and antigen-specific T cell activation by dendritic cells. *Proc Natl Acad Sci U S A* **100**, 7749–7754 (2003).

75. Sica, A. *et al.* Interaction of NF-kappaB and NFAT with the interferon-gamma promoter. *J Biol Chem* **272**, 30412–30420 (1997).

76. Buxadé, M. *et al.* Macrophage-specific MHCII expression is regulated by a remote Ciita enhancer controlled by NFAT5. *Journal of Experimental Medicine* **215**, 2901–2918 (2018).

77. Samten, B. *et al.* CREB, ATF AND AP-1 TRANSCRIPTION FACTORS REGULATE IFN-γ SECRETION BY HUMAN T CELLS IN RESPONSE TO MYCOBACTERIAL ANTIGEN. *J Immunol* **181**, 2056 (2008).

78. Wang, L. *et al.* Repression of interferon-γ expression in T cells by Prospero-related Homeobox protein. *Cell Research 2008 18:9* **18**, 911–920 (2008).

79. Ricote, M. & Glass, C. K. PPARs and molecular mechanisms of transrepression.

80. Waite, K. J., Floyd, Z. E., Arbour-Reily, P. & Stephens, J. M. Interferon-gamma-induced regulation of peroxisome proliferator-activated receptor gamma and STATs in adipocytes. *J Biol Chem* **276**, 7062–7068 (2001).

81. Lin, J. T., Martin, S. L., Xia, L. & Gorham, J. D. TGF-beta 1 uses distinct mechanisms to inhibit IFN-gamma expression in CD4+ T cells at priming and at recall: differential involvement of Stat4 and T-bet. *J Immunol* **174**, 5950–5958 (2005).

82. Park, I.-K., Shultz, L. D., Letterio, J. J. & Gorham, J. D. TGF-beta1 inhibits T-bet induction by IFN-gamma in murine CD4+ T cells through the protein tyrosine phosphatase Src homology region 2 domain-containing phosphatase-1. *J Immunol* **175**, 5666–5674 (2005).

83. Schoenborn, J., Dorschner, M., … M. S.-N. & 2007, undefined. Comprehensive epigenetic profiling identifies multiple distal regulatory elements directing transcription of the gene encoding interferon-γ. *nature.com*.

84. Nathan, C. F. *et al.* Brief Definitive Report ACTIVATION OF HUMAN MACROPHAGES Comparison of Other Cytokines with Interferon-y.

85. Kotenko, S., Oncogene, S. P.- & 2000, undefined. Jak-Stat signal transduction pathway through the eyes of cytokine class II receptor complexes. *nature.com*.

86. Nambi, S. *et al.* The Oxidative Stress Network of Mycobacterium tuberculosis Reveals Coordination between Radical Detoxification Systems. *Cell Host Microbe* **17**, 829–837 (2015).

87. Darwin, K. H., Ehrt, S., Gutierrez-Ramos, J. C., Weich, N. & Nathan, C. F. The Proteasome of Mycobacterium tuberculosis Is Required for Resistance to Nitric Oxide. *Science (1979)* **302**, 1963–1966 (2003).

88. Denis, M. Interferon-gamma-treated murine macrophages inhibit growth of tubercle bacilli via the generation of reactive nitrogen intermediates. *Cell Immunol* **132**, 150–157 (1991).

89. Olive, A. J., Smith, C. M., Baer, C. E., Coers, J. & Sassetti, C. M. Mycobacterium tuberculosis Evasion of Guanylate Binding Protein-Mediated Host Defense in Mice Requires the ESX1 Secretion System. *Int J Mol Sci* **24**, 2861 (2023).

90. Springer, H. M., Schramm, M., Taylor, G. A. & Howard, J. C. Irgm1 (LRG-47), a Regulator of Cell-Autonomous Immunity, Does Not Localize to Mycobacterial or Listerial Phagosomes in IFN-γ–Induced Mouse Cells. *The Journal of Immunology* **191**, 1765–1774 (2013).

91. Wilburn, K. M. *et al.* Differential Requirement for IRGM Proteins during Tuberculosis Infection in Mice. (2023) doi:10.1128/iai.00510-22.

92. Sakai, S. *et al.* CD4 T Cell-Derived IFN-γ Plays a Minimal Role in Control of Pulmonary Mycobacterium tuberculosis Infection and Must Be Actively Repressed by PD-1 to Prevent Lethal Disease. *PLoS Pathog* **12**, e1005667 (2016).

93. Boom, H., Harding, C. v, Pai, R. K., Convery, M. & Hamilton, T. A. A Potential Mechanism for Immune Evasion Mycobacterium tuberculosis Lipoprotein from Transactivator Expression by a 19-kDa-Induced Class II γ Inhibition of IFN-Downloaded from. *J Immunol References The Journal of Immunology by guest on* **171**, 175–184 (2003).

94. Harding, C. v, Pennini, M. E., Pai, R. K., Schultz, D. C. & Henry, W. TLR2 and MAPK Signaling by MHC2TA Chromatin Remodeling of-Induced γ Lipoprotein Inhibits IFN-19-kDa Mycobacterium tuberculosis. (2018) doi:10.4049/jimmunol.176.7.4323.

95. Gehring, A. J. *et al.* The Mycobacterium tuberculosis 19-Kilodalton Lipoprotein Inhibits Gamma Interferon-Regulated HLA-DR and FcγR1 on Human Macrophages through Toll-Like Receptor 2. *Infect Immun* **71**, 4487 (2003).

96. Masood, K. I. *et al.* Expression of M. tuberculosis-induced suppressor of cytokine signaling (SOCS) 1, SOCS3, FoxP3 and secretion of IL-6 associates with differing clinical severity of tuberculosis. *BMC Infect Dis* **13**, 1–9 (2013).

97. Carow, B. *et al.* Silencing suppressor of cytokine signaling-1 (SOCS1) in macrophages improves Mycobacterium tuberculosis control in an interferon-γ (IFN-γ)-dependent manner. *Journal of Biological Chemistry* **286**, 26873–26887 (2011).

98. Jayaraman, P. *et al.* TIM3 Mediates T Cell Exhaustion during Mycobacterium tuberculosis Infection. *PLoS Pathog* **12**, e1005490 (2016).

99. Pollock, K. M. *et al.* PD-1 Expression and Cytokine Secretion Profiles of Mycobacterium tuberculosis-Specific CD4+ T-Cell Subsets; Potential Correlates of Containment in HIV-TB Co-Infection. *PLoS One* **11**, e0146905 (2016).

100. Condos, R., Rom, W. N. & Schluger, N. W. Treatment of multidrug-resistant pulmonary tuberculosis with interferon-γ via aerosol. *Lancet* **349**, 1513–1515 (1997).

101. Koh, W. J. *et al.* Six-month therapy with aerosolized interferon-γ for refractory multidrug-resistant pulmonary tuberculosis. *J Korean Med Sci* **19**, 167–171 (2004).

102. Dawson, R. *et al.* Immunomodulation with Recombinant Interferon-γ1b in Pulmonary Tuberculosis. *PLoS One* **4**, e6984 (2009).

CHAPTER 2: A genetic screen in macrophages identifies new regulators of IFNγ-inducible MHCII that contribute to T-cell activation

DECLARATIONS

Authors

Michael Kiritsy[2], Laurisa Ankley[1], Justin Trombley[1], Gabrielle Huizinga[1], Audrey Lord[2], Pontus Orning[2], Roland Elling[2], Katherine Fitzgerald[2], Andrew Olive[1]

1 Michigan State University

2 University of Massachusetts Medical School

Contributions

The following dissertation chapter identifies and describes novel regulators of IFNγ-dependent MHCII expression on macrophages. Together, Andrew Olive, Michael Kiritsy, and I completed data analysis and writing of the manuscript. The CRISPR-Cas9 screen and analysis of the screen was completed by Michael Kiritsy and Andrew Olive during Andrew's post-doc at UMass prior to starting the Olive lab here at Michigan State. I completed validation of the top 20 genes identified in the screen and characterization of Med16 and GSK3 using flow cytometry and qRT-PCR. The RNAseq experiment was completed by me and Andrew Olive and Michael Kiritsy worked together to analyze the data. Andrew Olive supported the characterization of GSK3 and Med16 by conducting the T-cell co-culture experiments and supervised the conception and development of defining IFNγ-dependent MHCII expression using a CRISPR Cas9 screen.

Publication Notice

The following chapter is published at doi.org/10.7554/eLife.65110. Reprint permission is granted by the Creative Commons Attribution license. This chapter was also published as a preprint at doi.org/10.1101/2020.08.12.248252.

ABSTRACT

Cytokine-mediated activation of host immunity is central to the control of pathogens. Interferon-gamma (IFNγ) is a key cytokine in protective immunity that induces major histocompatibility complex class II molecules (MHCII) to amplify $CD4^+$ T cell activation and effector function. Despite its central role, the dynamic regulation of IFNγ-induced MHCII is not well understood. Using a genome-wide CRISPR-Cas9 screen in murine macrophages, we identified genes that control MHCII surface expression. Mechanistic studies uncovered two parallel pathways of IFNγ-mediated MHCII control that require the multifunctional glycogen synthase kinase three beta (GSK3β) or the mediator complex subunit 16 (MED16). Both pathways control distinct aspects of the IFNγ response and are necessary for IFNγ-mediated induction of the MHCII transactivator *Ciita*, MHCII expression, and $CD4^+$ T cell activation. Our results define previously unappreciated regulation of MHCII expression that is required to control $CD4^+$ T cell responses.

INTRODUCTION

Activation of the host response to infection requires the coordinated interaction between antigen presenting cells (APCs) and T cells [1–3]. For $CD4^+$ T cells, the binding of the T cell receptor (TCR) to the peptide-loaded major histocompatibility complex class II (MHCII) on the surface of APCs is necessary for both $CD4^+$ T cell activation and their continued effector function in peripheral tissues [3–5] Dysregulation of MHCII control leads to a variety of conditions including the development of autoimmunity and increased susceptibility to pathogens and cancers [6–9]. While MHCII is constitutively expressed on dendritic cells and B cells, the production of the cytokine IFNγ promotes MHCII expression broadly in other cellular populations including macrophages [10–13]. The induction of MHCII in these tissues activates a

feedforward loop wherein IFNγ-producing $CD4^+$ T cells induce myeloid MHCII expression, which in turn amplifies $CD4^+$ T cell responses [13–15]. Thus, IFNγ-mediated MHCII expression is essential for protective immunity.

The IFNγ-dependent control of MHCII is complex [1,5,11,16,17]. Binding of IFNγ to its receptor induces cytoskeletal and membrane rearrangement that results in the activation of JAK1 and JAK2 and STAT1-dependent transcription [18,19]. STAT1 induces *Irf1*, which then drives the expression of the MHCII master regulator, *Ciita* [20]. The activation of CIITA opens the chromatin environment surrounding the MHCII locus and recruits transcription factors, including CREB1 and RFX5 [5,21]. MHCII is also regulated post-translationally to control the trafficking, peptide loading, and stability of MHCII on the surface of cells [22–24]. While recent evidence points to additional regulatory mechanisms of IFNγ-mediated MHCII expression, including the response to oxidative stress, these have not been investigated directly in macrophages [1].

In non-inflammatory conditions, macrophages express low levels of MHCII that is uniquely dependent on NFAT5 [14]. While basal MHCII expression on macrophages plays a role in graft rejection, it is insufficient to control intracellular bacterial pathogens, which require IFNγ-activation to propagate protective $CD4^+$ T cell responses [25–27]. Many pathogens including *Mycobacterium tuberculosis* and *Chlamydia trachomatis* inhibit IFNγ-mediated MHCII induction to evade $CD4^+$ T-cell-mediated control and drive pathogen persistence [28–30] Overcoming these pathogen immune evasion tactics is essential to develop new treatments or immunization strategies that provide long-term protection [25]. Without a full understanding of the global mechanisms controlling IFNγ-mediated MHCII regulation in macrophages, it has proven difficult to dissect the mechanisms related to MHCII expression that cause disease or lead to infection susceptibility.

Here, we globally defined the regulatory networks that control IFNγ-mediated MHCII surface expression on macrophages. Using CRISPR-Cas9 to perform a forward genetic screen, we identified the major components of the IFNγ-regulatory pathway in addition to many genes with no previously known role in MHCII regulation. Follow-up studies identified two critical regulators of IFNγ-dependent *Ciita* expression in macrophages, MED16 and GSK3β. Loss of either MED16 or GSK3β resulted in significantly reduced MHCII expression on macrophages, unique changes in the IFNγ-transcriptional landscape, and prevented the effective activation of $CD4^+$ T cells. These results show that IFNγ-mediated MHCII expression in macrophages is finely tuned through parallel regulatory networks that interact to drive efficient $CD4^+$ T cell responses.

RESULTS

Optimization of CRISPR-Cas9 editing in macrophages to identify regulators of IFNγ-inducible MHCII

To better understand the regulation of IFNγ-inducible MHCII, we optimized gene-editing in immortalized bone marrow-derived macrophages (iBMDMs) from C57BL/6 J mice. iBMDMs were transduced with Cas9-expessing lentivirus and Cas9-mediated editing was evaluated by targeting the surface protein CD11b with two distinct single guide RNAs (sgRNA). When we compared CD11b surface expression to a non-targeting control (NTC) sgRNA by flow cytometry, we observed less than 50 % of cells targeted with either of the *Cd11b* sgRNA were successfully edited (Figure 1.1—figure supplement 1A). We hypothesized that the polyclonal Cas9-iBMDM cells variably expressed Cas9 leading to inefficient editing. To address this, we isolated a clonal population of Cas9-iBMDMs using limiting dilution plating. Using the same *Cd11b* sgRNAs in a clonal population (clone L3) we found 85–99% of cells were deficient

in CD11b expression by flow cytometry compared to NTC (Figure 1.1—figure supplement 1B). Successful editing was verified by genotyping the *Cd11b* locus for indels at the sgRNA targeting sequence using Tracking of Indels by Decomposition (TIDE) analysis [31]. Therefore, clone L3 Cas9^{+} iBMDMs proved to be a robust tool for gene editing in murine macrophages.

To test the suitability of these cells to dissect IFNγ-mediated MHCII induction, we next targeted *Rfx5*, a known regulator of MHCII expression, with two independent sgRNAs [9]. Since L3 macrophages do not express IFNγ, we stimulated *Rfx5 t*argeted and NTC cells with IFNγ for 18 hours and quantified the surface expression of MHCII by flow cytometry (Figure 1.1A and B and Figure 1.5—source data 1). In cells expressing the non-targeting sgRNA, IFNγ stimulation resulted in a 20-fold increase in MHCII. In contrast, cells transduced with either of two independent sgRNAs targeting *Rfx5* failed to induce the surface expression of MHCII following IFNγ stimulation. We further tested other activators that might impact MHCII expression in L3 cells. L3 cells were stimulated with IFNγ, LPS, Pam3CSK4, IFN-β, TNF and N-glycolylated muramyldipeptide (NG-MDP) and 24 hours later the surface expression of MHCII and PD-L1 was quantified. While each stimuli increased PD-L1 expression, only IFNγ significantly altered the expression of MHCII (Figure 1.1—figure supplement 1C,D). Thus, MHCII expression in macrophages is tightly controlled by IFNγ-dependent mechanisms and L3 cells can be effectively used to interrogate IFNγ-mediated MHCII expression in macrophages.

Forward genetic screen identifies known and novel regulators of MHCII surface expression in macrophages

To define the genetic networks required for IFNγ-mediated MHCII expression, we made a genome-wide library of mutant macrophages with sgRNAs from the Brie library to generate null alleles in all protein-coding genes [32]. After verifying coverage and minimal skew in the

initial library, we conducted a forward genetic screen to identify regulators of IFNγ-dependent MHCII expression (Figure 1.1C and Supplementary file 1). The loss-of-function library was stimulated with IFNγ and 24 hours later, we selected MHCII^{high} and MHCII^{low} expressing cells by fluorescence activated cells sorting (FACS). Following genomic DNA extraction, sgRNA abundances for each sorted bin were determined by deep sequencing.

As our knockout library relied on the formation of Cas9-induced indels and was exclusive to protein-coding genes, we focused our analysis on genes expressed in macrophages under the conditions of interest, which we determined empirically in the isogenic cell line by RNA-seq (Figure 1.5—source data 1). We assumed that sgRNAs targeting non-transcribed genes are neutral in their effect on IFNγ-induced MHCII expression, which afforded us ~32,000 internal negative control sgRNAs [33]. To test for statistical enrichment of sgRNAs and genes, we used the modified robust rank algorithm (α-RRA) employed by Model-based Analysis of Genome-wide CRISPR/Cas9 Knockout (MAGeCK), which first ranks sgRNAs by effect and then filters low ranking sgRNAs to improve gene significance testing [34]. We tuned the sgRNA threshold parameter to optimize the number of significant hits without compromising the calculated q-values of known positive controls that are expected to be required for IFNγ-mediated MHCII expression. Further, by removing irrelevant sgRNAs that targeted genes not transcribed in our conditions, we removed potential false positives and improved the positive predictive value of the screen (Figure 1.1—figure supplement 2A and S2B).

Guide-level analysis confirmed the ability to detect positive control sgRNAs which had robust enrichment in the MHCII^{low} population (Figure 1.1—figure supplement 2C). Using the previously determined parameters, we tested for significantly enriched genes that regulated MHCII surface levels. As expected, sgRNAs targeting known components of the IFNγ-receptor

signal transduction pathway, such as *Ifngr1*, *Ifngr2*, *Jak1* and *Stat1*, as well as regulators and components of IFNγ–mediated MHCII expression, such as *Ciita*, *Rfx5*, and *Rfxank* were all significantly enriched [5,20]. These results validated our approach to identify functional regulators of IFNγ-mediated MHCII expression.

Stringent analysis revealed a significant enrichment of genes with no known involvement in interferon responses and antigen presentation. To identify functional pathways that are associated with these genes, we performed KEGG pathway analysis on the positive regulators of IFNγ-induced MHCII that met the FDR cutoff (Figure 1.1—figure supplement 2D; [35–37]). However, gene membership for the 10 most enriched KEGG pathways was largely dominated by known regulators of IFNγ signaling. To circumvent this redundancy and identify novel pathways enriched from our candidate gene list, the gene list was truncated to remove the 11 known IFNγ signaling regulators. Upon reanalysis, several novel pathways emerged, including mTOR signaling (Figure 1.1—figure supplement 2E). Thus, our genetic screen uncovered previously undescribed pathways that are critical to control IFNγ-mediated MHCII surface expression in macrophages.

The results of the genome-wide CRISPR screen highlight the sensitivity and specificity of our approach and analysis pipeline. To gain new insights into IFNγ-mediated MHCII regulation, we next validated a subset of candidates that were not previously associated with the IFNγ-signaling pathway. Using two independent sgRNAs for each of 15 candidate genes, we generated loss-of-function macrophages in the L3 clone. MHCII surface expression was quantified by flow cytometry for each cell line in the presence and absence of IFNγ activation. For all 15 candidates, we observed no changes in basal MHCII expression (Figure 1.1—figure supplement 2F) but found deficient MHCII induction following IFNγ stimulation with at least

one sgRNA (Figure 1.1E and Figure 1.1—figure supplement 2G). For 9 of 15 candidate genes, we observed a significant reduction in MHCII surface expression with both gene-specific sgRNAs These results show that our screen not only identified known regulators of IFNγ-mediated MHCII induction, but also uncovered new regulatory networks required for MHCII expression on macrophages.

We were interested in better understanding the IFNγ-mediated transcriptional activation of MHCII to determine if a subset of candidates reveal new regulatory mechanisms of MHCII-expression. Based on the screen and validation results, we examined the known functions of the candidates that were confirmed with two sgRNAs, and identified *Med16* and *Gsk3β* for follow-up study. MED16 is a subunit of the mediator complex that regulates transcription initiation while Glycogen synthase kinase 3β (GSK3β) is a multifunctional kinase that controls signaling pathways known to regulate transcription [38,39]. Thus, we hypothesized that MED16 and GSK3β would be required for effective IFNγ-mediated transcriptional control of MHCII.

MED16 is uniquely required for IFNγ-mediated CIITA expression

We first examined the role of MED16 in controlling IFNγ-mediated MHCII expression. Our validation results confirmed that MED16 was indeed an essential positive regulator of MHCII expression (Figure 1.1E). MED16 was the sixth ranked candidate from our screen results, with robust enrichment of all four sgRNAs in the MHCII^{low} population (Figure 1.2A). As part of the mediator complex, MED16 bridges the transcription factor binding and the chromatin remodeling that are required for transcriptional activation [40]. These changes then recruit and activate RNA polymerase II to initiate transcription. While the core mediator complex function is required for many RNA polymerase II dependent transcripts, distinct sub-units of the mediator complex can also play unique roles in gene regulation [38,40]. To examine if MED16 was uniquely

required for IFNγ-dependent MHCII expression, we probed our genetic screen data for all mediator complex subunits. The other 27 mediator complex subunits in our library did not show any significant changes in MHCII expression (Figure 1.2B). To test the specific requirement of MED16, we generated knockout macrophages in *Med16* (*Med16* KO) using two independent sgRNAs and targeted three additional mediator complex subunits, *Med1*, *Med12* and *Med17*. We treated with IFNγ and quantified the surface levels of MHCII by flow cytometry. In support of the screen results, *Med1*, *Med12* and *Med17* showed similar MHCII upregulation compared to NTC cells, while *Med16* targeted cells demonstrated defects in MHCII surface expression (Figure 1.2C and D). These results suggest that there is specificity to the requirement for MED16-dependent control of IFNγ-induced *Ciita* that is unique among the mediator complex subunits.

To understand the mechanisms of how MED16 regulates MHCII-induction, we assessed the transcriptional induction of MHCII in *Med16* KO cells. In macrophages, the IFNγ-mediated transcriptional induction of MHCII subunits requires the activation of CIITA that then, in complex with other factors like RFX5, initiates transcription at the MHCII locus [1,13]. To determine whether MED16 controls the transcriptional induction of MHCII, we stimulated NTC, *Med16* KO and *Rfx5* targeted cells with IFNγ for 18 hours and isolated RNA. Using qRT-PCR, we observed that loss of RFX5 did not impact the induction of *Ciita*, but had a profound defect in the expression of *H2aa* compared to NTC cells (Figure 1.2E and F). Loss of MED16 significantly inhibited the induction of both *Ciita* and *H2aa*. We further compared MHCII expression between NTC and *Med16* KO cells over time and with varying IFNγ concentrations observing robust inhibition of MHCII expression in all conditions (Figure 1.2—figure supplement 1B-D).

To ensure that the IFNγ treatments reflect physiological conditions, we developed a co-culture assay with macrophages and activated Natural Killer (NK) cells that produce IFNγ. NTC and *Med16* KO cells were left untreated or were incubated with activated NK cells for 18 hours then MHCII expression on the surface of the macrophages was quantified by flow cytometry (Figure 1.2G). In this model, induction of MHCII on macrophages was entirely dependent on NK cell-derived IFNγ as antibody-mediated blockade of IFNγ signaling or co-culture with IFNγ-/- NK cells did not significantly change macrophage surface expression of MHCII. While co-culture of NTC macrophages with wild type NK cells robustly induced MHCII on the surface, *Med16* KO macrophages had significantly reduced MHCII expression. Altogether these data suggest that MED16 controls the IFNγ-mediated induction of MHCII through upstream regulation of CIITA.

GSK3 regulates the IFNγ-dependent induction of CIITA

We next examined the mechanisms of GSK3β control of IFNγ-mediated MHCII expression in more detail. GSK3β is involved in many cellular pathways, yet no role in regulating IFNγ-mediated MHCII expression has previously been described [39,41–43]. *Gsk3β* was highly ranked in the screen showing strong effects of multiple sgRNAs (Figure 1.3A; [42]). Our validation studies further showed that GSK3β is required for the effective induction of IFNγ-dependent MHCII (Figure 1E). To begin to understand the mechanisms controlling GSK3β-dependent regulation of MHCII expression, we generated *Gsk3β* knockout cells (*Gsk3β* KO) and verified that the loss of *Gsk3β* inhibited IFNγ-mediated MHCII surface expression (Figure 1.3B and Figure 1.3—figure supplement 1A). We next examined if the IFNγ-mediated transcriptional induction of *Ciita* or *H2aa* were reduced in *Gsk3β* KO cells. Loss of *Gsk3β* significantly inhibited the expression of both CIITA and H2-Aa after IFNγ-treatment

compared to NTC controls (Figure 1.3C and D). These data suggest that GSK3β, similar to MED16, is an upstream regulator of IFNγ-mediated MHCII induction and controls the expression of CIITA following IFNγ-activation. As with the *Med16* KO, we further compared MHCII expression between NTC and *Gsk3β* KO macrophages over time and with varying IFNγ concentrations observing significant inhibition of MHCII expression in all conditions (Figure 1.3—figure supplement 1B-D).

To confirm the genetic evidence using an orthogonal method, we next used the well-characterized small molecule CHIR99021, which inhibits both GSK3β and the GSK3β paralog GSK3α ([39,44]). NTC macrophages were treated with CHIR99021 and cells were then stimulated with IFNγ, and MHCII expression was quantified by flow cytometry. Inhibition of GSK3α/β activity reduced the induction of surface MHCII and was more deleterious than genetic loss of *Gsk3β* alone (Figure 1.3E). These data suggest a possible role for GSK3α in controlling IFNγ-mediated MHCII expression (Huang et al., 2017). While we did not observe enrichment for GSK3α in the screen (Figure 1.2—figure supplement 1D and Supplementary file 1), we could not exclude the possibility that GSK3α plays a key regulatory role during IFNγ activation when GSK3β is dysfunctional. We hypothesized that GSK3α can partially compensate for total loss of *Gsk3β*, resulting in some remaining IFNγ-induced MHCII expression. To test this hypothesis, we treated *Gsk3β* KO macrophages with CHIR99021 or DMSO and quantified MHCII surface expression. In support of an important regulatory role for GSK3α, CHIR99021 treatment of *Gsk3β* KO macrophages further reduced surface MHCII expression after IFNγ-stimulation compared to the *Gsk3β* KO alone (Figure 1.3E).

To exclude the possibility of CHIR99021 off-target effects we next targeted *Gsk3α* genetically. To enable positive selection of a second sgRNA, we engineered

vectors in the sgOpti background with distinct resistance markers for bacterial and mammalian selection that facilitated multiplexed sgRNA cloning (see materials and methods) [45]. These vectors could be used to improve knockout efficiency when targeting a gene with multiple sgRNAs or target multiple genes simultaneously (Figure 1.3—figure supplement 1E). We targeted *Gsk3α* with two unique sgRNAs in either NTC or *Gsk3β* KO macrophages and stimulated the cells with IFNγ. Cells with the sgRNA targeting *Gsk3α* alone upregulated MHCII expression similarly to NTC control cells (Figure 1.3F and Figure 1.3—figure supplement 1F). In contrast, targeting *Gsk3α* in *Gsk3β* KO macrophages (i.e. double knockout) led to a further reduction of MHCII surface expression, similar to what was observed with CHIR99021 treatment. This same trend was observed when we examined *Ciita* mRNA expression after IFNγ-activation (Figure 1.2—figure supplement 1G). To ensure physiological levels of IFNγ, we next repeated the NK cell co-culture experiment with *Gsk3β* KO and CHIR99021 treated cells. We observed over a 3-fold reduction in MHCII expression in both conditions compared to NTC cells and the reduction was greater in CHIR99021 treated cells compared to *Gsk3β* KO cells (Figure 1.3G). As observed before, the MHCII induction was dependent on IFNγ as blocking the IFNγR with antibodies or co-culturing with IFNγ-/- NK cells resulted in no change in MHCII expression compared to no co-culture controls. Therefore, both GSK3β and GSK3α have important regulatory functions that control IFNγ-mediated MHCII expression.

We next examined possible mechanisms by which GSK3α controls MHCII expression only in the absence of GSK3β. We hypothesized that *Gsk3α* expression or activation is increased in the absence of GSK3β. To test these hypotheses, NTC and *Gsk3β* KO cells were left untreated or stimulated with IFNγ for 30 min. We measured total and phosphorylated GSK3α by immunoblot and observed no significant difference between resting and IFNγ activation NTC

and *Gsk3β* KO macrophages (Figure 1.3H). We observed robust phosphorylation of STAT1 further suggesting this pathway remains intact even in the absence of GSK3β. Together these data suggests that GSK3α does not compensate for the loss of GSK3β by modulating its expression or activation.

To understand the kinetics of the GSK3α/β requirement for IFNγ responses, we conducted a time course experiment with CHIR99021. We hypothesized that GSK3α/β inhibition with CHIR99021 would block MHCII expression only if the inhibitor was present shortly after IFNγ stimulation. To test this hypothesis, iBMDMs were stimulated with IFNγ then treated with DMSO for the length of the experiment or with CHIR99021, 2, 6, 12, and 18 hours post-stimulation. When MHCII was quantified by flow cytometry we saw a reduction in MHCII expression when CHIR99021 was added 2 or 6 hours after IFNγ (Figure 1.3I). CHIR99021 addition at later time points resulted in similar MHCII expression compared to DMSO treated cells. When the expression of *H2aa* mRNA was quantified from a parallel experiment, a significant reduction in mRNA expression was only observed in macrophages that were treated with CHIR99021 2 hours following IFNγ-activation (Figure 1.2—figure supplement 1H). Thus, GSK3α/β activity is required early after IFNγ stimulation to activate the transcription of MHCII. We repeated this experiment in primary bone marrow-derived macrophages from HoxB8 conditionally immortalized progenitor cells and observed comparable results (Figure 1.2—figure supplement 1I) [46]. Therefore, GSK3α/β activity is required for the effective induction of IFNγ-mediated MHCII in immortalized and primary murine macrophages and has a negligible effect on the maintenance or stability of cell surface-associated MHCII.

GSK3α/β and MED16 function independently from mTORC1 to control IFNγ-mediated MHCII expression

Since the loss of either MED16 or GSK3β reduced IFNγ-mediated CIITA transcription, it remained possible that these two genes control MHCII expression through the same regulatory pathway. While *Med16* KO macrophages are greatly reduced in IFNγ-mediated MHCII induction, there remains a small yet reproducible increase in MHCII surface expression. We determined if this effect on MHCII expression after IFNγ-activation required GSK3 activity by treating *Med16* KO and NTC macrophages with CHIR99021. While DMSO-treated *Med16* KO cells showed a reproducible two- to threefold increase in MHCII expression after IFNγ stimulation, CHIR99021 treated *Med16* KO cells showed no change whatsoever (Figure 1.4A). CHIR99021 treatment of NTC cells resulted in a significant reduction in MHCII compared to vehicle controls. However, we observed more MHCII expression compared to CHIR99021 treated *Med16* KO cells. These results suggest that MED16 and GSK3α/β control IFNγ-mediated *Ciita* induction and MHCII expression through independent mechanisms.

Our bioinformatic analysis identified an enrichment for the mTOR pathway among positive regulators of MHCII expression. In contrast, a previous study linked IFNγ activation in human monocyte derived macrophages with the inhibition of mTORC1 [47]. Given this inconsistency and the previously described role of mTORC1 modulating GSK3 activity, we next examined how mTORC1 contributes to IFNγ-mediated MHCII expression. As a first step, we tested how the inhibition of mTORC1 impacts IFNγ responses in murine macrophages. NTC macrophages were treated with and without the mTORC1 inhibitor Torin2 then were left untreated or were stimulated with IFNγ. The surface expression of MHCII was then quantified by flow cytometry. While Torin2 alone had no effect on MHCII expression, blocking mTORC1

resulted in a significant reduction in surface MHCII following IFNγ activation, consistent with our screen analysis (Figure 1.4C). To determine the specificity of mTORC1 inhibition on other IFNγ responses we also examined the induction of the immunoinhibitory molecule programmed death ligand 1 (PD-L1) (Figure 1.4D). In contrast to MHCII, blockade of mTORC1 resulted in a significant increase in IFNγ-dependent PD-L1 expression compared to vehicle controls. Thus, the expression of distinct IFNγ-mediated genes are differentially controlled by mTOR signaling.

Since blocking mTORC1 inhibited IFNγ-mediated MHCII expression, we next tested whether mTORC1 functions in the same pathway as GSK3α/β or MED16. NTC cells with and without the inhibitor CHIR99021 in addition to *Gsk3β* KO and *Med16* KO macrophages were treated with low and high concentrations of Torin2. These cells were then activated with IFNγ and the surface expression of MHCII and PD-L1 was quantified by flow cytometry 24 hours later (Figure 1.4D and E). Consistent with our findings above, for all genotypes and treatments the inhibition of mTORC1 resulted in a significant reduction in MHCII expression and a significant increase in PD-L1. Taken together these data suggest that while mTORC1 is required for robust IFNγ-mediated MHCII expression, it functions independently of Med16 and GSK3α/β.

GSK3β and MED16 control the expression of distinct IFNγ-mediated genes in macrophages

While GSK3β and MED16 independently regulate MHCII expression, their overlap in transcriptional regulation globally remained unknown. To test this, we compared the transcriptional profiles of *Med16* KO and *Gsk3β* KO cells to NTC cells by performing RNAseq on cells that were left untreated or were stimulated with IFNγ (See materials and methods). Principal component analysis of these six transcriptomes revealed distinct effects of IFNγ-

stimulation ('condition'; PC1) and genotype (PC2) gene expression (Figure 1.5A). Both *Med16* and *Gsk3β* knockout macrophages had distinct transcriptional signatures in the absence of cytokine stimulation, which were further differentiated with IFNγ-stimulation. The PCA analysis suggested that MED16 and GSK3β control distinct transcriptional networks in macrophages following IFNγ-activation.

Transcriptional analysis confirmed a critical role of GSK3β and MED16 in regulating IFNγ-dependent *Ciita* and MHCII expression in macrophages compared to NTC controls (Figure 1.5B and C). However, the extent to which MED16 or GSK3β controlled the overall response of macrophages to IFNγ remained unclear. To directly assess how MED16 and GSK3β regulate the general response to IFNγ, we queried IFNγ-regulated genes from our dataset that are annotated as part of the cellular response to IFNγ stimulation (GeneOntology:0071346). Hierarchical clustering found that, of the 20 most induced IFNγ-regulated transcripts, the expression of eight were unaffected by loss of either *Gsk3β* and *Med16* (Figure 1.5D, Cluster 2). Importantly, these genes included a major regulator of the IFNγ response, *Irf1*, as well as canonical STAT1-target genes (*Gbp2, Gbp3, Gbp5, Gbp6 and Gbp7*). This suggests that neither GSK3β nor MED16 are global regulators of the IFNγ response in macrophages, but rather are likely to exert their effect on particular genes at the level of transcription or further downstream. In contrast, only two genes, out of the top 20 IFNγ-regulated genes, were similarly reduced in both *Med16* KO and *Gsk3β* KO cells (Cluster 4), one of which was *H2ab1*. This shows that while GSK3β and MED16 both regulate IFNγ-mediated MHCII expression, they otherwise control distinct aspects of the IFNγ-mediated response in macrophages. The remaining clusters from this analysis showed specific changes in either *Med16* KO or *Gsk3β* KO cells. Clusters 1 and 3 showed a subset of genes that were more robustly induced in *Gsk3β* KO cells compared to NTC

and *Med16* KO cells. These genes included *Nos2, Il12rb1* and chemokines *Ccl2, Ccl3, Ccl4,* and *Ccl7*. In contrast, Cluster five showed a subset of genes that were reduced only in macrophages lacking MED16, including *Irf8* and *Stat1*; as these effects were modest, and did not reach statistical significance, they may be suggestive of an incomplete positive feedforward in which MED16 plays a role. Further stringent differential gene expression analysis (FDR < 0.05, absolute LFC > 1) of the IFNγ-stimulated transcriptomes identified 69 and 90 significantly different genes for MED16 and GSK3β respectively. Of these differentially expressed genes (DEGs), eight non-MHCII genes were shared between MED16 and GSK3β, including five genes that are involved in controlling the extracellular matrix (*Mmmp8, Mmp12, Tnn, and Clec12a*). Taken together these results suggest that while MED16 and GSK3β both regulate IFNγ-mediated *Ciita* and MHCII expression in macrophages, they otherwise control distinct regulatory networks in response to IFNγ.

We next used the transcriptional dataset to understand what aspects of IFNγ-mediated signaling MED16 and GSK3β specifically control. To resolve the transcriptional landscape of *Med16* KO macrophages and to understand the specific effect that MED16 loss has on the host response to IFNγ, we analyzed the DEGs for upstream regulators whose effects would explain the observed gene expression signature. The analysis correctly predicted a relative inhibition on IFNγ signaling compared to NTC due to the muted induction of *Ciita, H2-Ab1* and *Cd74*. This analysis also identified signatures of *Il10, Stat3*, and *Pparγ* activation that included *Socs3* induction and *Ptgs2* downregulation (Figure 1.5E and Figure 1.5—figure supplement 1A and S5B). As the DEG analysis relied on a stringent threshold that filtered the great majority of the transcriptome from analysis, we sought to incorporate a more comprehensive analysis capable of capturing genes with more modest effects based on pathway

enrichment. To this end, we performed gene set enrichment analysis (GSEA) using a ranked gene list derived from the differential gene expression analysis [48]. Of the ~10,000 gene sets tested, 11 sets were enriched for NTC+ IFNγ and 76 for MED16+ IFNγ (FDR < 0.1). To reduce pathway redundancy and infer biological relevance from the gene sets, we consolidated the signal into pathway networks (Figure 1.5—figure supplement 1C), and observed a significant enrichment for genes involved in xenobiotic and steroid metabolism, including many cytochrome p450 family members and glutathione transferases. We also observed an elevated type I interferon transcriptional response in *Med16* KO cells stimulated with IFNγ that included components of IFNα/β signal transduction (*Ifnar2*), transcription factors (*Stat2, Irf7*) and antiviral mediators (*Oas2, Ifitm1, Ifitm2, Ifitm3, Ifitm6*) (Figure 1.6F and G). Type I IFN production is described to have varying effects on MHCII expression [49–52]. While some studies indicate type I IFN can enhance MHCII in DCs, other studies in distinct cell types suggest type I IFN blunts IFNγ-mediated MHCII expression. We reasoned that if increased type I IFN in *Med16* KO cells was blocking MHCII expression the type I IFN would also inhibit MHCII expression in wild type cells in *trans*. To test the hypothesis that *Med16* KO cells produce elevated type I IFN that blocks IFNγ-mediated MHCII induction we conducted a co-culture experiment. *Med16* KO and GFP expressing NTC macrophages were mixed equally, and the following day stimulated with IFNγ. The surface expression of MHCII was then quantified by flow cytometry. While *Med16* KO cells were unable to robustly induce MHCII, NTC cells from the same well induced MHCII over 30-fold (Figure 1.5H). These data suggest that the effect of Med16 on IFNγ-mediated MHCII expression is cell-autonomous. Thus, MED16 is a critical regulator of the overall interferon response in macrophages.

We next examined the regulatory networks that were specifically controlled by GSK3β. As observed by the initial PCA (Figure 1.5A), the transcriptional landscape of GSK3β deficient macrophages was altered in unstimulated cells. We hypothesized that these widespread differences may alter cellular physiology and explain, in part, the varied responsiveness of *Gsk3β* KO cells to IFNγ. DEG analysis of unstimulated macrophages identified 284 differentially expressed genes due to *Gsk3β* loss. Functional enrichment by STRING identified three major clusters that included dysregulation of chemokines, cell surface receptors, growth factor signaling, and cellular differentiation (Figure 1.5—figure supplement 1D). GSEA identified a strong enrichment for chemotaxis and extracellular matrix remodeling pathways including several integrin subunits and matrix metalloproteinase members (Figure 1.5I and J). These results suggest that GSK3β is an important regulator of both macrophage homeostasis and the response to IFNγ. Altogether the global transcriptional profiling suggests that while MED16 and GSK3β are both critical regulators of IFNγ-mediated MHCII expression, they each control distinct aspects of the macrophage response to IFNγ.

Loss of MED16 or GSK3 inhibits macrophage-mediated CD4$^+$ T cell activation

While the data to this point suggested that MED16 and GSK3β control the IFNγ-mediated induction of MHCII, in addition to distinct aspects of the IFNγ-response, it remained unclear how loss of GSK3β or MED16 in macrophages altered the activation of CD4$^+$ T cells. To test this, we optimized an *ex vivo* T cell activation assay with macrophages and TCR-transgenic CD4$^+$ T cells (NR1 cells) that are specific for the *Chlamydia trachomatis* antigen Cta1 [53]. Resting NR1 cells were added to non-targeting control macrophages that were untreated, IFNγ stimulated, Cta1 peptide-pulsed, or IFNγ-stimulated and Cta1 peptide-pulsed. Five hours later, we harvested T cells and used intracellular cytokine staining to identify IFNγ producing cells by

flow cytometry. Only macrophages that were treated with IFNγ and pulsed with Cta1 peptide were capable of stimulating NR1 cells to produce IFNγ (Figure 1.6A-C). Additionally, when *Rfx5* deficient macrophages were pulsed with peptide in the presence and absence of IFNγ, we observed limited IFNγ production by NR1 cells in both conditions suggesting this approach is peptide-specific and sensitive to macrophage MHCII surface expression.

We next determined the effectiveness of macrophages lacking GSK3 components to activate $CD4^+$ T cells. Macrophages deficient in *Gsk3α*, *Gsk3β* or both along with NTC and *Rfx5* controls were left untreated or stimulated with IFNγ for 16 hours, then all cells were pulsed with Cta1 peptide. Resting NR1 cells were then added and the production of IFNγ by NR1 cells from each condition was quantified by flow cytometry five hours later. In agreement with our findings on MHCII expression, loss of *Gsk3α* did not inhibit the production of IFNγ by NR1 cells (Figure 1.6D-F). In contrast, *Gsk3β* KO cells reduced the number of $IFN\gamma^+$ NR1 cells over twofold and reduced the mean fluorescence intensity of IFNγ production over 4-fold. Furthermore, macrophages deficient in *Gsk3α* and *Gsk3β* were almost entirely blocked in their ability to activate IFNγ production by NR1 cells. Thus, macrophages deficient in GSK3 function are unable to serve as effective antigen-presenting cells to $CD4^+$ T cells.

The *ex vivo* T cell assay was next used to test the effectiveness of *Med16* KO macrophages as APCs. NR1 cells stimulated on IFNγ-activated *Med16* KO macrophages were reduced in the number of $IFN\gamma^+$ T cells by 10-fold and the fluorescence intensity of IFNγ by 100-fold compared to NTC (Figure 1.6G-I). Similar to what we observed with MHCII expression, there was a small yet reproducible induction of $IFN\gamma^+$ NR1 cells incubated with IFNγ-activated *Med16* KO macrophages. We hypothesized that inhibition of GSK3 and MED16 simultaneously would eliminate all NR1 activation on macrophages. Treatment of *Med16* KO

macrophages with CHIR99021 prior to IFNγ-stimulation and T cell co-incubation, eliminated the remaining IFNγ production by NR1 cells seen in the DMSO treated *Med16* KO condition. Altogether these results show that GSK3β and MED16 are critical regulators of IFNγ mediated antigen presentation in macrophages and their loss prevents the effective activation of $CD4^+$ T cells.

FIGURES

Figure 1.1. Genome-wide CRISPR Cas9 screen identifies regulators of IFNγ-dependent MHCII expression. (**A**) Cas9+ iBMDMs (Clone L3) expressing the indicated sgRNAs were left untreated or treated with IFNγ (6.25 ng/ml) for 24 hours. Surface MHCII was quantified by flow cytometry. Shown is a representative histogram of MHCII surface staining and (**B**) the quantification of the mean fluorescence intensity (MFI) in the presence and absence of IFNγ stimulation from three biological replicates. **** $p < 0.0001$ by one-way ANOVA with tukey correction for multiple hypotheses. These data are representative of three independent experiments. (**C**) A schematic representation of the CRISPR-Cas9 screen conducted to identify regulators of IFNγ-inducible MHCII surface expression on macrophages. A genome-wide CRISPR Cas9 library was generated in L3 cells using sgRNAs from the Brie library (four sgRNAs per gene). The library was treated with IFNγ and MHCII^{hi} and MHCII^{low} populations were isolated by FACS. The representation of sgRNAs in each population in addition to input library were sequenced. (**D**) Shown is score for each gene in the CRISPR-Cas9 library that passed filtering metrics as determined by the alpha-robust rank algorithm (a-RRA) in MAGeCK from two independent screen replicates. (**E**) The L3 clone was transduced with the indicated sgRNAs for candidates (two per candidate gene) in the top 100 candidates from the CRISPR-Cas9 screen. All cells were left untreated or treated with 10 ng/µl of IFNγ for 24 hours then were analyzed by flow cytometry. The fold-increase in MFI was calculated for triplicate samples for each cell line (MFI IFNγ+/MFI IFNγ-). The results are representative of at least two independent experiments. Candidates that were significant for two sgRNAs (Red) or one sgRNA (Blue) by one-way ANOVA compared to the mean of NTC1 and NTC2 using Dunnets multiple comparison test. Non-significant results are shown in gray bars.

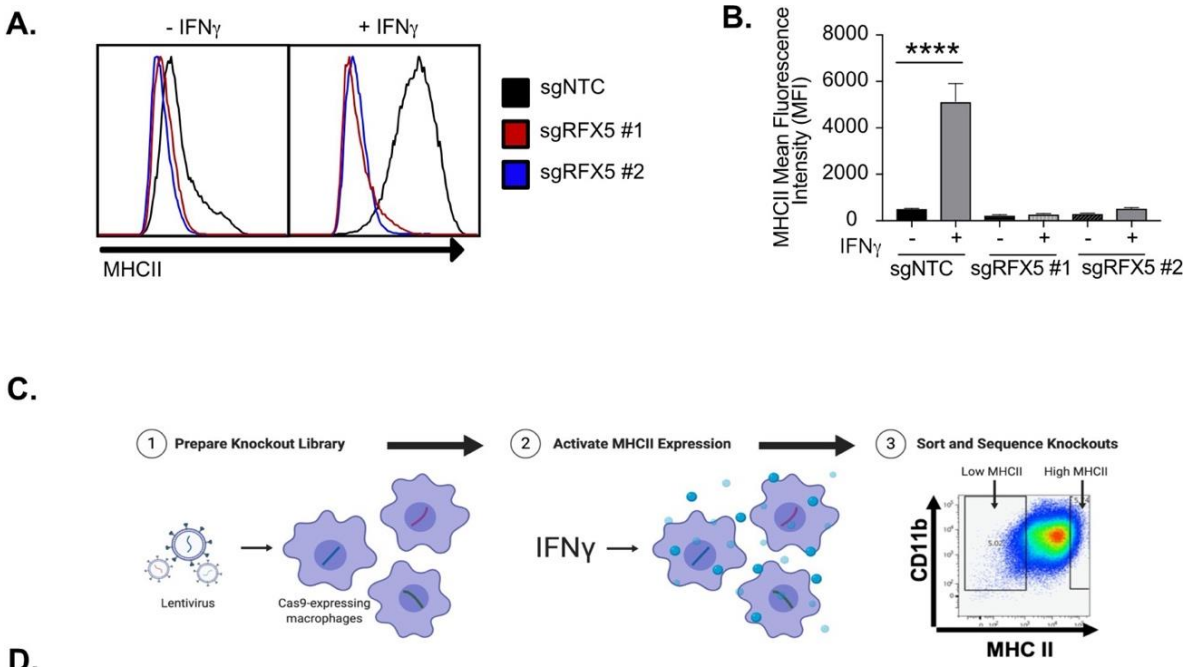

Figure 1.1 (cont'd)

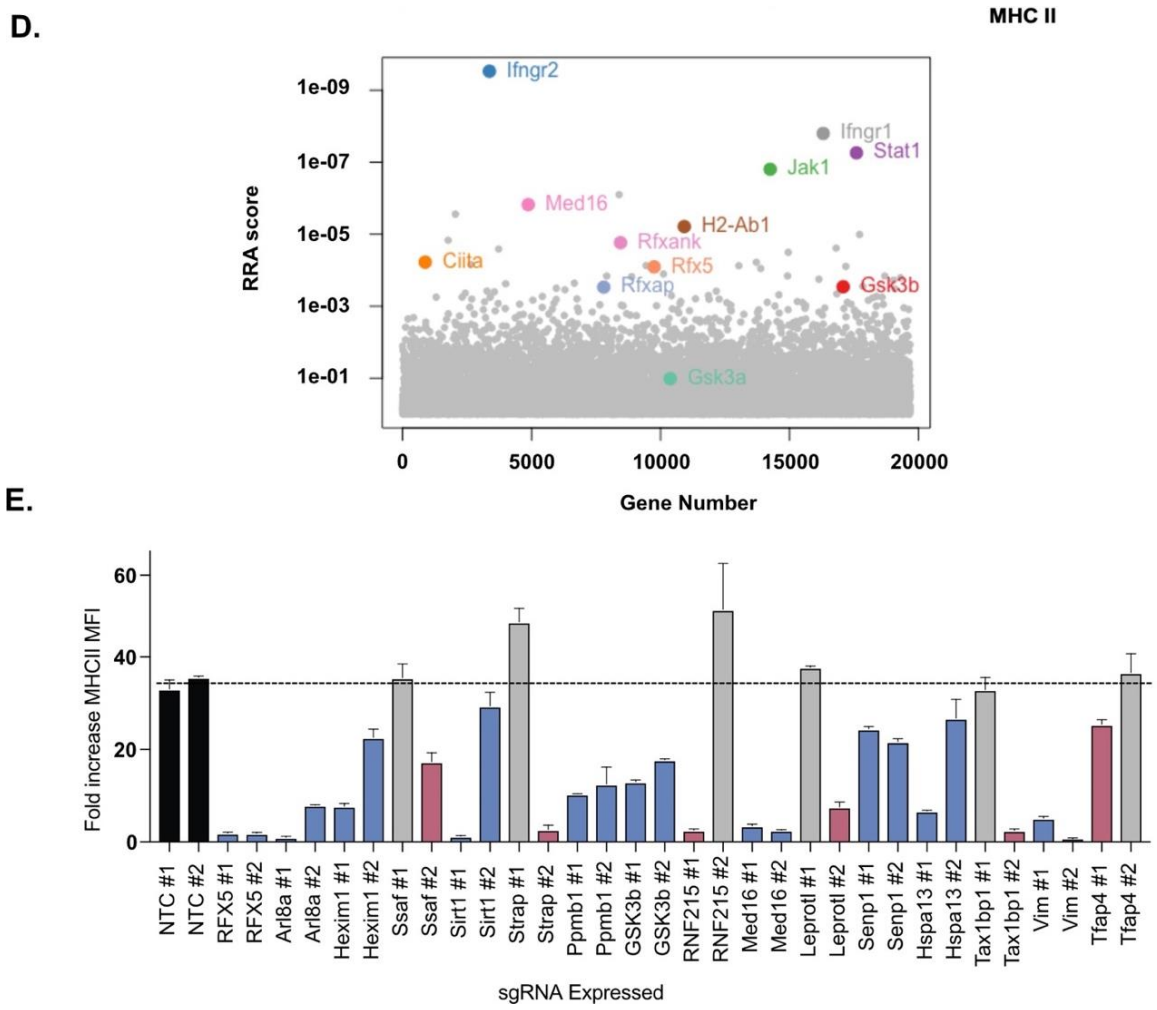

Figure 1.2. The mediator complex subunit MED16 is uniquely required for IFNγ-mediated MHCII surface expression. (**A**) Shown is the normalized mean read counts from FACS sorted MHCII^{low} and MHCII^{hi} populations for the four sgRNAs targeting *Med16* within the genome-wide CRISPR-Cas9 library. (**B**) The mean of the log fold change (normalized counts in MHCII^{hi}/normalized counts in MHCII^{low}) for each mediator complex subunit that passed quality control metrics described in Materials and methods. The bar colors indicate the number of sgRNAs out of four possible that pass the alpha cutoff using the MAGeCK analysis pipeline as described in material and methods. (**C**) *Med16* KO cells or L3 cells targeted with the indicated sgRNA were left untreated or were treated with 6.25 ng/ml of IFNγ for 18 hours. Cells were then analyzed for surface MHCII expression by flow cytometry. Shown are representative comparing the MHCII surface expression of indicated mediator complex subunit (Black solid line) treated with IFNγ overlayed with NTC (Gray-dashed line) treated with IFNγ. (**D**) Quantification of the MFI of surface MHCII from the experiment in (**C**) from three biological replicates. These results are representative of two independent experiments. (**E**) NTC L3 cells, RFX5 sg#1 cells, and *Med16* KO cells were left untreated or were treated with 6.25 ng/ml of IFNγ. 18 hours later cells RNA was isolated and qRT-PCR was used to determine the relative expression of *Ciita* and (**F**) *H-2aa* compared to GAPDH controls from three biological replicates. (**G**) NK cells from wild type or IFNγ-/- mice were activated with IL12/IL18 overnight then added to NTC or *Med16* KO cells in the presence or absence of IFNγR blocking antibody. Twenty-four hours later MHCII expression on macrophages was quantified by flow cytometry. The results are representative of three independent experiments. ***p < 0.001 as determined one-way ANOVA compared to NTC cells with a Dunnets test.

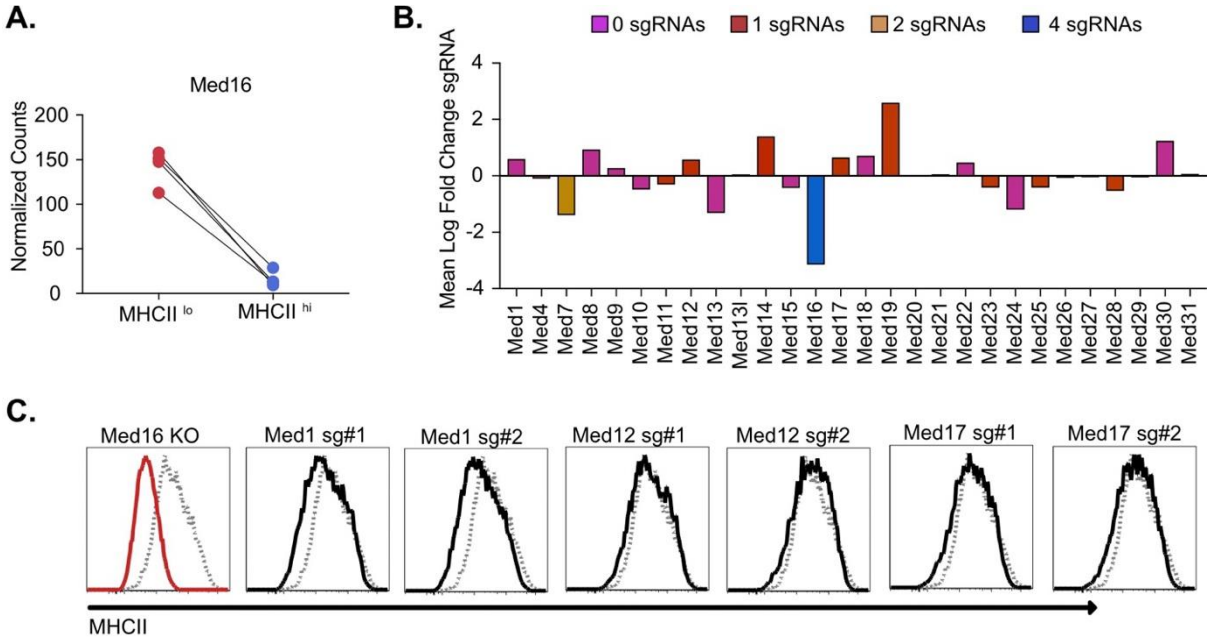

Figure 1.2 (cont'd)

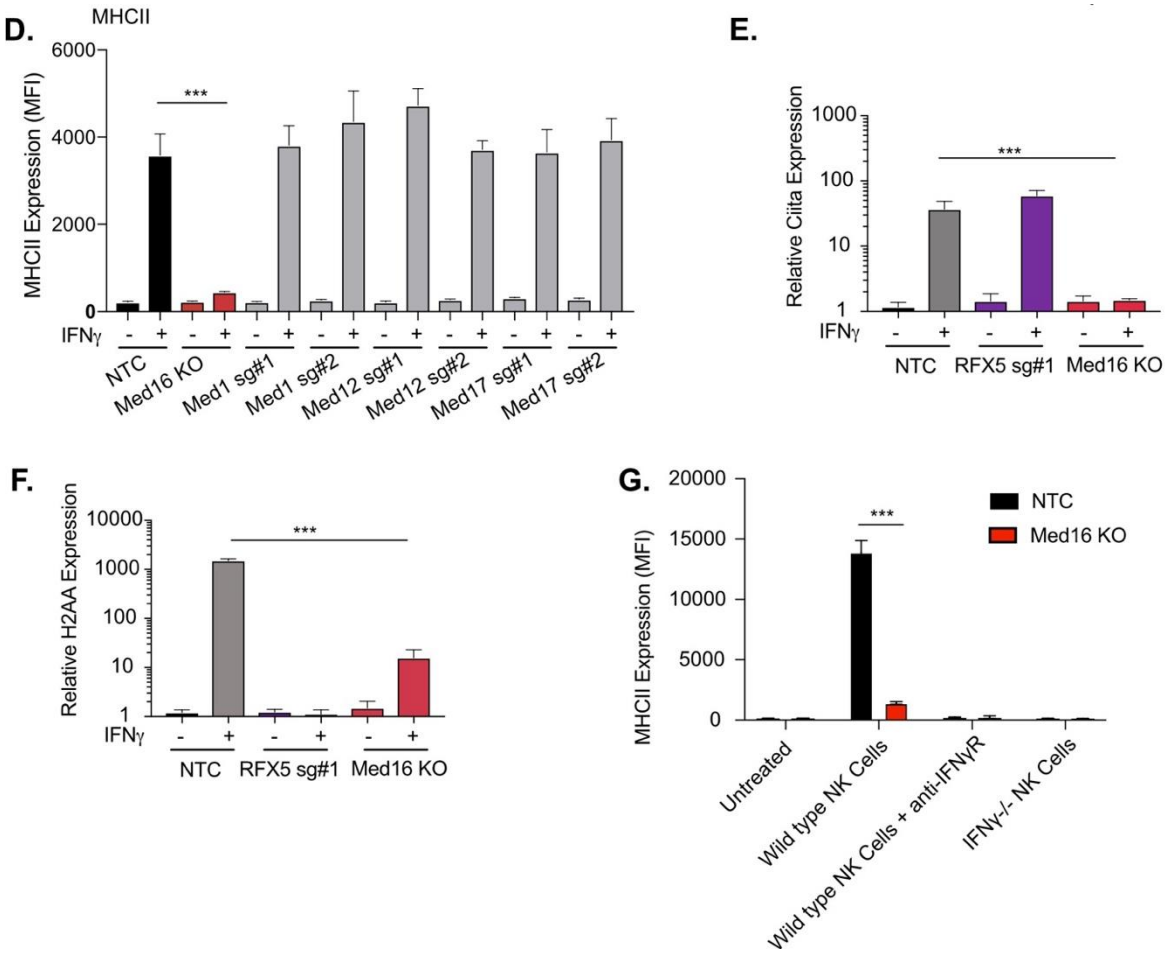

Figure 1.3. GSK3β and GSK3α coordinate IFNγ-mediated CIITA and MHCII expression. (**A**) Shown is the normalized mean read counts from FACS sorted MHCII^{low} and MHCII^{high} populations for the four sgRNAs targeting *Gsk3b* within the genome-wide CRISPR-Cas9 library. (**B**) NTC L3 cells and *Gsk3b* KO cells were treated with 6.25 ng/ml of IFNγ. Eighteen hr later, cells were stained for surface MHCII and analyzed by flow cytometry. Shown is a representative flow cytometry plot overlaying *Gsk3b* KO (blue line) with NTC (grey line). The results are representative of five independent experiments. (**C**) NTC L3 cells, *Rfx*5 sg#1 cells, and *Gsk3b* KO cells were left untreated or were treated with 6.25 ng/ml of IFNγ. Eighteen hr later, cells RNA was isolated and qRT-PCR was used to determine the relative expression of *Ciita* and (**D**) *H2aa* compared to *Gapdh* controls from three biological replicates. The results are representative of three independent experiments. (**E**) NTC L3 cells or Gsk3β KO were treated with DMSO or 10 μM CHIR99021 as indicated then left untreated or stimulated with IFNγ for 18 hr. MHCII surface expression was then quantified by flow cytometry. The mean fluorescence intensity was quantified from three biological replicates. These results are representative of three independent experiments. (**F**) L3 cells or *Gsk3b* KO transduced with the indicated sgRNAs were treated with IFNγ and 18 hr later the surface levels of MHCII were quantified by flow cytometry. The mean fluorescence intensity of surface MHCII was quantified from three biological replicates from this experiment that is representative of 4 independent experiments. (**G**) NK cells from wild type or IFNγ-/- mice were activated with IL12/IL18 overnight then added to NTC or *Gsk3b* KO cells in the presence or absence of IFNγR blocking antibody, 10 μM CHIR99021 or DMSO. Twenty-four hours later, MHCII expression on macrophages was quantified by flow cytometry from three biological replicates. The results are representative of three independent experiments. (**H**) NTC or *Gsk3b* KO cells were left untreated or were stimulated with 6.25 ng/ml IFNγ for 30 min. Cell lysates were used for immunoblot analysis with the indicated antibodies for pSTAT1, total GSK3α, pGSK3α, and Beta-actin. (**J**) Immortalized bone marrow macrophages were treated with IFNγ. Control cells were treated with DMSO and for the remaining cells CHIR999021 was added at the indicated times following IFNγ treatment. 24 hours after IFNγ stimulation the levels of surface MHCII were quantified by flow cytometry. Shown is the MFI for biological triplicate samples. ***p < 0.001 **p < 0.01 *p < 0.05 by one-way ANOVA with a Tukey Correction test.

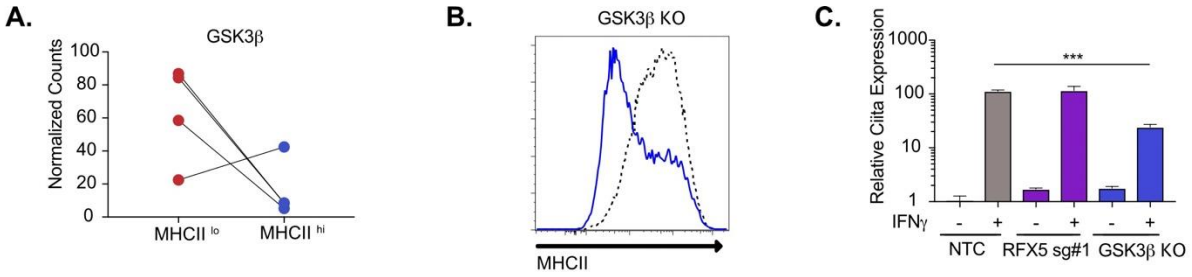

Figure 1.3 (cont'd)

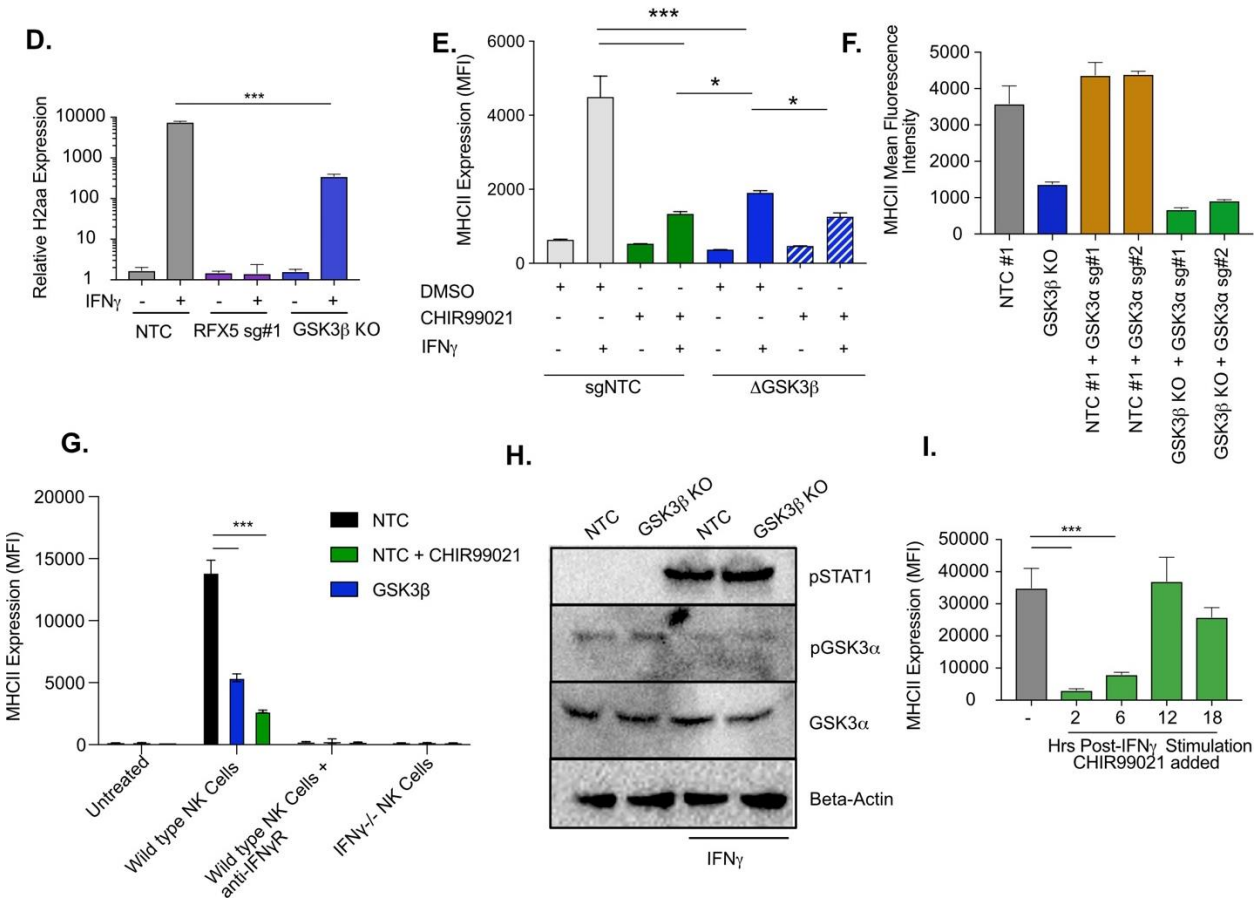

Figure 1.4. GSK3α/β and Med16 function independently from mTORC1 to control IFNγ-mediated MHCII expression. (**A**) NTC or *Med16* KO cells were treated with DMSO or CHIR99021 then left untreated or stimulated with IFNγ overnight. The following day MHC II cell surface expression was determined by flow cytometry. The quantification of the MFI of MHCII from four biological replicates is shown. **p < 0.001 by two-way ANOVA with multiple comparison correction. (**B and C**) NTC cells were treated with DMSO or 30 nM Torin2 for 2-hr then were stimulated with 6.25 ng/ml IFNγ overnight. Eighteen hr later (**B**) MHCII expression and (**C**) PD-L1 expression were quantified by flow cytometry. Shown is the MFI of the indicated marker from three biological replicates and is representative of three independent experiments. (**D and E**) NTC, *Gsk3b* KO and *Med16* KO cells were treated with DMSO or 10 uM CHIR99021 and/or the indicated Torin2 for 2 hours. Cells were then treated with IFNγ and the surface expression of (**D**) MHCII and (**E**) PD-L1 were quantified by flow cytometry. Shown is the MFI of the indicated marker from three biological replicates and is representative of three independent experiments. *p < 0.05, **p < 0.01, ***p < 0.001, **** p < 0.0001 by one or two-way ANOVA with correction for multiple comparisons.

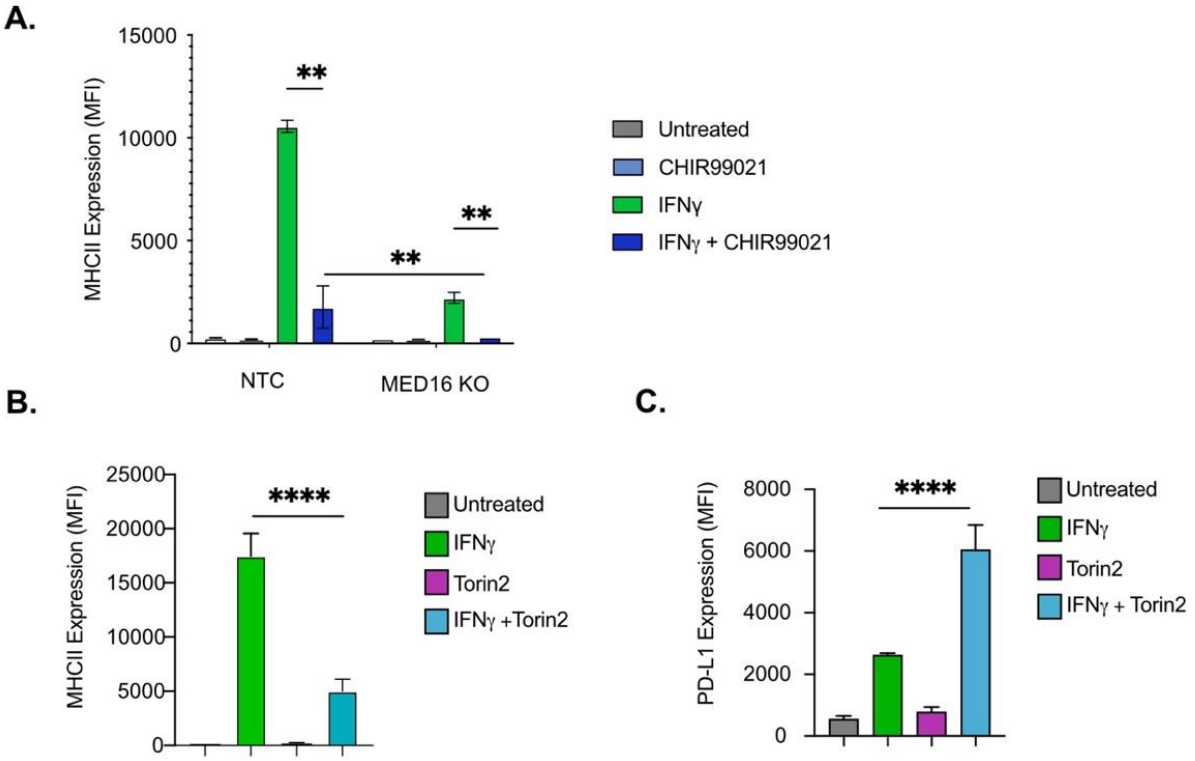

Figure 1.4 (cont'd)

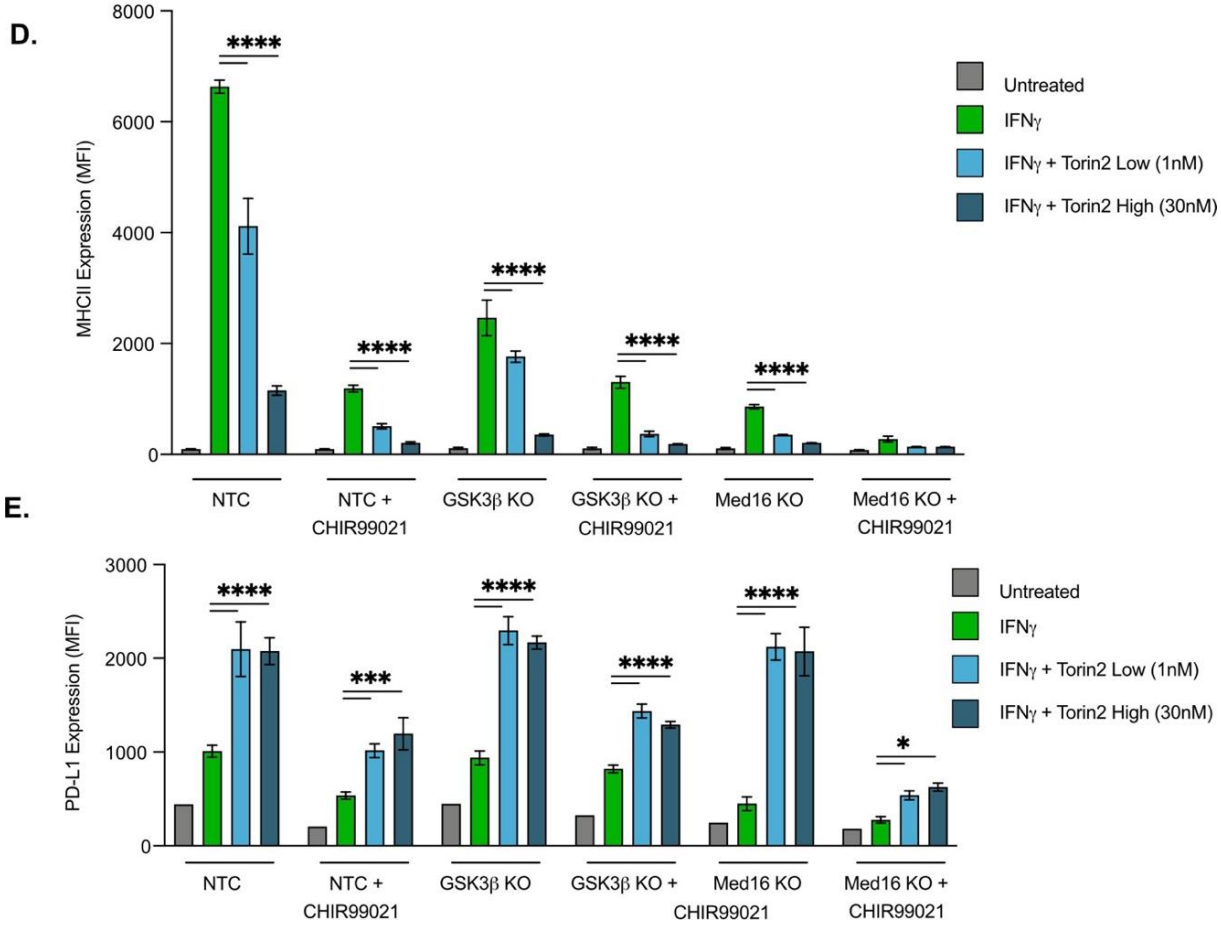

Figure 1.5. Transcriptomic analysis reveals distinct regulatory mechanisms of IFNγ signaling mediated by MED16 and GSK3β. (**A**) The Global transcriptomes of NTC, *Gsk3b* KO and *Med16* KO was determined in the presence and absence of IFNγ-stimulation for 18 hours by RNA sequencing. Shown is the principal component analysis of the transcriptomes from three biological replicates for each condition. Dotplot showing the normalized read counts for (**B**) CIITA and (**C**) H2-Aa. (**D**) Shown is a heatmap showing the relative expression (log normalized, row-scaled) of the most varied 20 genes involved in the cellular response to type II interferon (Gene Ontology GO:0071346). (**E**) Shown is a Dotplot visualizing the normalized counts of the type I IFN signature Socs3 from all RNAseq conditions. Clustering was used to (**F**) Significant gene sets from *Med16* KO cells that were uniquely regulated from the RNAseq dataset were analyzed by gene set enrichment analysis (GSEA) then subjected to Leading Edge analysis, which identified a significant enrichment of the cellular responses to type I interferons (normalized enrichment score 2.81, FDR < 0.01). (**G**) Shown is a heatmap demonstrating the relative expression of the type I interferon signature identified in IFNγ-stimualted *Med16* KO macrophages from the RNAseq analysis. (**H**) GFP+ NTC cells were mixed equally with GFP- NTC or GFP- *Med16* KO cells. The following day cells were stimulated with 6.25 ng/ml IFNγ and 24 hours later MHCII expression was quantified on each cell type. (**Top**) Shown is a representative flow cytometry plot to identify the cells of interest and MHCII expression. (**Bottom**) the % MHCII positive was calculated for cells in each population in each well. Lines link samples that were within the same well. These data are from three biological replicates and represent three independent experiments. **p < 0.01 by two-tailed t-test. (**I**) Shown is a heatmap demonstrating the relative expression of unique differentially expressed genes from the *Gsk3b* KO in the presence (Top) and absence (Bottom) of IFNγ-stimulation. (**J**) These differentially expressed genes were used in GSEA to identify Leading Edge networks that are specific to *Gsk3b* KO cells. (Top) Shown is the leading-edge analysis of the UPAR pathway that was identified from IFNγ-stimulated *Gsk3b* KO cells. (Bottom) Shown is the leading-edge analysis of the Granulocyte chemotaxis pathway that was identified as differentially regulated in resting *Gsk3b* KO cells.

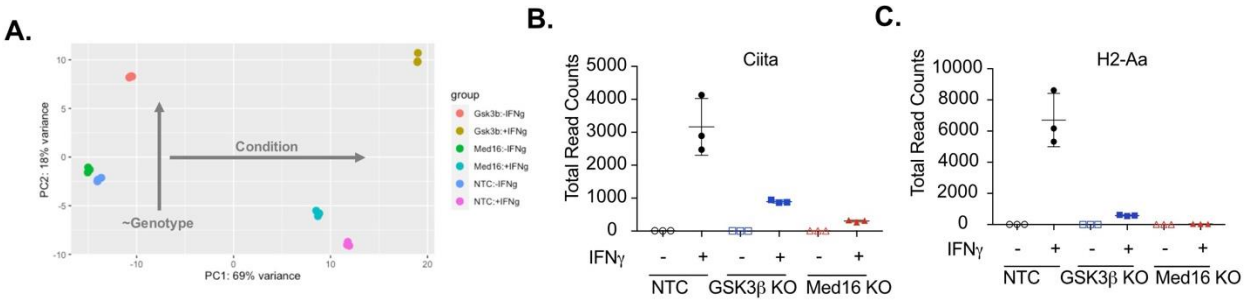

Figure 1.5 (cont'd)

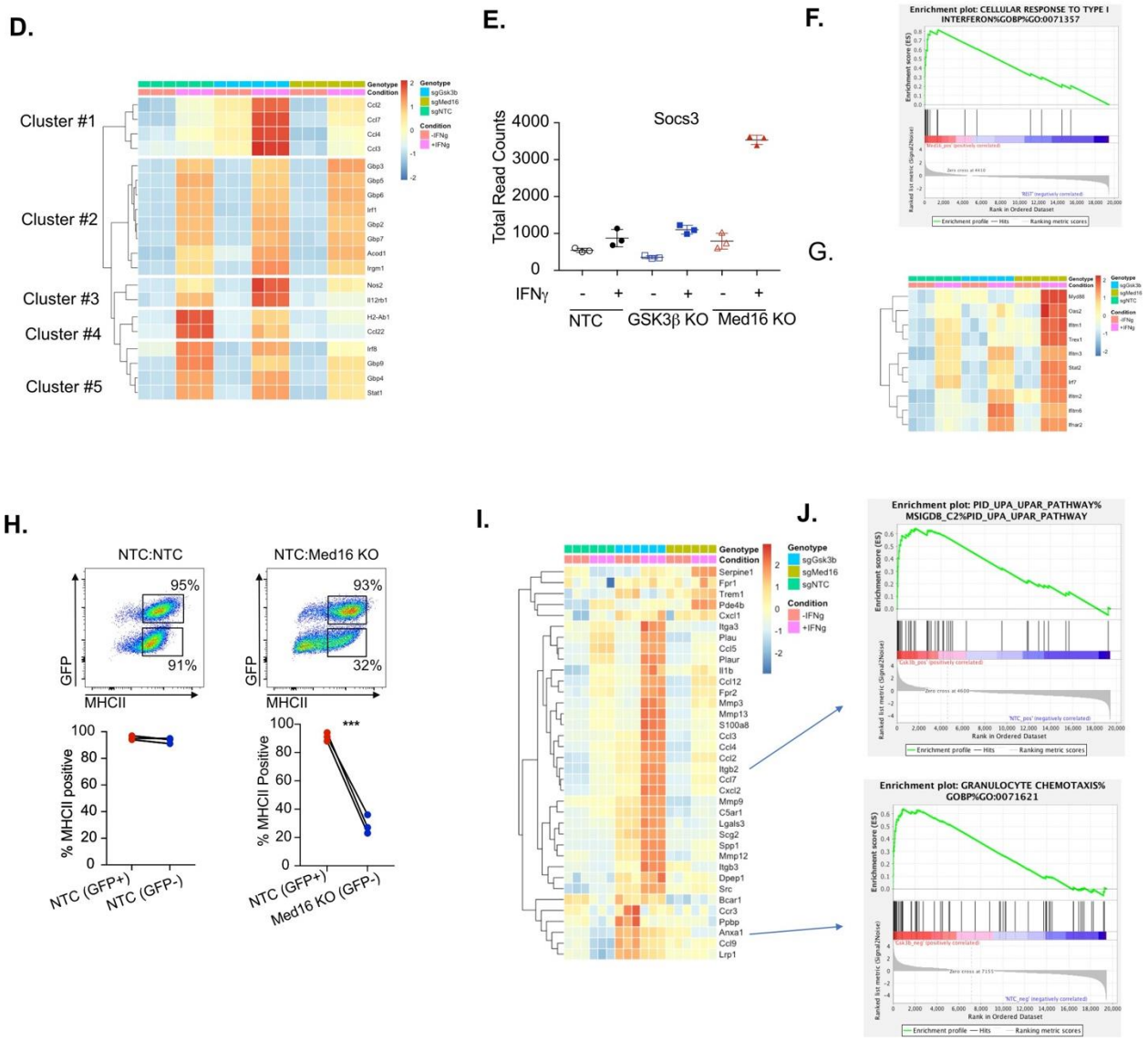

Figure 1.6. IFNγ-stimulated macrophages require MED16 or GSK3 to activate CD4+ T cells.

(**A**) Macrophages were left untreated, treated with 10 ng/ml IFNγ overnight, 5 μM peptide for 1 hr or both IFNγ and peptide as indicated. TCR-transgenic NR1 CD4+ T cells specific for the peptide Cta1 from *Chlamydia trachomatis* were then added to L3 macrophages of the indicated genotypes at a 1:1 ratio. Four hr after the addition of T cells, NR1 cells were harvested and the number of IFNγ-producing CD4+ T cells was quantified by intracellular staining and flow cytometry. Shown is a representative flow cytometry plot gated on live/CD4+ cells. Gates for IFNγ+ T cells were determined using an isotype control antibody. (**B**) The percent of live CD4+ T cells producing IFNγ and (**C**) the MFI of IFNγ production by live CD4+ T cells was quantified from triplicate samples. These results are representative of three independent experiments. (**D**) L3 cells targeted with the indicated sgRNAs were left untreated or treated overnight with IFNγ then pulsed with Cta1 peptide for 1 hr. NR1 cells were then added at a 1:1 ratio and 4 hr later NR1 cells were harvested and the number of IFNγ-producing CD4+ T cells was quantified by intracellular staining and flow cytometry. Shown is a representative flow cytometry plot gated on live/CD4+ cells. Gates for IFNγ+ T cells were determined using an isotype control antibody. (**E**) The percent of live CD4+ T cells producing IFNγ and (**F**) the MFI of IFNγ production by live CD4+ T cells was quantified from triplicate samples. These results are representative of three independent experiments. (**G**) NTC L3 cells or *Med16* KO cells were left untreated or treated overnight with DMSO, IFNγ, and DMSO or IFNγ and CHIR999021 then pulsed with Cta1 peptide for 1 hour. NR1 cells were then added at a 1:1 ratio and 4 hours after the addition of T cells, NR1 cells were harvested and the number of IFNγ-producing CD4+ T cells was quantified by intracellular staining and flow cytometry. Shown is a representative flow cytometry plot gated on live/CD4+ cells. Gates for IFNγ+ T cells were determined using an isotype control antibody. (**H**) The percent of live CD4+ T cells producing IFNγ and (**I**) the MFI of IFNγ production by live CD4+ T cells was quantified from triplicate samples. These results are representative of three independent experiments. *** $p < 0.001$, *$p < 0.05$ by one-way ANOVA with a Tukey correction test.

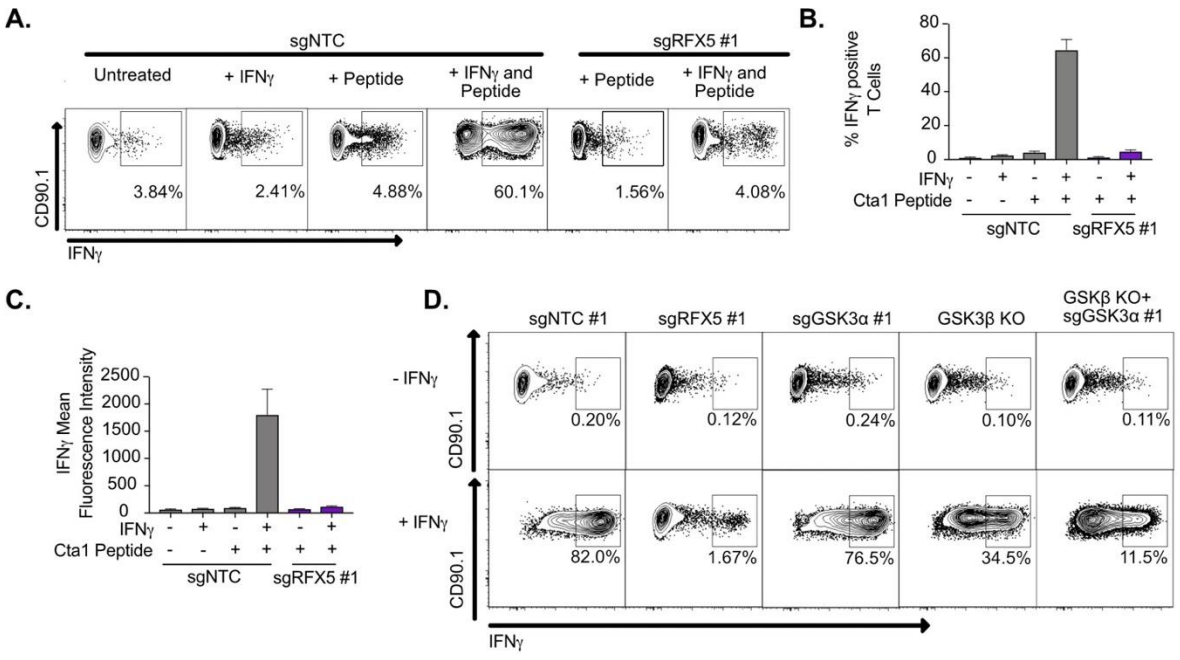

Figure 1.6 (cont'd)

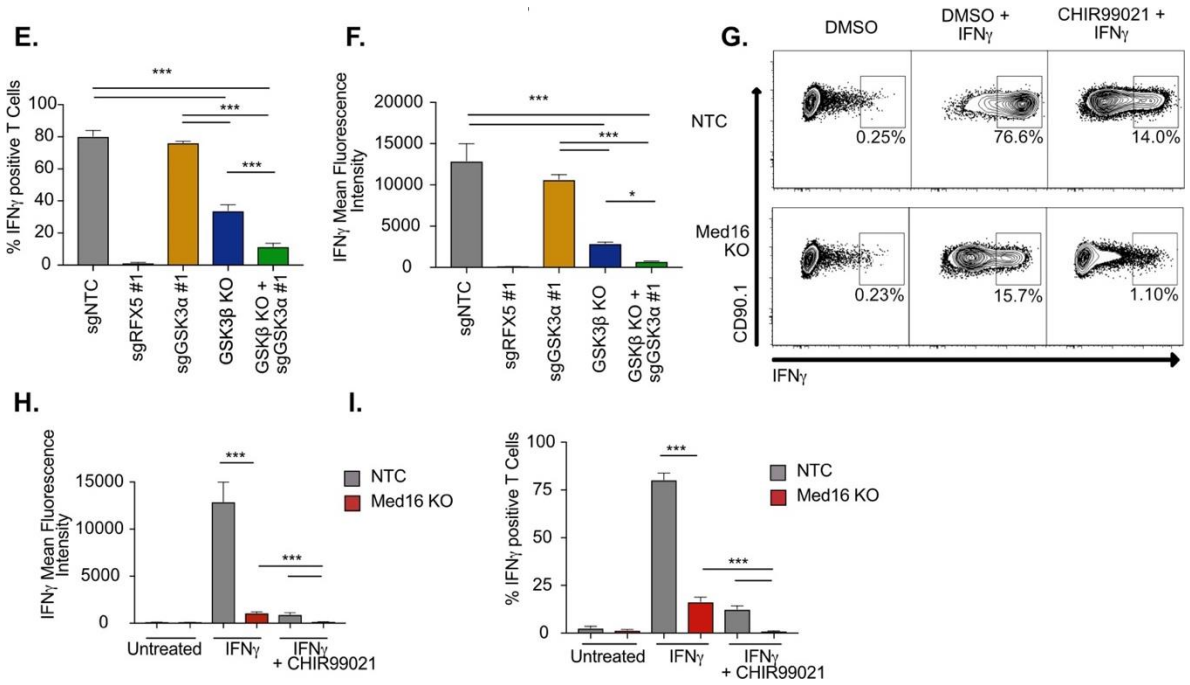

Figure 1.7. Model of GSK3β− and Med16-mediated control of IFNγ-activated MHCII expression.
Shown is a model of how GSK3β and MED16 regulate IFNγ-mediated MHCII expression. In the absence of IFNγ (**Left**) GSK3β controls the transcription of many macrophage genes related to inflammation such as CCLs. In contrast, *Med16* KO cells shows minimal transcriptional changes in resting macrophages. Additionally, IFNγ-mediated gene expression is low. Following the activation of macrophages with IFNγ (**Right**), STAT1 becomes phosphorylated and translocates to the nucleus to drive gene transcription. The IFNγ-mediated induction of *Irf1* does not require either GSK3β or MED16. While GSK3β continues to negatively regulate inflammatory genes like CCLs it also positively regulates the transcriptional activation of *Ciita* following IFNγ-activation. Through a parallel but distinct mechanism, IFNγ-mediated induction of *Ciita* also requires MED16 function. The expression of *Ciita* then recruits other transcription factors such as RFX5 to the MHCII locus where it induces the expression of MHCII, which allows for the activation of CD4+ T cells. Figure created using Biorender.

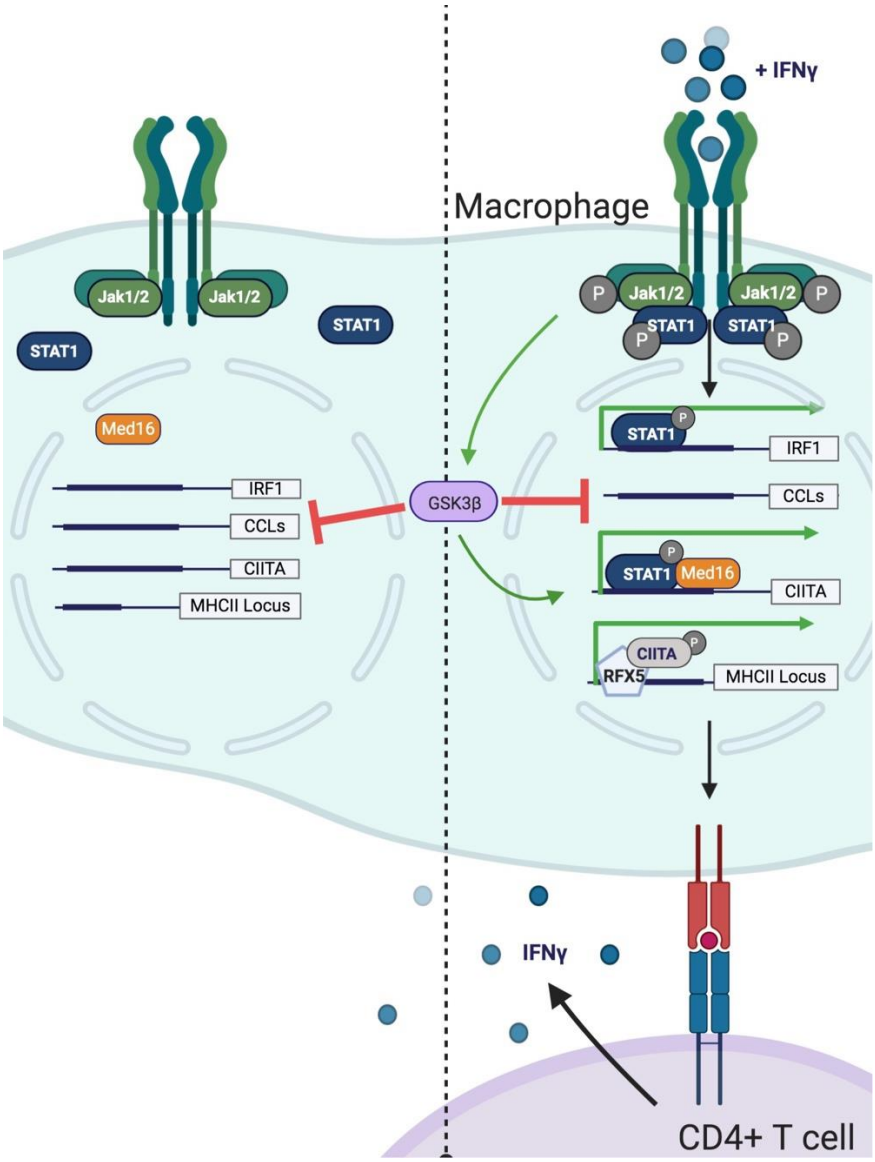

DISCUSSION

IFNγ-mediated MHCII is required for the effective host response against infections. Here, we used a genome-wide CRISPR library in macrophages to globally examine mechanisms of IFNγ-inducible MHCII expression. The screen correctly identified major regulators of IFNγ-signaling, highlighting the specificity and robustness of the approach. In addition to known regulators, our analysis identified many new positive regulators of MHCII surface expression. While we validated only a subset of these candidates, the high rate of validation suggests many new regulatory mechanisms of IFNγ-inducible MHCII expression in macrophages. While the major pathways identified from the candidates in CRISPR screen were related to IFNγ-signaling, we also identified an important role for other pathways including the mTOR signaling cascade. Within the top 100 candidates of the screen several genes related to metabolism and lysosome function including *Lamtor2* and *Lamtor4* were found. Given the known effects of IFNγ in modulating host metabolism, these results suggest that the metabolic changes following IFNγ-activation of macrophages is critical for key macrophage functions including the surface expression of MHCII [54]. Future studies will need to dissect the metabolism specific mechanisms that macrophages use to control the IFNγ response, including the regulation of MHCII.

In this study, we focused our followup efforts from validated candidates on genes that might control MHCII transcriptional regulation. We identified MED16 and GSK3β as strong regulators of IFNγ-mediated *Ciita* induction. Using global transcriptomics we found that loss of either *Med16* or *Gsk3β* in macrophages inhibited subsets of IFNγ-mediated genes including MHCII. Importantly, the evidence here strongly supports a model where MED16 and GSK3β control IFNγ-mediated MHCII expression through distinct mechanisms (Figure 1.7). Our results

uncover previously unknown regulatory control of CIITA-mediated expression that is biologically important to activate CD4+ T cells.

MED16 is a subunit of the mediator complex that is critical to recruit RNA polymerase II to the transcriptional start site [38]. While the mediator complex can contain over 20 unique subunits and globally regulate gene expression, individual mediator subunits control distinct transcriptional networks by interacting with specific transcription factors [38,40]. Our data shows that MED16 is uniquely required among the mediator complex for IFNγ-mediated MHCII expression. While we observed a strong reduction in *Ciita* expression in the absence of Med16, some *Ciita* expression remained driving reduced MHCII expression (Figure 5—source data 1). Yet how MED16 controls *Ciita* expression upstream of MHCII remains an open question. One recent study showed that MED16 controls NRF2 related signaling networks that respond to oxidative stress [55]. A major finding of our MED16 transcriptional analysis was the identification of several metabolic pathways involved in oxidative stress and xenobiotics. Given the previous work that described how oxidative stress and the NRF2 regulator KEAP1 regulated IFNγ-mediated MHCII expression in human melanoma cells, NRF2 regulation and redox dysregulation could explain a possible mechanism for MED16 control of MHCII [1]. Intriguingly, the effect of MED16 loss was negligible on many STAT1 and IRF1 targets, and, in fact, resulted in a type I interferon gene signature. Further experiments found that co-culture of *Med16* KO with NTC cells did not alter MHCII expression in either population suggesting a cell-autonomous effect of *Med*16 KO. Thus, what is driving the type I signature following type II interferon activation remains unknown suggesting a careful balance between regulation of distinct IFN-mediated gene expression signatures.

Previous studies showed that CDK8, a kinase that can associate with the mediator complex, controls a subset of IFNγ-dependent gene transcription [56]. However, our results strongly support a model where MED16 acts independently of CDK8. Not only was CDK8 not identified in the initial CRISPR screen, but our transcriptional profiling showed that the major IFNγ-dependent genes controlled by *Cdk8, Tap1* and *Irf1*, remain unchanged in *Med16* KO macrophages. Thus, understanding what transcription factors MED16 interacts with in the future will be needed to fully determine the mechanisms of MED16-dependent transcription and its control over *Ciita* and IFNγ-mediated gene expression.

While we hypothesize that MED16 directly controls *Ciita* transcription, GSK3 likely regulates MHCII through signaling networks upstream of transcription initiation. GSK3α and GSK3β are multifunctional kinases that regulate diverse cellular functions including inflammatory and developmental cascades [39]. Our studies found that GSK3β and GSK3α coordinate IFNγ-mediated MHCII expression, with GSK3β playing a primary role and GSK3α contributing in the absence of GSK3β. The mechanism of this compensation, however, appears independent of protein abundance or phosphorylation and remains unclear. One possibility is that GSK3β outcompetes GSK3α for substrates related to MHCII expression but testing this hypothesis will require further biochemical studies. Thus, GSK3α and GSK3β are partially redundant in their control of IFNγ-mediated MHCII expression highlighting the interlinked regulation of MHCII.

Because GSK3α/β control many pathways, careful work is needed to determine which networks upstream and downstream of GSK3α/β are responsible for controlling *Ciita* expression. Previous studies suggested that GSK3 controls IFNγ mediated STAT3 activation, LPS-mediated nitric oxide production, and IRF1 transcriptional activity but our transcriptional results clearly

show these do not explain the requirement for GSK3-dependent MHCII expression [57–59]. Work in human monocyte-derived macrophages showed previously that IFNγ primed macrophages activate mTORC1 resulting in blunted TLR2 responses opposite of the results from the MHCII genetic screen [47]. Given GSK3 was previously shown to be modified by mTORC1, we directly examined how mTORC1 modulates IFNγ-mediated responses in the presence and absence of functional GSK3α/β [60]. Our study provides new evidence that mTORC1 differentially controls the expression of distinct IFNγ-inducible genes. Blocking mTORC1 activation enhanced IFNγ-mediated PD-L1 surface expression in line with observations in human cells [47]. In contrast, mTOR activity was required for robust IFNγ-mediated MHCII expression, in agreement with the bioinformatic analysis from our screen. We also observed that mTORC1 inhibition further diminished MHCII expression in *Gsk3β* KO or CHIR99021 cells suggesting GSK3α/β functions independently of mTOR to control IFNγ-inducible MHCII. Thus, our findings suggest that mTORC1 is both a positive and negative regulator of IFNγ responses that functions independently of GSK3β and Med16 to control MHCII expression. Given mTORC1 is the target of many therapeutics, the mechanisms regulating this differential control of IFNγ-activated pathways will be important to understand.

One additional function of GSK3 is to modulate the activation of the Wnt signaling cascade [39]. Inhibition or loss of GSK3 results in the constitutive stabilization of Beta-Catenin and *Tcf* expression. If the constitutive activation of Beta-catenin and Wnt signaling prevents effective *Ciita* expression remains to be determined. Interestingly, another Wnt signaling pathway member *Fzd4* was identified in our screen as required for MHCII expression in our screen, supporting a possible role for Wnt in IFNγ-induced MHCII regulation. It is tempting to speculate that Wnt signaling balances IFNγ-induced activation, resulting in distinct MHCII

upregulation between cells with different Wnt activation states. While there is data supporting interactions between Wnt pathways and Type I IFN during viral infections, this has not been explored yet in the context of IFNγ [61,62].

GSK3 was recently found to be co-opted by the *Salmonella enterica* serovar Typhimurium effector SteE to skew infected macrophage polarization and allow infection to persist [63,64]. Our results suggest another possible effect of targeting GSK3 may be the inefficient upregulation of MHCII on Salmonella-infected macrophages in response to IFNγ. While it is known that *Salmonella* and other pathogens including *M. tuberculosis* and *C. trachomatis*, modulate the expression of MHCII, the precise mechanisms underlying many of these virulence tactics remains unclear [24,65]. Our screening results provide a framework to test the contribution of each candidate MHCII regulator during infection with pathogens that target MHCII. These directed experiments would allow the rapid identification of possible host-pathogen interactions. It will be important to determine if augmenting specific MHCII pathways identified by our screen overcomes pathogen-mediated inhibition and induces robust MHCII expression to better activate CD4+ T cells and protect against disease using *in vivo* models. Conditional knockout mice were recently developed for GSK3α and Gsk3β and can now be used to specifically ablate *Gsk3β* in macrophages *in vivo* and examine IFNγ responses. However, previous work targeting *Med16* found this knockout is embryonic lethal thus work is underway to develop conditional *Med16* knockout animals to specifically test Med16 function in IFNγ responses to infection *in vivo*.

Beyond infections, our dataset provides an opportunity to examine the importance of newly identified MHCII regulators in other diseases such as tumor progression and autoimmunity. Of course, MHCII is not the only surface marker that is targeted by pathogens

and malignancy. Other important molecules including MHCI, CD40, and PD-L1 are induced by IFNγ stimulation and are targeted in different disease states [66–69]. Employing our screening pipeline for a range of surface markers will identify regulatory pathways that are shared and unique at high resolution and provide insights into targeting these pathways therapeutically. Taken together, the tools and methods developed here identified new regulators of IFNγ-inducible MHCII that will illuminate the underlying biology of the host immune response.

MATERIALS AND METHODS

Mice

C57BL/6J (stock no. 000664) were purchased from The Jackson Laboratory. NR1 mice were a gift of Dr. Michael Starnbach [53]. Mice were housed under specific pathogen-free conditions and in accordance with the Michigan State University Institutional Animal Care and Use Committee guidelines. All animals used for experiments were 6–12 weeks of age.

Cell culture

Macrophage cell lines were maintained in Dulbecco's Modified Eagle Medium (DMEM; Hyclone) supplemented with 5% fetal bovine serum (Seradigm). Cells were kept in 5% CO2 at 37 C. For HoxB8- conditionally immortalized macrophages, bone marrow from C57BL/6J mice was transduced with retrovirus containing estradiol-inducible HoxB8 then maintained in media containing 10% GM-CSF conditioned supernatants, 10% FBS and 10 μM Beta-Estradiol as previously described (Wang et al., 2006). To generate BMDMs cells were washed 3 x in PBS to remove estradiol then plated in 20% L929 condition supernatants and 10% FBS. Eight to 10 days later cells were plated for experiments as described in the figure legends.

CRISPR screen and analysis

The mouse BRIE knockout CRISPR pooled library was a gift of David Root and John Doench (Addgene #73633) [32]. Using the BRIE library, 4 sgRNAs targeting every coding gene in mice in addition to 1000 non-targeting controls (78,637 sgRNAs total) were packaged into lentivirus using HEK293T cells and transduced in L3 cells at a low multiplicity of infection (MOI <0.3) and selected with puromycin two days after transduction. Sequencing of the input library showed high coverage and distribution of the library (Figure 1.1—figure supplement 1). We next treated the library with IFNγ (10 ng/ml) and 24 hr later the cells were fixed and fluorescence activated cell sorting (FACS) was used to isolate the MHCIIhigh and MHCIIlow bins. Bin size was guided by the observed phenotypes of positive control sgRNAs, such as RFX5, which were tested individually and to ensure sufficient coverage (> 25 x unselected library) in the sorted populations. Genomic DNA was isolated from sorted populations from two biological replicate experiments using Qiagen DNeasy kits. Amplification of sgRNAs by PCR was performed as previously described using Illumina compatible primers from IDT [32], and amplicons were sequenced on an Illumina NextSeq500.

Sequence reads were first trimmed to remove any adapter sequence and to adjust for p5 primer stagger. We used bowtie two via MAGeCK to map reads to the sgRNA library index without allowing for any mismatch. Subsequent sgRNA counts were median normalized to control sgRNAs in MAGeCK to account for variable sequencing depth. Control sgRNAs were defined as non-targeting controls as well as genes not-transcribed in our macrophage cell line as determined empirically by RNA-seq (Figure 5—source data 1). To test for sgRNA and gene enrichment, we used the 'test' command in MAGeCK to compare the distribution of sgRNAs in the MHCIIhigh and MHCIIlow bins. Notably, we included the input libraries in the count

analysis in order to use the distribution of sgRNAs in the unselected library for the variance estimation in MAGeCK. sgRNA cloning sgOpti was a gift from Eric Lander & David Sabatini (Addgene plasmid #85681) [45]. Individual sgRNAs were cloned as previously described [70]. Briefly, annealed oligos containing the sgRNA targeting sequence were phosphorylated and cloned into a dephosphorylated and BsmBI (New England Biolabs) digested SgOpti (Addgene#85681) which contains a modified sgRNA scaffold for improved sgRNA-Cas9 complexing. A detailed cloning protocol is available in supplementary methods. To facilitate rapid and efficient generation of sgRNA plasmids with different selectable markers, we further modified the SgOpti vector such that the mammalian selectable marker was linked with a distinct bacterial selection. Subsequent generation of SgOpti-Blasticidin-Zeocin (BZ), SgOpti-Hygromycin-Kanamycin (HK), and SgOpti-G418-Hygromycin (GH) allowed for pooled cloning in which a given sgRNA was ligated into a mixture of BsmBI-digested plasmids. Successful transformants for each of the plasmids were selected by plating on ampicillin (SgOpti), zeocin (BZ), kanamycin (HK), or hygromycin (GH) in parallel. In effect, this reduced the cloning burden 4 x and provided flexibility with selectable markers to generate near-complete editing in polyclonal cells and/or make double knockouts.

Flow cytometry

Cells were harvested at the indicated times post-IFNγ stimulation by scraping to ensure intact surface proteins. Cells were pelleted and washed with PBS before staining for MHCII. MHCII expression was analyzed on the BD LSRII cytometer or a BioRad S3E cell sorter. All flow cytometry analysis was done in FlowJo V9 or V10 (TreeStar).

Chemical inhibitors and agonists

CHIR99021 (Sigma) was resuspended in DMSO at 10 mM stock concentration. DMSO was added at the same concentration to the inhibitors as a control. Cells were maintained in 5 % CO2. Cells were stimulated with 6.25 ng/ml of IFNγ (Biolegend) for the indicated times in each figure legend before analysis. Torin2 (Sigma) was resuspended in DMSO and diluted to the concentrations indicated in each experiment. PAM3SK4 (Invivogen) NG-MDP (Invivogen), IFNβ (BEI Resources), and TNF (Peprotech) were resuspending in sterile PBS and added to cells at the indicated concentrations in the figure legends.

NK cell isolation, activation, and co-culture

Untouched naïve NK cells were isolated from spleen homogenates of C57BL/6 J mice using the MojoSort Mouse NK cell isolation kit (Biolegend). NK cells were grown for 7–10 days in RPMI with 10 % FBS, non-essential amino acids, 50 µM b-mercaptoethanol and 50 nM murine IL-15 (Biolegend). NK cells were then activated for 18 hr by adding 2 nM IL-12 and 20 nM IL-18 to cells. NK cells viability, differentiation, and activation was confirmed prior to experiments by flow cytometry using anti-CD335 and anti- IFNγ antibodies in combination with a viability live/dead stain (biolegend).

Isolation of knockout cells

Cells transduced with either MED16 or GSK3β sgRNAs were stimulated with IFNγ then stained for MHCII 24 hr later. Cells expressing low MHCII were then sorted using a BioRad S3e cell sorter and plated for expansion. Gene knockouts were confirmed by amplifying the genomic regions encoding either MED16 or GSK3β from each cell population in addition to NTC cells using PCR. PCR products were purified by PCR-cleanup Kit (Qiagen) and sent for Sanger

Sequencing (Genewiz). The resultant ABI files were used for TIDE analysis to assess the frequency and size of indels in each population compared to control cells.

RNA isolation

Macrophages were homogenized in 500 µL of TRIzol reagent (Life Technologies) and incubated for 5 minutes at room temperature. A total of 100 µL of chloroform was added to the homogenate, vortexed, and centrifuged at 12,000 x g for 20 min at 4 C to separate nucleic acids. The clear, RNA containing layer was removed and combined with 500 µL of ethanol. This mixture was placed into a collection tube and protocols provided by the Zymo Research Direct-zol RNA extraction kit were followed. Quantity and purity of the RNA was checked using a NanoDrop and diluted to 5 ng/µL in nuclease-free water.

RNA-sequencing analysis

To generate RNA for sequencing, macrophages were seeded in 6-well dishes at a density of 1 million cells/well. Cells were stimulated for 18 hr with IFNγ (Peprotech) at a final concentration of 6.25 ng/mL, after which RNA was isolated as described above. RNA quality was assessed by qRT-PCR as described above and by TapeStation (Aligent); the median RIN value was 9.5 with a ranger of 8.6–9.9. A standard library preparation protocol was followed to prepare sequencing libraries on poly-A tailed mRNA using the NEBNext Ultra RNA Library Prep Kit for Illumina. In total, 18 libraries were prepared for dual index paired-end sequencing on a HiSeq 2500 using a high-output kit (Illumina) at an average sequencing depth of 38.6e6 reads per library with >93 % of bases exceeding a quality score of 30. FastQC (v0.11.5) was used to assess the quality of raw data. Cutadapt (v2.9) was used to remove TruSeq adapter sequences with the parameters --cores = 15 m 1 a AGATCGGAAGAGCACACGTCTGAACTCCAGTCA -A AGATCGGAAGAGCGTCGTGTAGGGAAAGAGTGT. A transcriptome was prepared with

the rsem (v1.3.0) command rsem-prepare-reference using bowtie2 (v2.3.5.1) and the gtf and primary *Mus musculus* genome assembly from ENSEMBL release 99. Trimmed sequencing reads were aligned and counts quantified using rsem-calculate-expression with standard bowtie2 parameters; fragment size and alignment quality for each sequencing library was assessed by estimating the read start position distribution (RSPD) via --estimate-rspd. aBriefly, counts were imported using tximport (v1.16.0) and differential expression was performed with non-targeting control ('NTC') and unstimulated ('Condition A') as reference levels for contrasts. For visualization via PCA, a variance stabilizing transformation was performed in DESeq2. Pathway enrichment utilized R packages gage and fgsea or Ingenuity Pathway Analysis (Qiagen). Gene-set enrichment analysis (GSEA) was performed utilized gene rank lists as calculated from defined comparisons in DeSeq2 and was inclusive of gene sets comprised of 10–500 genes that were compiled and made available by the Bader lab [71]. Pathway visualization and network construction was performed in CytoScape 3.8 using the apps STRING and EnrichmentMap. Pathway significance thresholds were set at an FDR of 0.1 unless specified otherwise.

Quantitative real-time PCR

PCR amplification of the RNA was completed using the One-step Syber Green RT-PCR Kit (Qiagen). 25 ng of total RNA was added to a master mix reaction of the provided RT Mix, Syber green, gene specific primers (5 uM of forward and reverse primer), and nuclease-free water. For each biological replicate (triplicate), reactions were conducted in technical duplicates in 96-well plates. PCR product was monitored using the QuantStudio3 (ThermoFisher). The number of cycles needed to reach the threshold of detection (Ct) was determined for all reactions. Relative gene expression was determined using the 2^-ddCT method. The mean CT of each experimental sample in triplicate was determined. The average mean of glyceraldehyde 3-phosphate

dehydrogenase (GAPDH) was subtracted from the experimental sample mean CT for each gene of interest (ΔCT). The average ΔCT of the untreated control group was used as a calibrator and subtracted from the ΔCT of each experimental sample (ΔΔCT). $2^{-\Delta\Delta CT}$ shows the fold change in gene expression of the gene of interest normalized to GAPDH and relative to untreated control (calibrator).

Immunoblot analysis

At the indicated times following stimulation, cells were washed with PBS once and lysed in on ice using the following buffer: 1 % Triton X-100, 150 mM NaCl, 5 mM KCl, 2 mM MgCl2, 1 mM EDTA, 0.1 % SDS, 0.5 % DOC, 25 mM Tris-HCl, pH 7.4, with protease and phosphatase inhibitor (Sigma #11873580001 and Sigma P5726). Lysates were further homogenized using a 25 g needle and cleared by centrifugation before quantification (Pierce BCA Protein Assay Kit, 23225). Parallel blots were run with the same samples, 15 µg per well. The following antibodies were used according to the manufacturer's instructions:

- Anti-GSK3a - #4,337 Cell Signaling Technology
- Anti-pGSK3a - #9,316 Cell Signaling Technology
- Anti-pStat1 0 #8,826 Cell Signaling Technology
- Anti-mouse β-Actin Antibody, Biolegend Cat# 66,480
- Goat anti-Rabbit IgG (H + L) Secondary Antibody, HRP, Invitrogen 31,460
- Goat anti-Mouse IgG (H + L) Secondary Antibody, HRP, Invitrogen 31,430

T cell activation assays

CD4+ T cells were harvested from the lymph nodes and spleens of naive NR1 mice and enriched with a mouse naïve CD4-negative isolation kit (BioLegend) following the manufacturer's

protocol. CD4+ T cells were cultured in media consisting of RPMI 1640 (Invitrogen), 10 % FCS, l-glutamine, HEPES, 50 μM 2-ME, 50 U/ml penicillin, and 50 mg/ml streptomycin. NR1 cells were activated by coculture with mitomycin-treated splenocytes pulsed with 5 μM Cta1133–152 peptide at a stimulator/T cell ratio of 4:1. Th1 polarization was achieved by supplying cultures with 10 ng/ml IL-12 (PeproTech, Rocky Hill, NJ) and 10 μg/ml anti–IL-4 (Biolegend) One week after initial activation resting NR1 cells were co-incubated with untreated or IFNγ-treated macrophages of different genotypes, that were or were not pulsed with Cta1 peptide. Six hours following co-incubation NR1 cells were harvested and stained for intracellular IFNγ (BioLegend) using an intracellular cytokine staining kit (BioLegend) as done previously. Analyzed T cells were identified as live, CD90.1+ CD4+ cells.

Statistical analysis, replicates, grouping, and figures

Statistical analysis was done using Prism Version 7 (GraphPad) as indicated in the figure legends. Data are presented, unless otherwise indicated, as the mean ±the standard deviation. Throughout the manuscript, no explicit power analysis was used, but group size was based on previous studies using similar approaches. Throughout the manuscript biological replicate refers to independent wells or experiments processed at similar times. For RT-PCR experiments technical replicates were used and are defined as repeat measures from the same well. Throughout the manuscript groups were assigned based on genotypes and blinding was not used throughout. Independent personnel completed several key figures to ensure robustness. Figures were created in Prism V7 or were created with BioRender.com.

REFERENCES

1. Wijdeven, R. H. *et al.* Chemical and genetic control of IFN γ-induced MHCII expression . *EMBO Rep* **19**, (2018).

2. Iwasaki, A. & Medzhitov, R. Control of adaptive immunity by the innate immune system. *Nat Immunol* **16**, 343–353 (2015).

3. Tubo, N. J. & Jenkins, M. K. CD4+ T cells: Guardians of the phagosome. *Clin Microbiol Rev* **27**, 200–213 (2014).

4. DeSandro, A., Nagarajan, U. M. & Boss, J. M. The bare lymphocyte syndrome: Molecular clues to the transcriptional regulation of major histocompatibility complex class II genes. *Am J Hum Genet* **65**, 279–286 (1999).

5. Reith, W., LeibundGut-Landmann, S. & Waldburger, J. M. Regulation of MHC class II gene expression by the class II transactivator. *Nat Rev Immunol* **5**, 793–806 (2005).

6. Koyama, M. *et al.* Recipient nonhematopoietic antigen-presenting cells are sufficient to induce lethal acute graft-versus-host disease. *Nat Med* **18**, 135–142 (2012).

7. Abrahimi, P. *et al.* Blocking MHC class II on human endothelium mitigates acute rejection. *JCI Insight* **1**, (2016).

8. Thelemann, C. *et al.* Absence of nonhematopoietic MHC class II expression protects mice from experimental autoimmune myocarditis. *Eur J Immunol* **46**, 656–664 (2016).

9. Steimle, V. *et al.* A novel DNA-binding regulatory factor is mutated in primary MHC class II deficiency (bare lymphocyte syndrome). *Genes Dev* **9**, 1021–1032 (1995).

10. Jakubzick, C. v., Randolph, G. J. & Henson, P. M. Monocyte differentiation and antigen-presenting functions. *Nat Rev Immunol* **17**, 349–362 (2017).

11. Unanue, E. R., Turk, V. & Neefjes, J. Variations in MHC Class II Antigen Processing and Presentation in Health and Disease. *Annu Rev Immunol* **34**, 265–297 (2016).

12. Collins, T. *et al.* Immune interferon activates multiple class II major histocompatibility complex genes and the associated invariant chain gene in human endothelial cells and dermal fibroblasts. *Proc Natl Acad Sci U S A* **81**, 4917–4921 (1984).

13. Neefjes, J., Jongsma, M. L. M., Paul, P. & Bakke, O. Towards a systems understanding of MHC class i and MHC class II antigen presentation. *Nat Rev Immunol* **11**, 823–836 (2011).

14. Buxadé, M. *et al.* Macrophage-specific MHCII expression is regulated by a remote Ciita enhancer controlled by NFAT5. *Journal of Experimental Medicine* **215**, 2901–2918 (2018).

15. Ivashkiv, L. B. IFNγ: signalling, epigenetics and roles in immunity, metabolism, disease and cancer immunotherapy. *Nat Rev Immunol* **18**, 545–558 (2018).

16. Herrero, C., Marqués, L., Lloberas, J. & Celada, A. IFN-γ-dependent transcription of MHC class II IA is impaired in macrophages from aged mice. *Journal of Clinical Investigation* **107**, 485–493 (2001).

17. Ting, J. P. Y. & Trowsdale, J. Genetic control of MHC class II expression. *Cell* **109**, (2002).

18. Bousoik, E. & Montazeri Aliabadi, H. "Do We Know Jack" About JAK? A Closer Look at JAK/STAT Signaling Pathway. *Front Oncol* **8**, (2018).

19. Hu, X. & Ivashkiv, L. B. Cross-regulation of Signaling Pathways by Interferon-γ: Implications for Immune Responses and Autoimmune Diseases. *Immunity* **31**, 539–550 (2009).

20. Schroder, K., Hertzog, P. J., Ravasi, T. & Hume, D. A. Interferon-γ: an overview of signals, mechanisms and functions. *J Leukoc Biol* **75**, 163–189 (2004).

21. Beresford, G. W. & Boss, J. M. CIITA coordinates multiple histone acetylation modifications at the HLA-DRA promoter. *Nat Immunol* **2**, 652–657 (2001).

22. Paul, P. *et al.* A genome-wide multidimensional RNAi screen reveals pathways controlling MHC class II antigen presentation. *Cell* **145**, 268–283 (2011).

23. Oh, J. *et al.* MARCH1-mediated MHCII ubiquitination promotes dendritic cell selection of natural regulatory T cells. *Journal of Experimental Medicine* **210**, 1069–1077 (2013).

24. Alix, E. *et al.* The Tumour Suppressor TMEM127 Is a Nedd4-Family E3 Ligase Adaptor Required by Salmonella SteD to Ubiquitinate and Degrade MHC Class II Molecules. *Cell Host Microbe* **28**, 54-68.e7 (2020).

25. Ankley, L., Thomas, S. & Olive, A. J. Fighting persistence: How chronic infections with mycobacterium tuberculosis evade T cell-mediated clearance and new strategies to defeat them. *Infect Immun* **88**, (2020).

26. Grau, V., Herbst, B. & Steiniger, B. Dynamics of monocytes/macrophages and T lymphocytes in acutely rejecting rat renal allografts. *Cell Tissue Res* **291**, 117–126 (1997).

27. Underhill, D. M., Bassetti, M., Rudensky, A. & Aderem, A. Dynamic interactions of macrophages with T cells during antigen presentation. *Journal of Experimental Medicine* **190**, 1909–1914 (1999).

28. Pai, R. K., Convery, M., Hamilton, T. A., Boom, W. H. & Harding, C. v. Inhibition of IFN-γ-Induced Class II Transactivator Expression by a 19-kDa Lipoprotein from Mycobacterium tuberculosis : A Potential Mechanism for Immune Evasion . *The Journal of Immunology* **171**, 175–184 (2003).

29. Pennini, M. E., Pai, R. K., Schultz, D. C., Boom, W. H. & Harding, C. v. Mycobacterium tuberculosis 19-kDa Lipoprotein Inhibits IFN-γ-Induced Chromatin Remodeling of MHC2TA by TLR2 and MAPK Signaling . *The Journal of Immunology* **176**, 4323–4330 (2006).

30. Zhong, G., Fan, T. & Liu, L. Chlamydia inhibits interferon γ-inducible major histocompatibility complex class II expression by degradation of upstream stimulatory factor 1. *Journal of Experimental Medicine* **189**, 1931–1937 (1999).

31. Brinkman, E. K., Chen, T., Amendola, M. & van Steensel, B. Easy quantitative assessment of genome editing by sequence trace decomposition. *Nucleic Acids Res* **42**, (2014).

32. Doench, J. G. *et al.* Optimized sgRNA design to maximize activity and minimize off-target effects of CRISPR-Cas9. *Nat Biotechnol* **34**, 184–191 (2016).

33. Hart, T., Brown, K. R., Sircoulomb, F., Rottapel, R. & Moffat, J. Measuring error rates in genomic perturbation screens: gold standards for human functional genomics. *Mol Syst Biol* **10**, 733 (2014).

34. Li, W. *et al.* MAGeCK enables robust identification of essential genes from genome-scale CRISPR/Cas9 knockout screens. *Genome Biol* **15**, 554 (2014).

35. Kanehisa, M. & Goto, S. KEGG: Kyoto Encyclopedia of Genes and Genomes. *Nucleic Acids Res* **28**, 27–30 (2000).

36. Kanehisa, M., Sato, Y., Furumichi, M., Morishima, K. & Tanabe, M. New approach for understanding genome variations in KEGG. *Nucleic Acids Res* **47**, D590–D595 (2019).

37. Kanehisa, M. Toward understanding the origin and evolution of cellular organisms. *Protein Science* **28**, 1947–1951 (2019).

38. Poss, Z. C., Ebmeier, C. C. & Taatjes, D. J. The Mediator complex and transcription regulation. *Crit Rev Biochem Mol Biol* **48**, 575–608 (2013).

39. Wu, D. & Pan, W. GSK3: a multifaceted kinase in Wnt signaling. *Trends Biochem Sci* **35**, 161–168 (2010).

40. Conaway, R. C. & Conaway, J. W. Origins and activity of the Mediator complex. *Semin Cell Dev Biol* **22**, 729–734 (2011).

41. Beurel, E., Michalek, S. M. & Jope, R. S. Innate and adaptive immune responses regulated by glycogen synthase kinase-3 (GSK3). *Trends Immunol* **31**, 24–31 (2010).

42. Thomson, A. W., Turnquist, H. R. & Raimondi, G. Immunoregulatory functions of mTOR inhibition. *Nat Rev Immunol* **9**, 324–337 (2009).

43. Xu, Y., Harton, J. A. & Smith, B. D. CIITA mediates interferon-γ repression of collagen transcription through phosphorylation-dependent interactions with co-repressor molecules. *Journal of Biological Chemistry* **283**, 1243–1256 (2008).

44. Ring, D. B. *et al.* Selective glycogen synthase kinase 3 inhibitors potentiate insulin activation of glucose transport and utilization in vitro and in vivo. *Diabetes* **52**, 588–595 (2003).

45. Fulco, C. P. *et al.* Systematic mapping of functional enhancer-promoter connections with CRISPR interference. *Science (1979)* **354**, 769–773 (2016).

46. Wang, G. G. *et al.* Quantitative production of macrophages or neutrophils ex vivo using conditional Hoxb8. *Nat Methods* **3**, 287–293 (2006).

47. Su, X. *et al.* Interferon-γ regulates cellular metabolism and mRNA translation to potentiate macrophage activation. *Nat Immunol* **16**, 838–849 (2015).

48. Subramanian, A. *et al.* Gene set enrichment analysis: A knowledge-based approach for interpreting genome-wide expression profiles. *Proc Natl Acad Sci U S A* **102**, 15545–15550 (2005).

49. Jayarapu, K., Kerr, M. S., Katschke, A. & Johnson, R. M. Chlamydia muridarum-specific CD4 T-cell clones recognize infected reproductive tract epithelial cells in an interferon-dependent fashion. *Infect Immun* **77**, 4469–4479 (2009).

50. Kurche, J. S., Haluszczak, C., McWilliams, J. A., Sanchez, P. J. & Kedl, R. M. Type I IFN-Dependent T Cell Activation Is Mediated by IFN-Dependent Dendritic Cell OX40 Ligand Expression and Is Independent of T Cell IFNR Expression. *The Journal of Immunology* **188**, 585–593 (2012).

51. Lu, H. T. *et al.* Interferon (IFN) β acts downstream of IFN-γ-induced class II transactivator messenger RNA accumulation to block major histocompatibility complex class II gene expression and requires the 48-kD DNA-binding protein, ISGF3-γ. *Journal of Experimental Medicine* **182**, 1517–1525 (1995).

52. Simmons, D. P. *et al.* Type I IFN Drives a Distinctive Dendritic Cell Maturation Phenotype That Allows Continued Class II MHC Synthesis and Antigen Processing. *The Journal of Immunology* **188**, 3116–3126 (2012).

53. Roan, N. R., Gierahn, T. M., Higgins, D. E. & Starnbach, M. N. Monitoring the T cell response to genital tract infection. *Proc Natl Acad Sci U S A* **103**, 12069–12074 (2006).

54. Siska, P. J. & Rathmell, J. C. Metabolic Signaling Drives IFN-γ. *Cell Metab* **24**, 651–652 (2016).

55. Sekine, H. *et al.* The Mediator Subunit MED16 Transduces NRF2-Activating Signals into Antioxidant Gene Expression. *Mol Cell Biol* **36**, 407–420 (2016).

56. Bancerek, J. *et al.* CDK8 Kinase Phosphorylates Transcription Factor STAT1 to Selectively Regulate the Interferon Response. *Immunity* **38**, 250–262 (2013).

57. Beurel, E. & Jope, R. S. Differential regulation of STAT family members by glycogen synthase kinase-3. *Journal of Biological Chemistry* **283**, 21934–21944 (2008).

58. Huang, W. C. *et al.* Glycogen synthase kinase-3 negatively regulates anti-inflammatory interleukin-10 for lipopolysaccharide-induced iNOS/NO biosynthesis and RANTES production in microglial cells. *Immunology* **128**, (2009).

59. Garvin, A. J. *et al.* GSK3-SCFFBXW7 mediated phosphorylation and ubiquitination of IRF1 are required for its transcription-dependent turnover. *Nucleic Acids Res* **47**, 4476–4494 (2019).

60. Turnquist, H. R. *et al.* mTOR and GSK-3 shape the CD4+ T-cell stimulatory and differentiation capacity of myeloid DCs after exposure to LPS. *Blood* **115**, 4758–4769 (2010).

61. Smith, J. L., Jeng, S., McWeeney, S. K. & Hirsch, A. J. A MicroRNA Screen Identifies the Wnt Signaling Pathway as a Regulator of the Interferon Response during Flavivirus Infection. *J Virol* **91**, (2017).

62. Baizabal-Aguirre, V. M. Editorial: Cross-Talk Mechanisms of Wnt/Beta-Catenin Signaling Components with TLR-Activated Signaling Molecules in the Inflammatory Response. *Front Immunol* **8**, 1396 (2017).

63. Gibbs, K. D. *et al.* The Salmonella Secreted Effector SarA/SteE Mimics Cytokine Receptor Signaling to Activate STAT3. *Cell Host Microbe* **27**, 129-139.e4 (2020).

64. Panagi, I. *et al.* Salmonella Effector SteE Converts the Mammalian Serine/Threonine Kinase GSK3 into a Tyrosine Kinase to Direct Macrophage Polarization. *Cell Host Microbe* **27**, 41-53.e6 (2020).

65. Ankley, L., Thomas, S. & Olive, A. Fighting persistence; how chronic infections with Mycobacterium tuberculosis evade T cell-mediated clearance and new strategies to defeat them. *Infect Immun* (2020).

66. Garcia-Diaz, A. *et al.* Interferon Receptor Signaling Pathways Regulating PD-L1 and PD-L2 Expression. *Cell Rep* **19**, 1189–1201 (2017).

67. Mandai, M. *et al.* Dual faces of ifnγ in cancer progression: A role of pd-l1 induction in the determination of proand antitumor immunity. *Clinical Cancer Research* **22**, 2329–2334 (2016).

68. Gu, W., Chen, J., Yang, L. & Zhao, K. N. TNF-α promotes IFN-α-induced CD40 expression and antigen process in Myb-transformed hematological cells. *The Scientific World Journal* **2012**, (2012).

69. Zhou, F. Molecular mechanisms of IFN-γ to up-regulate MHC class i antigen processing and presentation. *Int Rev Immunol* **28**, 239–260 (2009).

70. Shalem, O. *et al.* Genome-scale CRISPR-Cas9 knockout screening in human cells. *Science (1979)* **343**, 84–87 (2014).

71. Reimand, J. *et al.* Pathway enrichment analysis and visualization of omics data using g:Profiler, GSEA, Cytoscape and EnrichmentMap. *Nat Protoc* **14**, 482–517 (2019).

CHAPTER 3: GSK3α/β restrains IFNγ-inducible co-stimulatory molecule expression in AMs limiting their ability to activate CD4+ T-cells

DECLARATIONS

Authors

Laurisa Ankley, Kayla Connor, Taryn Vielma, Mahima Thapa, Andrew Olive

Contributions

LA and AO designed the studies. KC analyzed and curated figures for all RNAseq data. AO characterized primary alveolar macrophages. LA investigated the role of GSK3 in the IFNγ responses of both iBMDMs and FLAMs. TV completed flow cytometry to determine the combined role of IFNβ and TNF in GSK3-dependent IFNγ responses. MT completed the T-cell co-culture experiments. LA and AO wrote the chapter and all other authors reviewed it.

ABSTRACT

Macrophages play a crucial role in eliminating respiratory pathogens. Both the pulmonary resident macrophage population, alveolar macrophages (AMs), and recruited macrophages contribute to detecting, responding, and resolving infections in the lungs. Despite their distinct functions, it remains unclear how these macrophage subsets regulate their host responses, including how they regulate activation by the key cytokine IFNγ. To better understand this regulation, we used a new *ex vivo* model of AMs and immortalized bone marrow-derived macrophages (iBMDMs) from mice to define shared and unique changes to the transcriptional landscape following IFNγ activation. Our findings reveal that IFNγ robustly activates both macrophage types; however, the profile of activated IFNγ-stimulated genes varies significantly. Notably, FLAMs show limited activation of costimulatory markers essential for T-cell activation upon IFNγ stimulation alone. To understand the cell specific differences, we examined how the inhibition of the key regulatory kinases GSK3α/β alter the IFNγ-response. GSK3α/β controlled distinct IFNγ-responses and in AM-like cells we found GSK3α/β restrains the induction of type I IFN and TNF that prevents robust expression of co-stimulatory molecules and limits CD4+ T cell activation. Together, these data suggest that the capacity of AMs to respond to IFNγ is restricted in a GSK3α/β dependent manner and that IFNγ responses differ across distinct macrophage populations.

INTRODUCTION

Macrophages are important innate immune cells that sense the environment, initiate inflammation, and help activate the adaptive immune response. Throughout the body there are distinct macrophage subsets that are broadly broken into two categories, circulating monocytes/macrophages and tissue resident macrophages. Tissue resident macrophages are self-

renewing, derived from the fetal liver, and are maintained by local cues where they contribute to tissue homeostasis [1–3]. In contrast, recruited macrophages are derived from myeloid progenitors circulating throughout the bloodstream and lymphatics until they are actively recruited to sites of infection where they mature into macrophages and help contain infections [4,5].

In the lungs both resident and recruited macrophages play important roles in maintaining pulmonary function and protecting against respiratory pathogens. Resident lung macrophages, known as alveolar macrophages (AMs), reside in the airspace to recycle surfactants produced by the lungs [6]. AMs are the first immune cells to detect pathogens in the airspace and are tasked with appropriately responding while maintaining pulmonary function [7]. During respiratory infections monocyte-derived inflammatory macrophages are recruited to the lung tissues to support antimicrobial responses and resolve infections [8,9]. Dysregulation of these two important macrophage populations can result in pulmonary dysfunction, susceptibility to infection and autoinflammatory disease [5,6,10].

While both resident and recruited macrophages contribute to immune responses in the lungs, their regulation and functional mechanisms are distinct. One key difference is the baseline metabolism of these cells. Given their role in recycling lipids, AMs are heavily dependent on fatty acid oxidation and oxidative phosphorylation [11–13], whereas recruited macrophages are highly glycolytic [14]. These metabolic differences have functional implications as AMs are generally thought to be hypo-inflammatory and skewed towards alternative activation. In contrast, the high glycolysis rates in recruited macrophages drives robust activation of inflammatory cytokines and antimicrobial poisons such as nitric oxide [15]. In addition, several studies suggest differences in the ability of AMs or recruited macrophages to robustly activate protective T-cell responses [16–18]. While recruited inflammatory macrophages robustly drive T-

helper 1 responses to activate the production of the protective cytokine interferon-gamma (IFNγ), AMs have been shown to drive immunosuppressive regulatory T-cell activation [16–18]. Several questions remain regarding the functional differences between AMs and recruited macrophages including how they respond to cues like IFNγ during an active infection. Following IFNγ binding to the IFNγR, Jak/Stat pathways become activated and drive transcriptional induction of hundreds of genes that are mediated by interferon regulatory factors (Irfs) [19]. IFNγ responses can be further fine-tuned through the activity of key regulators including the kinases glycogen synthase kinase 3α and 3β (GSK3α/β) and the mammalian target of rapamycin (Mtor) [20–23]. Whether this regulation is conserved in both AMs and recruited macrophages remains to be understood, limiting our ability to effectively leverage IFNγ pathways therapeutically in the lung environment.

The dichotomy between AMs and recruited macrophages in the lungs is critical during infections with *Mycobacterium tuberculosis*, the leading cause of infectious disease mediated death worldwide. Several studies have shown that *M. tuberculosis* resides almost exclusively in AMs over the first two weeks of infection, yet AMs are unable to mount an effective cell-autonomous response to eradicate the infection [7]. This results in *M. tuberculosis* using AMs as an intracellular niche allowing uncontrolled growth and delayed onset of adaptive immunity. Whether these AMs can control Mtb after the activation of Th1 responses remains unclear, but data suggests infected AMs do not robustly respond to IFNγ [24]. As infection progresses, *M. tuberculosis* no longer resides in AMs but rather is found within recruited macrophages that are better equipped to restrict bacterial replication, modulate T-cell effector functions, and drive protective immune responses [25].

Developing new host-directed therapies to combat *M. tuberculosis* and other respiratory infections will require a better understanding of differences between resident AMs and recruited macrophages. Dissecting the mechanisms controlling the function of distinct macrophage subsets requires *ex vivo* models that faithfully recapitulate *in vivo* macrophage biology. Bone-marrow derived macrophages (BMDMs) are differentiated from myeloid progenitors and are a widely used model for recruited inflammatory macrophages [26]. Following activation with IFNγ, BMDMs become highly glycolytic driving inflammatory cytokine production and directly modulating T-cell responses similar to recruited macrophages [20,27,28]. Until recently, *ex vivo* models for AMs remained challenging. AMs are present in very low numbers in the lungs and once isolated and grown in culture they rapidly lose surface markers and functions associated with AMs [29,30]. Thus, this technical hurdle has limited our ability to dissect regulatory networks that maintain AM functionality. Recently several groups, including our own, have described approaches to culture AM-like cells *ex vivo* while maintaining AM functions [29,31–33]. While the details of these approaches differ, they all leverage lung-specific cytokine cues from GM-CSF and TGFβ that are required to maintain AM populations in the lung environment. We developed an *ex vivo* AM model known as fetal liver-derived alveolar-like macrophages (FLAMs) that takes advantage of the fetal liver cells that are the progenitors of AMs during development. Our previous work shows that FLAMs maintain high expression of the AM surface markers SiglecF and CD14 and the key transcription factor Pparg [29]. The advantage of FLAMs is their ease of isolation, culture, and expansion along with their genetic tractability that will enable a new understanding of mechanisms underlying AM functions.

Here, we examined the transcriptional profile of resting and IFNγ-activated FLAMs and immortalized BMDMs (iBMDMs) to better define functional differences between these key

macrophage subsets. Our results show that FLAMs are highly similar to primary AMs and while both FLAMs and iBMDMs respond to IFNγ, they induce unique transcriptional profiles. The regulation of these IFNγ-responses is also distinct, with GSK3α/β playing unique roles in FLAMs and iBMDMs. Modulating GSK3 activity in IFNγ-activated FLAMs results in the robust production of IFNβ1 that contributes induction of co-stimulatory molecules and increases the capacity of FLAMs and AMs to activate CD4+ T-cells. Our results suggest that AMs are restrained in their capacity to activate CD4+ T-cells and that the IFNγ-response in different macrophage subsets is uniquely regulated. These results have implications when considering host-directed therapies that target distinct macrophage populations.

RESULTS

FLAMs are phenotypically like AMs and distinct from BMDMs

We recently optimized FLAMs as an *ex vivo* approach to interrogate the function of AMs. While we found FLAMs faithfully recapitulate a subset of AM gene expression patterns, a global understanding of FLAM transcription and the similarities or differences from standard bone marrow-derived macrophages remained unclear. To address this gap in knowledge we conducted RNA sequencing analysis on resting FLAMs and iBMDMs. Differential expression analysis identified hundreds of genes that were differentially expressed in FLAMs or iBMDMs (Figure 2.1A). To globally identify pathways that were uniquely enriched in FLAMs we used gene set enrichment analysis (GSEA) using a ranked gene list generated from the differential expression analysis. Among the top hallmark pathways enriched in FLAMs, we identified fatty acid metabolism, TGFβ-signaling, cholesterol homeostasis and peroxisome pathways (Figure 2.1B). Given AMs are known to drive lipid metabolism that is dependent on the transcription factor Ppar-gamma, these data suggest the FLAM transcriptional profile is similar to primary AMs [34].

To directly test this hypothesis, we compared the FLAM and iBMDM RNAseq transcriptional profiles with previously published datasets examining primary AMs and peritoneal macrophages [35]. In line with our prediction, we found that FLAMs were more similar to AMs while iBMDMs were more similar to peritoneal macrophages suggesting that FLAMs are a robust ex vivo model for AMs (Figure 2.1C). We furthered this analysis by examining a subset of genes that were previously associated with recruited macrophages like peritoneal and iBMDMs or AMs [36]. We found iBMDMs and peritoneal macrophages expressed high levels of genes associated with recruited macrophages including CD14, ApoE and the key transcription factor MafB (Figure 2.1D). In contrast, FLAMs and AMs expressed high levels of transcription factors associated with resident lung macrophages such as Pparg, Car4, Maff, Fosl2, Bhlhe41, and runx2. In addition, AMs and FLAMs expressed high levels of resident macrophage associated surface markers including SiglecF, Siglec1, Marco, CD200, TLR2, MRC1, Itgal and Itgax which were lowly or not expressed in iBMDMs and peritoneal macrophages. In line with functional similarities between AMs and FLAMs we observed a high expression of genes associated with lipid and cholesterol metabolism genes [37]. Interestingly, when we examined genes that modulate T-cell activation, we observed high expression of the co-inhibitory markers PDL1 and PDL2 on FLAMs in line with a recent report (Figure 2.1D and 2.1E) [38]. In contrast, we observed very low expression of co-stimulatory molecules including CD40, CD80, and CD86 (Figure 2.1D and 1E).

To confirm our transcriptional results through an orthologous method we compared the expression of surface markers predicted to be different between FLAMs and iBMDMs by flow cytometry. We found the surface markers Siglec1, CD11a, MRC1, and TLR2 were all highly expressed on both resting FLAMs and primary AMs while resting iBMDMs expressed higher

levels of CD14 (Figure 2.1F and 2.1G). In agreement with our transcriptional profiling, we also found low expression of co-stimulatory markers on FLAMs and AMs compared to iBMDMs but high expression of the co-inhibitory marker PD-L1 (Figure 2.1H and 2.1I). Taken together these results show that FLAMs are transcriptionally distinct from iBMDMs, are a faithful surrogate for primary AMs, and these cells express low levels of T-cell activating co-stimulatory markers in resting conditions.

IFNγ induces distinct transcriptional programs in FLAMs and does not broadly induce T-cell co-stimulatory molecules.

The cytokine IFNγ is an important regulator of the host response in macrophages [39–41]. IFNγ stimulation of macrophages induces the expression of antimicrobial molecules and T-cell modulatory markers to help drive T-cell activation [42–44]. Given transcriptional differences between FLAMs and iBMDMs at baseline, we wondered if IFNγ responses between these cells would be similar or distinct. To examine this question, we conducted global RNA sequencing analysis on FLAMs and iBMDMs following IFNγ activation for 24 hours. We first used differential expression analysis comparing IFNγ-activated FLAMs or iBMDMs to their resting counterparts from above. For both iBMDMs and FLAMs IFNγ-stimulation resulted in the induction of hundreds of genes suggesting that IFNγ robustly activates both iBMDMs and FLAMs (Figure 2.2A and 2.2B).

To directly compare the IFNγ-mediated responses of iBMDMs and FLAMs we visualized the normalized reads for genes associated with a curated IFNγ-stimulated gene (ISG) set based on the Hallmark pathway for both resting and IFNγ-activated cells (Figure 2.2C). We found that many ISGs including antigen presentation machinery for MHCI and MHCII were robustly induced following activation of both FLAMs and iBMDMs (Figure 2.2D). However, we

observed that many ISGs were differentially induced in FLAMs and iBMDMs. For example, the co-stimulatory molecules CD40 and CD80 were robustly expressed in iBMDMs but expression remained low in FLAMs (Figure 2.2E). In contrast, we noted many cell-autonomous restriction factors including OAS2, Irgm1, and RNF213 were induced more than 10-fold higher in FLAMS than iBMDMs (Figure 2.2F). We additionally noted the transcription factor IRF7 was induced 2-4-fold in iBMDMs following IFNγ activation, whereas in FLAMs it was induced over 100-fold. In line with our observations in resting cells we found that the expression of the co-inhibitory markers PDL1 remained over 10-fold higher following IFNγ activation of FLAMs compared to iBMDMs.

To confirm our transcriptional results, we examined the change in expression of T-cell modulatory markers on FLAMs and primary AMs in the presence and absence of IFNγ by flow cytometry (Figure 2.2D). In line with our RNAseq analysis we found similar changes in MHCII, CD40 and CD80 following IFNγ-activation of both FLAMs and AMs. Together these data suggest that while both iBMDMs and FLAMs respond to IFNγ-activation, each cell type uniquely regulates ISGs that may differentially impact the functionality of these distinct macrophage subtypes.

GSK3α/β inhibition during IFNγ-activation of AMs and FLAMs results in the robust upregulation of co-stimulatory molecules and a shift in the transcriptional landscape.

While we found that FLAMs and AMs differentially regulate IFNγ responses compared to iBMDMs, what controls the underlying regulation of these responses remained unclear. We previously identified GSK3α and GSK3β as key regulators that fine-tune the IFNγ response in iBMDMs [20]. Our previous work showed that inhibiting GSK3α/β in iBMDMs blocks a subset of IFNγ responses including the expression of the MHCII transactivator Ciita and subsequent

MHCII expression. However, the core IFNγ signaling pathways including Stat1 and Irf1 remained intact following GSK3α/β inhibition. We hypothesized that GSK3α/β contribute to the differential IFNγ responses observed between iBMDMs and AMs. To test this hypothesis, we treated resting or IFNγ-activated iBMDMs or FLAMs with and without the GSK3α/β inhibitor CHIR99021 then analyzed the expression of MHCII by flow cytometry. In agreement with our previous results blockade of GSK3α/β in iBMDMs led to a significant reduction in MHCII on IFNγ-activated cells. In contrast, inhibiting GSK3α/β in IFNγ-activated FLAMs had no effect on MHCII expression. (Figure 2.3A) These data suggest distinct functions for GSK3α/β in controlling the IFNγ response between AMs and BMDMs.

GSK3α/β were previously shown to modulate co-stimulatory molecule expression [45,46]. Thus, we next tested if GSK3α/β inhibition alters the IFNγ-mediated induction of co-stimulatory molecules. Resting or IFNγ-activated iBMDMs and FLAMs were treated with DMSO or CHIR99021 and flow cytometry was used to quantify the surface expression of CD40, CD80 and CD86. We found that while IFNγ increased the expression of all markers on iBMDMs, blocking GSK3α/β had no effect on this induction (Figure 2.3B). In contrast, while IFNγ alone resulted in minimal changes to co-stimulatory molecule expression on FLAMs, GSK3α/β blockade in IFNγ-activated FLAMs resulted in a robust increase in all co-stimulatory molecules. These results for MHCII and co-stimulatory markers were confirmed in primary AMs suggesting that GSK3α/β plays distinct functions in regulating the response to IFNγ in AMs and BMDMs (Figure 2.3C).

Since GSK3α/β inhibition differentially impacted a subset of IFNγ-responses in BMDMs and FLAMs we next wanted to understand the global transcriptional changes that occur during GSK3α/β inhibition. RNA sequencing analysis was conducted on resting and IFNγ-activated

iBMDMs and FLAMs in the presence of CHIR99021 and we compared these results to our previous RNA sequencing analysis above in resting and IFNγ-activated iBMDMs and FLAMs. First, we confirmed the changes in co-stimulatory marker expression on FLAMs that were IFNγ-activated and blocked for GSK3α/β activity (Figure 2.3D). Principal component analysis of these 8 conditions revealed stark differences in the transcriptional landscape of iBMDMs and FLAMs (Figure 2.3E). All iBMDM samples clustered closely within the PCA plot with distinct but small shifts in the transcriptomes following IFNγ and/or GSK3α/β inhibition. Compared to resting iBMDMs, resting FLAMs were shifted significantly along PC1 in line with our results from above showing distinct transcriptional landscapes in these resting cells. While either IFNγ activation or GSK3α/β blockade alone shifted the transcriptional profile of FLAMs similarly to shifts observed iBMDMs, the combination of IFNγ and CHIR99021 resulted in a major shift of the transcriptional landscape of FLAMs along PC2. These results show that GSK3α/β are key regulators of the IFNγ response in FLAMs, and the combination of IFNγ activation and GSK3α/β blockade drives a synergistic transcriptional response not observed in any other FLAM or iBMDM condition.

To understand what pathways are altered during GSK3α/β inhibition in IFNγ-activated FLAMs we next used GSEA based on a differential expression ranked list between IFNγ-activated FLAMs in the presence and absence of GSK3α/β inhibition. We found both IFNα and TNF pathways, in addition to IFNγ, were all significantly enriched in GSK3α/β inhibited IFNγ activated FLAMs (Figure 2.3F). These results suggest that blockade of GSK3α/β during IFNγ activation of FLAMs drives inflammatory cytokine responses that may contribute to the expression of key IFNγ-inducible genes including co-stimulatory markers.

Type I IFN and TNF contribute to the upregulation of co-stimulatory molecules on IFNγ-activated FLAMs when GSK3α/β are inhibited

We were interested in understanding the mechanisms resulting in co-stimulatory marker induction on GSK3α/b inhibited IFNγ-activated FLAMs. Our GSEA analysis identified TNF and IFNβ, which were previously associated with modulating co-stimulatory marker expression [28,47]. We observed in iBMDMs that TNF was expressed following IFNγ activation regardless of GSK3α/β inhibition but in FLAMs TNF was highly expressed only following IFNγ-activation and GSK3α/β inhibition (Figure 2.4A). We found no expression of IFNβ in iBMDMs under any conditions and high expression of IFNβ only in IFNγ-activated GSK3α/β inhibited FLAMs. To confirm the results from the RNAseq analysis we examined the production of cytokines using a multiplex Luminex assay of the supernatants from resting and IFNγ-activated iBMDMs and FLAMs in the presence and absence of GSK3α/β inhibition. In agreement with the transcriptomic studies, we found increased TNF and type I IFN in FLAMs only following IFNγ-activation and GSK3α/β inhibition (Figure 2.4B). These data show that inhibition of GSK3α/β in IFNγ-activated FLAMs, results in increased expression of co-stimulatory modulating cytokines.

We next tested the sufficiency of either TNF or IFNβ to drive co-stimulatory marker expression on IFNγ-activated FLAMs. Resting or IFNγ-activated FLAMs were treated with recombinant TNF or IFNβ and the surface levels of CD40 were quantified by flow cytometry. While TNF alone did not increase CD40 expression on resting FLAMs, TNF addition to IFNγ-activated FLAMs resulted a synergistic increase in CD40 expression (Figure 2.4C). The addition of Type I IFN significantly increased CD40 expression in all conditions, and the combination

treatment of IFNγ and IFNβ did resulted in higher CD40 expression than IFNβ alone (Figure 4D). These data suggest that both IFNβ and TNF contribute to the increased CD40 expression during IFNγ-activation of FLAMs when GSK3α/β are inhibited.

We next wanted to test whether the production of either TNF or IFNβ was required for the enhanced co-stimulatory marker expression on GSK3α/β inhibited IFNγ-activated FLAMs. To block the function of IFNβ and TNF we isolated FLAMs from IFNAR-/- mice and used a TNFR neutralizing antibody which enabled the role of both cytokines to be tested simultaneously. Resting and IFNγ-activated wild type and IFNAR-/- FLAMs in the presence and absence of CHIR99021 and/or Anti-TNFR antibody were analyzed for CD40 expression by flow cytometry. We observed that blockade of TNF signaling minimally decreased CD40 expression in IFNγ-activated GSK3α/β inhibited FLAMs while blockade of IFNβ signaling dramatically reduced CD40 expression (Figure 2.4E). When we blocked TNF in IFNAR-/- FLAMs we observed a further reduction in CD40 surface expression although this was small. Taken together these data suggest that both TNF and IFNβ contribute to the increase in co-stimulatory marker expression seen in IFNγ-activated GSK3α/β inhibited FLAMs.

Inhibition of GSK3α/β following IFNγ activation of FLAMs and AMs drives the activation of CD4+ T-cells.

Co-stimulatory marker expression is necessary to activate the adaptive immune response during infection [48]. Our previous studies found that the increase in antigen presentation and co-stimulatory markers following IFNγ-activation of BMDMs is sufficient to activate CD4+ T-cells [20,28]. Given that AMs or FLAMs did not induce co-stimulatory marker expression with IFNγ alone but only in combination with GSK3α/β inhibition, we hypothesized IFNγ-activated AMs or FLAMs would not robustly activate CD4+ T-cells while IFNγ-activated GSK3α/β inhibited

cells would. To test this prediction, we used a previously optimized co-culture assay with macrophages and TCR-transgenic CD4+ T-cells that are specific for the *M. tuberculosis* peptide p25 [49–51]. Naïve p25 CD4+ T-cells were added to peptide-pulsed resting or IFNγ-activated iBMDMs or FLAMs that were or were not treated with CHIR99021 the previous day. As controls, p25 cells alone or p25 cells incubated with peptide pulsed splenocytes were included. Three days later co-culture supernatants were harvested and the levels of IFNγ produced by the CD4+ T cells was measured by ELISA. We found that p25 cells alone produced no IFNγ while co-culture with peptide pulsed splenocytes resulted in robust IFNγ production (Figure 2.4G). As expected, co-culture of p25 CD4+ T-cells with resting or CHIR99021 treated iBMDMs or FLAMs resulted in no IFNγ production by p25 cells. In agreement with our previous studies, co-culture of p25 cells with IFNγ-activated iBMDMs resulted in the production of IFNγ while blockade of GSK3α/β in IFNγ-activated iBMDMs prevented CD4+ T-cell activation [20]. In FLAMs we observed that IFNγ-activation alone was insufficient to activate p25 CD4+ T-cells during co-culture. In contrast, GSK3α/β inhibition in IFNγ-activated FLAMs resulted in the robust production of IFNγ by p25 cells. We repeated this experiment with primary AMs finding similar results (Figure 2.4H). The only condition that drove CD4+ T-cells activation was AMs that were IFNγ-activated with GSK3α/β inhibited. Taken together these data suggest differences in the capabilities of distinct macrophage populations to directly activate T-cell responses and highlight that AMs are restrained in their capacity to activate adaptive immune responses directly.

FIGURES

Figure 2.1. FLAMs are genetically like AMs. (A) Differentially expressed genes were identified using RNAseq between untreated FLAMs (blue) and iBMDMs (red). **(B)** Top 7 hallmark pathways that are enriched in untreated FLAMs **(C)** Normalized counts of core AM genes were compared between our iBMDMs, FLAMs and previous published data (Immgen PM and Immgen AM). Mann Whitney U Test used to compare medians. **(D)** Expression of genes previously associated with recruited macrophages were compared between FLAMs and iBMDMs. Each column represents one biological replicate from one experiment. **(E)** Normalized counts of costimulatory molecules between untreated FLAMs (blue) and iBMDMs (grey). Adjusted p-values were determined using DeSeq2. **(F-G)** Mean fluorescence intensity (MFI) of selected AM and BMDM surface markers between resting iBMDMs (grey), FLAMs (blue), and AMs (red). One-way ANOVA with a tukey test for multiple comparisons were used. **(H-I)** Flow cytometry comparing the expression of costimulatory surface markers on the surface of resting iBMDMs (grey), FLAMs (blue), and AMs (red). One-way ANOVA with a tukey test for multiple comparisons were used. *All data points represent one biological replicate from one experiment. ****p<0.0001, ***p<0.001, **p<0.01, *p<0. 05*

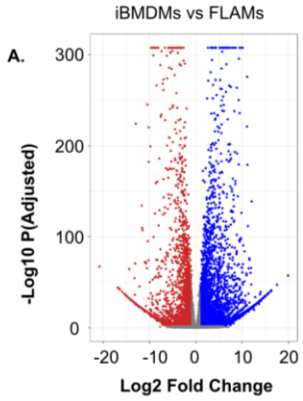

B.

HALLMARK PATHWAY	GENES ENRICHED	GROUP SIZE	NES
FATTY ACID METABOLISM	39	130	1.65
REACTIVE OXIGEN SPECIES PATHWAY	13	46	1.42
CHOLESTEROL HOMEOSTASIS	20	63	1.39
BILE ACID METABOLISM	17	73	1.17
ADIPOGENESIS	38	183	1.08
TGF BETA SIGNALING	13	52	1.01
PEROXISOME	23	85	0.94

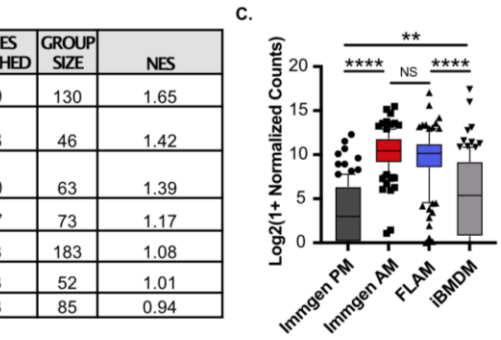

Figure 2.1 (cont'd)

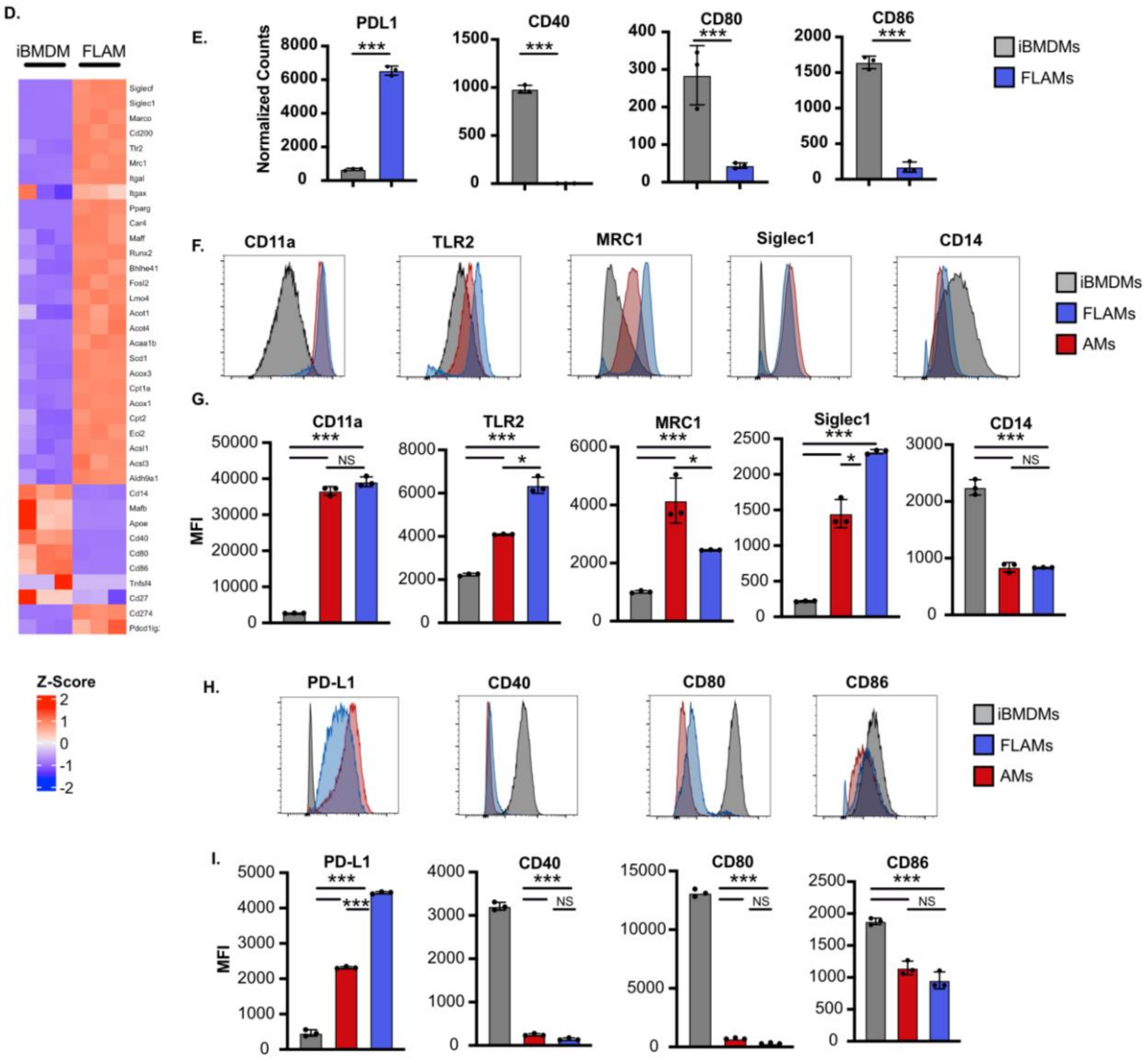

Figure 2.2. iBMDMs and FLAMs respond differently to IFNγ stimulation. **(A)** Differential expression of untreated (red) and IFNγ-stimulated (blue) iBMDMs colored symbols have an adjusted p-value <.05 and a fold change greater than 2 **(B)** Differential expression of untreated (red) and IFNγ-stimulated (blue) FLAMs. Colored symbols have an adjusted p-value <.05 and a fold change greater than 2 **(C)** Expression of subset of ISGs between untreated and IFNγ-stimulated iBMDMs and FLAMs **(D)** Normalized counts of ISGs that are differentially regulated between iBMDMs (grey) and FLAMs (blue) with and without IFNγ. Statistics were determined by adjusted p-values using DeSeq2. Data points represent one biological replicate from one experiment. **(E)** Normalized counts of costimulatory molecules that are differentially regulated between iBMDMs (grey) and FLAMs (blue) during untreated and IFNγ conditions. **(F)** Normalized counts of cell-autonomous restriction factors that are differentially regulated between iBMDMs (grey) and FLAMs (blue) during untreated and IFNγ conditions. **(G)** Mean fluorescence intensity T-cell modulating markers that are differentially regulated between untreated and IFNγ-stimulated FLAMs (blue) and AMs (red). Statistics were determined with a two-way ANOVA and tukey test for multiple comparisons. *Normalized counts points represent one biological replicate from one experiment. MFI points represent one biological replicate from one representative experiment of three. ****p<0.0001, ***p<0.001, **p<0.01, *p<0.05*

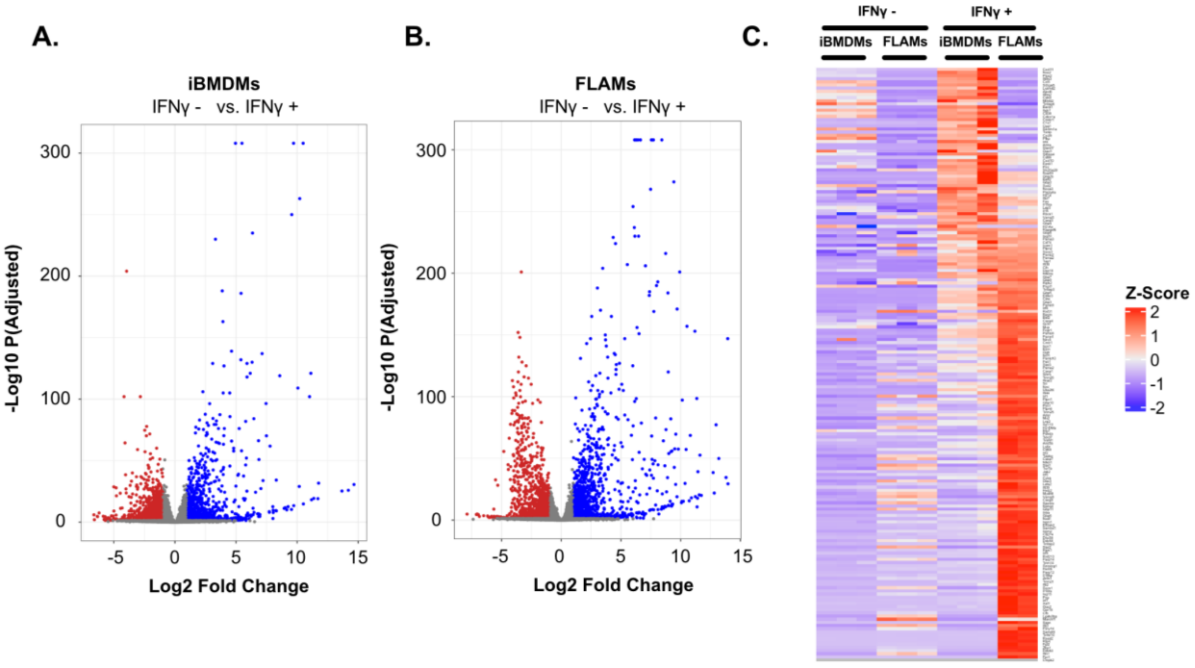

Figure 2.2 (cont'd)

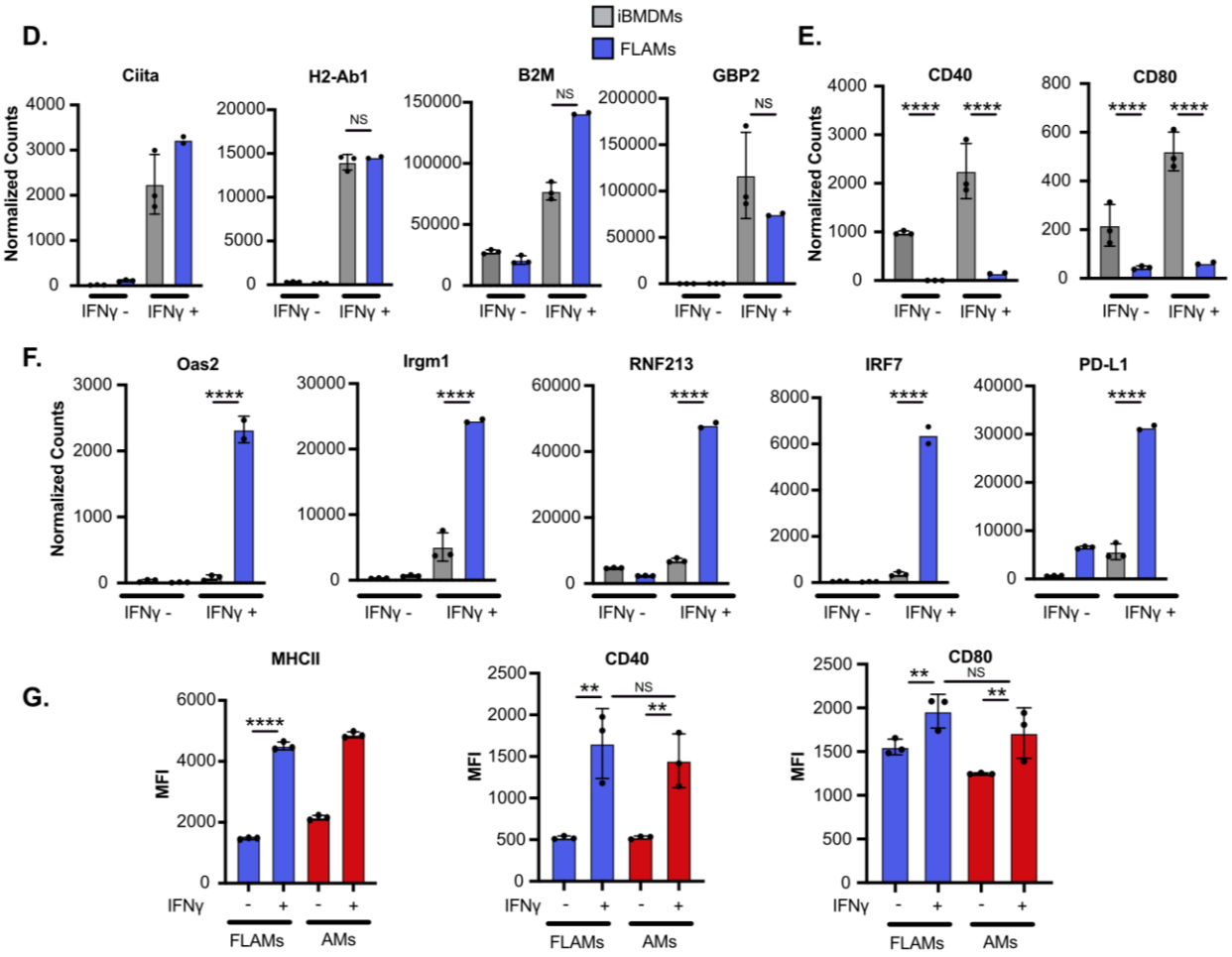

Figure 2.3. Blocking GSK3α/b during IFNγ activation of FLAMs drives co-stimulatory markers. (A) Mean fluorescence intensity of MHCII on iBMDMs and FLAMs treated with DMSO (grey), DMSO and IFNγ (blue), CHIR (yellow), or CHIR and IFNγ (green) for 24 hours. Statistics were determined with a two-way ANOVA and tukey test for multiple comparisons. **(B)** Mean fluorescence intensity of costimulatory molecules on iBMDMs and FLAMs under indicated conditions. Statistics were determined with a two-way ANOVA and tukey test for multiple comparisons. **(C)** MFI of T-cell modulatory markers on AMs under indicated conditions. Statistics were determined with a two-way ANOVA and tukey test for multiple comparisons. **(D)** Normalized counts of T-cell activation molecules between iBMDMs and FLAMs under indicated conditions. Statistics were determined by adjusted p-value calculated by DeSeq. **(E)** PCA plot comparing the likeness of iBMDMs and FLAMs under indicated conditions. **(F)** Top 4 hallmark pathways enriched in GSK3α/β inhibited, IFNγ stimulated FLAMs. *Normalized counts points represent one biological replicate from one experiment. MFI points represent one biological replicate from one representative experiment of three.* *****p<0.0001, ***p<0.001, **p<0.01, *p<0.05*

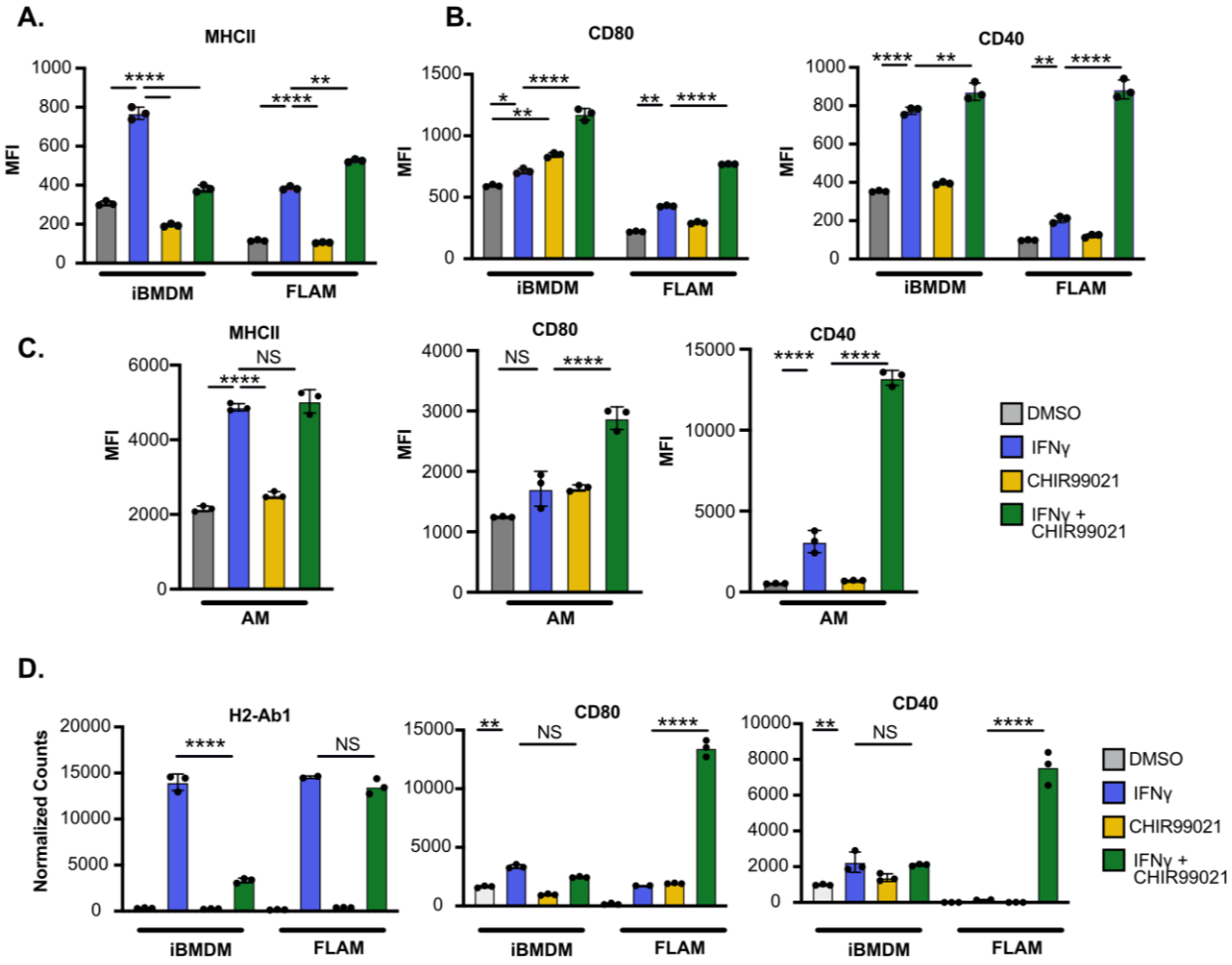

Figure 2.3 (cont'd)

E.

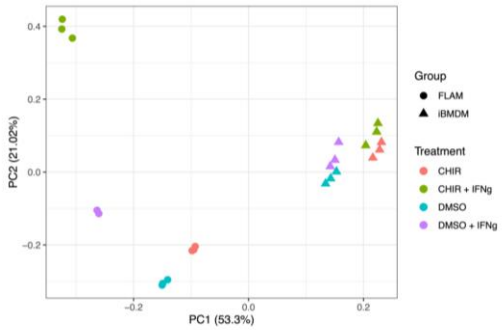

F.

HALLMARK PATHWAY	GENES ENRICHED	GROUP SIZE	NES
INTERFERON GAMMA RESPONSE	94	178	2.42
INTERFERON ALPHA RESPONSE	60	92	2.38
INFLAMMATORY RESPONSE	63	157	2.10
TNFA SIGNALING VIA NFKB	77	183	1.9

Figure 2.4. TNF and Type I IFN contribute to CD40 expression on IFNγ stimulated FLAMs. (A) Normalized counts of TNF (left) and IFNβ (right) compared between iBMDMs and FLAMs treated with DMSO (grey), DMSO and IFNγ (blue), CHIR (yellow), CHIR and IFNγ (green). Statistics were determined by adjusted p-value using DeSeq2. **(B)** Cytokine production of TNF (left) and IFNβ (right) from iBMDMs and FLAMs under the indicated treatments. Statistics were determined with a two-way ANOVA and tukey test for multiple comparisons. **(C)** MFI of CD40 for FLAMs treated with DMSO (grey), IFNγ (blue), TNF (red), or IFNγ and TNF (purple) for 24 hours. Statistics were determined with a two-way ANOVA and tukey test for multiple comparisons. **(D)** MFI of CD40 for FLAMs treated with DMSO (grey), IFNγ (blue), IFNβ1 (red), or IFNγ and IFNβ1 (purple) for 24 hours. Statistics were determined with a two-way ANOVA and tukey test for multiple comparisons. **(E)** MFI of CD40 for WT (grey), IFNAR-/- (blue), and WT + Anti-TNF(red) FLAMs were treated with the treatments indicated for 24 hours. Statistics were determined with a two-way ANOVA and tukey test for multiple comparisons. **(F)** MFI of CD40 for IFNAR-/- (blue) and IFNAR-/- + Anti-TNFR (purple) under indicated conditions. Statistics were determined with a one-way ANOVA and tukey test for multiple comparisons. **(G-H)** p25 peptide-pulsed macrophages with the indicated treatments were co-cultured with p25 specific T-cells and IFNγ release was used to quantify T-cell activation between iBMDMs and FLAMs or Primary AMs under the indicated conditions. Statistics were determined with a two-way ANOVA and tukey test for multiple comparisons. *Normalized counts points represent one biological replicate from one experiment. MFI and cytokine quantification points represent one biological replicate from one representative experiment of three. ****p<0.0001, ***p<0.001, **p<0.01, *p<0.05*

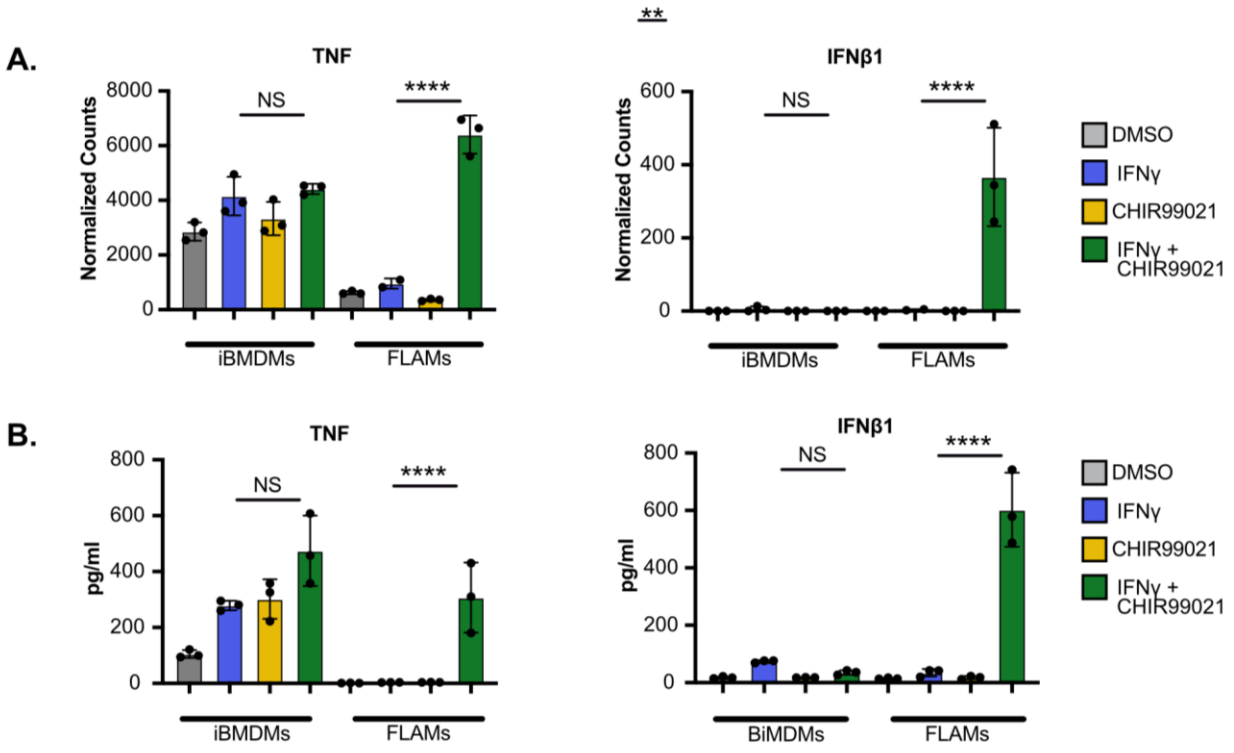

Figure 2.4 (cont'd)

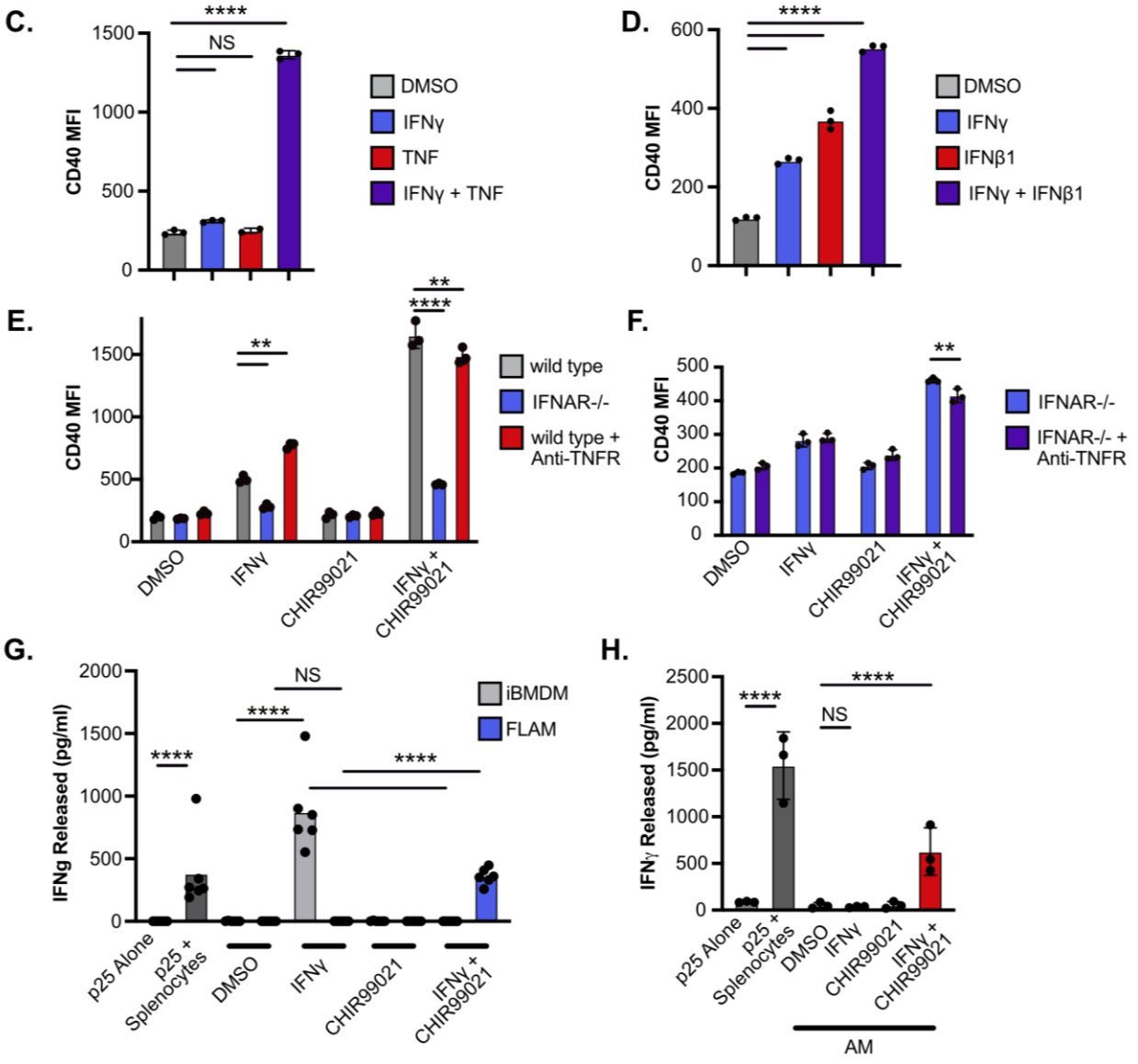

DISCUSSION

AMs are critical to lung immunity but are notoriously difficult to maintain and isolate. It is important to understand how these lung-resident-cells respond uniquely to inflammatory signals compared to other macrophages to develop lung specific therapies that protect against infection while maintaining pulmonary function. Here, we use FLAMs as an *ex vivo* AM model to globally understand transcriptional and functional differences of resident lung macrophages [29]. Overall, we found that FLAMs faithfully recapitulate AMs, uniquely regulate IFNγ responses and that GSK3α/β plays a key role in balancing AM responses to IFNγ and their ability to activate CD4+ T-cell responses. Taken together our results point towards the unique regulation of and responses to IFNγ by different macrophage populations that alter their functional capacity.

A strength of our approach was the use of FLAMs to model primary AMs present in the lung airspace. Our global transcriptional analysis of resting FLAMs confirmed the utility of this approach. By comparing iBMDMs and FLAMs to previously published datasets from immgen on various myeloid-derived cells we found strong similarity between AMs and FLAMs and a more distant relationship to iBMDMs and peritoneal macrophages [35]. Examination of pathways associated with FLAMs identified signatures previously associated with AMs including activation of Ppar signaling, unsaturated fatty acid synthesis, lipid metabolism, and lysosome and peroxisome pathways [37,52–56]. These results suggest that AMs are metabolically distinct from BMDMs and drive high levels of lipid metabolism in line the role of AMs in metabolizing surfactant in the lung environment. Based on the transcriptional results we further confirmed a subset of markers that are highly expressed on the surface FLAMs and AMs compared to iBMDMs, including CD11a, Siglec1 and TLR2. While the role of these surface markers on AM function remains unclear, future studies can now leverage these unique markers to better define

genetic regulatory pathways that control AMs using genome-wide CRISPR approaches as we have done previously with SiglecF [29]. Thus, we have convincingly shown that FLAMs are a tractable model that can be leveraged to dissect mechanisms regulating AM maintenance and function in the lungs.

We next used FLAMs to dissect how lung macrophages respond to the pro-inflammatory cytokine IFNγ. IFNγ is an important regulator of immunity in the lungs and is required protection against respiratory infections such as *M. tuberculosis* [57–62]. IFNγ is known to activate a range of IFN-stimulated genes (ISGs) that drive adaptive immunity cross-talk, cell autonomous effectors, and cytokines/chemokines that modulate inflammatory cell recruitment [19,63]. Interestingly, our transcriptional profiling found that while both iBMDMs and FLAMs are both responsive to IFNγ stimulation, they induce distinct transcriptional changes following activation. We noted that FLAMs robustly induce genes associated with cell-autonomous immunity and antiviral responses compared to iBMDMs including Oas2, RNF213, and Irgm proteins. In contrast, we noted iBMDMs robustly induced T-cell co-stimulatory molecules and nitric oxide production following IFNγ activation. These data suggested that iBMDMs and FLAMs differentially regulate IFNγ responses yet how these differences are regulated remains unclear. Given the metabolic differences between FLAMs and iBMDMs our current model predicts that baseline metabolism and differences in IFNγ-mediated shifts in metabolism drive distinct responses to IFNγ. Previous studies in BMDMs showed that IFNγ-activation drives a shift in cells towards aerobic glycolysis that is dependent on the activation of hypoxia -inducible factor 1 alpha (HIF1α). However, both aerobic glycolysis and oxidative phosphorylation are known to contribute to IFNγ responses [28,64]. Whether HIF1α plays a role in the differential IFNγ responses between BMDMs and AMs and how metabolism shifts in AMs following IFNγ-activation will

be directly examined in the future. In addition to metabolic differences, we noted distinct induction of transcription factors, including Irf7, that regulate downstream responses to IFNγ stimulation [19,63]. Whether differences in these transcriptional regulators are the cause or the result of metabolic differences in FLAMs and iBMDMs will need to be determined in the future. By coupling genetic approaches to remove single transcription factors with metabolic flux approaches including seahorse assays, we will be positioned to understand the mechanisms driving the interlinked metabolic and transcriptional responses following activation of AMs with IFNγ.

To begin understanding the mechanisms controlling the differential regulation of IFNγ responses between BMDMs and AMs, we examined the role of the kinase GSK3α/β. GSK3 has been associated with the regulation of several macrophage signaling pathways including polarization [65,66], inflammatory responses [67–75], and metabolism [76]. We also previously showed that GSK3 is a positive regulator of a subset of IFNγ-dependent responses in iBMDMs including the induction of MHCII antigen presentation machinery. In contrast to iBMDMs, we found that GSK3 does not control IFNγ-dependent MHCII upregulation in FLAMs or AMs. Thus, there are macrophage subset specific roles for GSK3 in regulating IFNγ responses, a hypothesis that was confirmed using global transcriptional profiling. While GSK3 does control a small subset of IFNγ-inducible genes in iBMDMs, the inhibition of GSK3 in combination with IFNγ activation in FLAMs resulted in a dramatic shift in the transcriptional landscape, beyond what was seen with either GSK3 inhibition or IFNγ activation alone. What drives the synergistic response of AMs to both IFNγ and GSK3 inhibition remains an open question. One clue to this synergy is the observation that type I IFN responses are robustly induced only in IFNγ-activated FLAMs with GSK3 inhibition. Type I IFNs can be induced by endogenous ligands from the mitochondria,

such as mitochondrial DNA or RNA, as well as changes in cholesterol metabolism[77–79]. Future work will determine the contribution of these distinct IFN pathways in FLAMs by examining mitochondrial dynamics, the production of mitochondrial ROS, and cholesterol metabolic flux. In addition, how type I IFNs drive the transcriptional changes in IFNγ-activated GSK3-inhibited FLAMs will need to be directly tested in the future using tools such as the IFNAR-/- FLAMs. Altogether our results show that GSK3 is an important regulator of the AM response to IFNγ and maintains AM functionality.

Throughout our study we noticed major differences in the regulation of T-cell modulatory markers between iBMDMs and FLAMs. In resting cells, FLAMs expressed very low levels the co-stimulatory molecules CD40, CD80, and CD86 compared to iBMDMs in line with previous studies on AMs. In contrast, FLAMs expressed high levels of the co-inhibitory molecules PD-L1 and PD-L2 compared to iBMDMs. These differences persisted after IFNγ activation with iBMDMs robustly upregulating both antigen presentation machinery and co-stimulatory markers while FLAMs only upregulated antigen presentation machinery. We found inhibiting GSK3 in IFNγ-activated FLAMs resulted in a robust increase in co-stimulatory molecules that was dependent on type I IFNs and was not observed in iBMDMs. These differences in MHCII and co-stimulatory molecule expression had functional implications as IFNγ-stimulated iBMDMs activated naïve CD4+ T-cells while IFNγ-stimulated FLAMs could not. In contrast, inhibiting GSK3 in IFNγ-stimulated iBMDMs reduced CD4+ T-cell activation while this treatment increased CD4+ T-cell activation by FLAMs. Our data support differential roles for macrophage subtypes in directly modulating the adaptive immune system. Previous studies suggest that AMs are not efficient activators of naïve T-cells [16,17]. In fact, robust activation of T-cells by AMs is associated with worse clinical outcomes during infection with SARS-CoV-2 in a manner that

was dependent on both IFNγ and TNF [41]. We speculate that AMs are inherently wired to respond to IFNγ in a way that prevents overly robust activation of T-cells and limits deleterious lung damage. However, when combined with other inflammatory signals including type I IFN or TNF, IFNγ robustly drives AMs to activate T-cell responses. It is possible that pathogens, such as *M. tuberculosis,* take advantage of the restrained T-cell activating capacity of AMs to prevent detection and initiate lung infections but this will need to be directly tested. Altogether our study shows that FLAMs are a useful model to probe mechanism that make AMs a unique macrophage population in the lung environment. Not only do AMs differentially regulate their IFNγ responses partially through the activity of GSK3α/β but they differentially control crosstalk with T-cells that alter the activation of adaptive immunity.

MATERIALS AND METHODS

Animal Experiments

All cells derived from live mice were performed in accordance using the recommendations from the Guide for the Care and Use of Laboratory Animals of the National Institutes of Health and the Office of Laboratory Animal Welfare. Mouse studies were performed using protocols approved by the Institutional Animal Care and Use Committee (IACUC). All mice were housed and bred under specific pathogen-free conditions and in accordance with Michigan State University (PROTO202200127) IACUC guidelines. All mice were monitored and weighed regularly. C57BL6/J mice (# 000664) and *Ifnar1-/-* mice (# 028288) were purchased from Jackson labs.

Cell Isolation

J2 virus immortalized Cas9 + BMDMs (iBMDMs) were isolated and immortalized as previously described from C57BL/6J mice [26,80]. Primary BMDMs were isolated from the femurs of C57BL/6J mice by cutting one end of the bone, placing the bone cut side down in 0.6mL tubes, and then centrifuging the bone at 16,000 x g for 25 seconds. The cells from several femurs were pooled together and pelleted in PBS. RBC lysis buffer (Alfa Aesar, Cat no. J62150) in combination with a 70-uM filter were used to remove red blood cells from the cell suspension. FLAMs were isolated as previously described from C57BL/6J mice [29,31]. Briefly, fetal livers were extracted from euthanized dams immediately after death. Livers were ground into a single cell suspension and plated. After approximately one-week cells are adherent, have an AM-like morphology, and express AM-like surface markers. Primary AMs were isolated by bronchoalveolar lavage of C57BL/J6 mice as previously described[81]. P25 TCR-Tg CD4+ T-cells [50,51] were isolated from the lymph nodes and spleens of transgenic P25TCR mice. The spleen and lymph nodes were homogenized over a 70uM strainer and washed with RPMI media. CD4+ T-

cells were enriched using the MojoSort ™ T-cell isolation kit (BioLegend, Cat no. 480006) following the manufacturer's protocol.

Cell Culture

iBMDMs were maintained in Dulbecco's Modified Eagle Medium (DMEM; HyClone Cytiva, Cat no. SH30243.01) supplemented with 10% fetal bovine serum (FBS) (R&D Systems, Cat no. S11550). iBMDMs were passaged once they reached 70-90% confluency by gently scraping and plating in 10cm TC treated dishes 1:10 (1 part-cell containing media, 9 parts fresh media). Primary BMDMs were cultured in RPMI 1640 complete media (HyClone Cytiva, Cat no. SH30027.02) supplemented with 10% FBS, 1% penicillin-streptomycin, and 20% L929 media 8. Cells were used after one week once fully differentiated. FLAMs were maintained in RPMI 1640 complete media supplemented with 10% FBS, 20 ng/mL recombinant human TGF-b1 (PeproTech, Cat no. 100-21), and 30ng/mL recombinant murine GM-CSF (PeproTech, Cat no. 300-03). FLAM media was refreshed every 3 days. When FLAMs were 70-90% confluent they were lifted by gentle scraping and plated 1:3 in 10cm TC treated dishes. Primary AMs were grown in complete RPMI 1640 supplemented with 10% FBS and 30ng/mL GM-CSF. CD4+ T-cells were cultured in complete RPMI 1640 media supplemented with 10% FBS and penicillin-streptomycin (50U/mL penicillin, 50mg/mL streptomycin) (Gibco, Cat no. 15140-122) All cells were incubated in 5% CO_2 at 37 ℃.

Generation of IFNAR KO

IFNAR KO FLAMs were isolated from IFNAR KO mice using the FLAM isolation and culture techniques described above.

Macrophage Treatment Conditions

FLAMs and iBMDMs were plated at $1x10^6$ cells per well in 6-well tissue culture plates and were allowed to adhere overnight. The following day, cells were treated with DMSO (Fisher Chemical, Cat no. D128500), DMSO and 6.25 ng/ml IFNγ (PeproTech, Cat no. 315-05) , 10 μM CHIR99021 (CHIR) (Sigma-Aldrich, Cat no. SML1046), or both 10 μM CHIR and 6.25 ng/ml IFNγ for 24 hours.

1. **Adding TNF Experiment**

   iBMDMs and FLAMs were incubated with IFNγ (6.25 ng/ml) and TNF-a (PeproTech, Cat no. 31501A) (20 ng/ul) for 24 hours prior to flow cytometry and qPCR.

2. **IFNβ**

   FLAMs and iBMDMs were plated in 12-well plates at 300,000 cells per well. FLAM and IFNAR KO FLAMs were treated as described above under "Macrophage IFNγ CHIR Treatments" but with the addition of IFN-B1 (BioLegend, Cat no. 581304) (20 ng/ml) or both IFNβ and TNF-a (20 ng/ml) for 24 hours prior to flow cytometry analysis.

3. **TNFR Blocking Experiment**

   FLAMs and iBMDMs were plated in 12-well plates at 300,000 cells per well in RPMI 1640 supplemented with 10% FBS, TGFβ, and GMCSF or DMEM supplemented with 10% FBS, respectively, that contained a TNFR blocking antibody (BioLegend, 113104) at 1.25 ng/ml for 24 hours. After 24 hours, the cells were treated with CHIR, IFNγ, and the TNFR blocking antibody for 24 hours prior to flow cytometry analysis.

Flow Cytometry

Cells were scraped and lifted, washed 3 times with PBS, and then stained. Each flow cytometry antibody was diluted 1:400 in PBS. The antibodies used were MHCII-FITC (BioLegend, Cat no.

107606, CD40-APC (BioLegend, Cat no. 124612), PDL1-BV421 (BioLegend, Cat no. 124315), CD80-PE (BioLegend, Cat no. 104708), and CD86-APC-Cy7 (BioLegend, Cat no. 104708). Cells were then washed 3 times and fixed with 1% formaldehyde (J.T. Baker , Cat no. JTB-2106-01) in PBS. Flow cytometry was performed with a BD LSR II flow cytometer at the MSU Flow Cytometry Core and data were analyzed using FlowJo (Version 10.8.1).

Quantitative Real-Time PCR

RNA from iBMDMs and FLAMs was PCR amplified using the One-step Syber Green RT-PCR Kit (Qiagen, Cat no. 210215). The PCR was monitored using the QuantStudio3 (ThermoFisher, Cat no. A28567).

Cytokine Profiling

FLAMs and iBMDMs were treated as described above for 24 hours, and supernatants were collected for cytokine profiling by Eve Technologies using the Mouse Cytokine/Chemokine 31-Plex Discovery Assay® Array.

RNA Sequencing and Analysis

FLAMs and iBMDMs were plated in 6-well plates at 1 x 10^6 cells/well and treated with IFNγ and CHIR as described above for 24 hours. The Direct-zol RNA Extraction Kit (Zymo Research, Cat no. R2072] was used to extract RNA according to the manufacturer's protocol. Quality was assessed by the MSU Genomics Core using an Agilent 4200 TapeStation System. Libraries were prepared using an Illumina Stranded mRNA Library Prep kit (Illumina, Cat no. 20040534) with IDT for Illumina RNA Unique Dual Index adapters following the manufacturer's recommendations, except that half-volume reactions were performed. Generated libraries were quantified and assessed for quality using a combination of Qubit™ dsDNA HS (ThermoFischer Scientific, Cat no. Q32851) and Agilent 4200 TapeStation HS DNA1000 assays (Agilent, Cat

no. 5067-5584). The libraries were pooled in equimolar amounts, and the pooled library was quantified using an Invitrogen Collibri Quantification qPCR kit (Invitrogen, Cat no. A38524100). The pool was loaded onto 2 lanes of a NovaSeq S1 flow cell, and sequencing was performed in a 1x100 bp single-read format using a NovaSeq 6000 v1.5 100-cycle reagent kit (Illumina, Cat no. 20028316). Base calling was performed with Illumina Real Time Analysis (RTA; Version 3.4.4), and the output of RTA was demultiplexed and converted to the FastQ format with Illumina Bcl2fastq (Version 2.20.0). All RNAseq analysis was performed using the MSU High Performance Computing Center (HPCC). Read quality was assessed using FastQC (Version 0.11.7) [83]. Read mapping was performed against the GRCm39 mouse reference genome using Bowtie2 (Version 2.4.1)[84] in Java (Version 1.8.0) with default settings. Aligned reads counts were assessed using feature counts from the Subread package (Version 2.0.0) [85]. Differential gene expression analysis was conducted using the DESeq2 package (Version 1.36.0) [86] in R (Version 4.2.1). One IFNγ treated FLAM samples did not pass QC and was not included in analysis.

T-cell Assays

A previously established co-culture system to assess antigen-specific T-cell activation was used. The CD4+ T-cells were stimulated with p25 peptide pulsed iBMDMs or FLAMs that were irradiated with Mitomycin (25ug/mL) (VWR, Cat no. TCM2320) and had been treated with DMSO, IFNγ, CHIR, and CHIR IFNγ as described under "Macrophage Treatment Conditions". Co-cultures were supplemented with 10ng/mL IL-12 (Peprotech, Cat no. 210-12) and 10ug/mL anti IL-4 (BioLegend, Cat no. 504-102) to achieve Th1 polarization. Supernatants were collected 3 days after the initial co-culture and used to quantify T-cell activation levels with ELISA (BioLegend, Cat no. 430801).

REFERENCES

1. Schneider, C. *et al.* Induction of the nuclear receptor PPAR-γ by the cytokine GM-CSF is critical for the differentiation of fetal monocytes into alveolar macrophages. *Nature Immunology 2014 15:11* **15**, 1026–1037 (2014).

2. Evren, E. *et al.* CD116+ fetal precursors migrate to the perinatal lung and give rise to human alveolar macrophages. *Journal of Experimental Medicine* **219**, (2022).

3. Sheng, J., Ruedl, C. & Karjalainen, K. Most Tissue-Resident Macrophages Except Microglia Are Derived from Fetal Hematopoietic Stem Cells. *Immunity* **43**, 382–393 (2015).

4. Serbina, N. V., Jia, T., Hohl, T. M. & Pamer, E. G. Monocyte-mediated defense against microbial pathogens. *Annu Rev Immunol* **26**, 421–452 (2008).

5. Dey, A., Allen, J. & Hankey-Giblin, P. A. Ontogeny and polarization of macrophages in inflammation: Blood monocytes versus tissue macrophages. *Front Immunol* **6**, 683 (2015).

6. Wynn, T. A., Chawla, A. & Pollard, J. W. Macrophage biology in development, homeostasis and disease. *Nature 2013 496:7446* **496**, 445–455 (2013).

7. Cohen, S. B. *et al.* Alveolar Macrophages Provide an Early Mycobacterium tuberculosis Niche and Initiate Dissemination. *Cell Host Microbe* **24**, 439-446.e4 (2018).

8. Peters, W. & Ernst, J. D. Mechanisms of cell recruitment in the immune response to Mycobacterium tuberculosis. *Microbes Infect* **5**, 151–158 (2003).

9. Shi, C. & Pamer, E. G. Monocyte recruitment during infection and inflammation. *Nat Rev Immunol* **11**, 762 (2011).

10. Bain, C. C. & MacDonald, A. S. The impact of the lung environment on macrophage development, activation and function: diversity in the face of adversity. *Mucosal Immunology 2022 15:2* **15**, 223–234 (2022).

11. Wessendarp, M. *et al.* Role of GM-CSF in regulating metabolism and mitochondrial functions critical to macrophage proliferation. *Mitochondrion* **62**, 85–101 (2022).

12. Wculek, S. K. *et al.* Oxidative phosphorylation selectively orchestrates tissue macrophage homeostasis. *Immunity* **56**, 516-530.e9 (2023).

13. Woods, P. S. *et al.* Tissue-Resident Alveolar Macrophages Do Not Rely on Glycolysis for LPS-induced Inflammation. (2020) doi:10.1165/rcmb.2019-0244OC.

14. Wang, T. *et al.* HIF1 α -Induced Glycolysis Metabolism Is Essential to the Activation of Inflammatory Macrophages. *Mediators Inflamm* **2017**, (2017).

15. Li, C. *et al.* HIF1α-dependent glycolysis promotes macrophage functional activities in protecting against bacterial and fungal infection. *Scientific Reports 2018 8:1* **8**, 1–11 (2018).

16. Coleman, M. M. *et al.* Alveolar macrophages contribute to respiratory tolerance by inducing FoxP3 expression in naive T cells. *Am J Respir Cell Mol Biol* **48**, 773–780 (2013).

17. Soroosh, P. *et al.* Lung-resident tissue macrophages generate Foxp3+ regulatory T cells and promote airway tolerance. *J Exp Med* **210**, 775–788 (2013).

18. Srivastava, S. & Ernst, J. D. Direct recognition of infected cells by CD4 T cells is required for control of intracellular Mycobacterium tuberculosis in vivo. *J Immunol* **191**, 1016 (2013).

19. Schneider, W. M., Chevillotte, M. D. & Rice, C. M. Interferon-stimulated genes: a complex web of host defenses. *Annu Rev Immunol* **32**, 513–545 (2014).

20. Kiritsy, M. C. *et al.* A genetic screen in macrophages identifies new regulators of ifnγ-inducible mhcii that contribute to t cell activation. *Elife* **10**, (2021).

21. Setoguchi, R., Matsui, Y. & Mouri, K. mTOR signaling promotes a robust and continuous production of IFN-γ by human memory CD8+ T cells and their proliferation. *Eur J Immunol* **45**, 893–902 (2015).

22. Kroczynska, B. *et al.* Interferon γ (IFNγ) Signaling via Mechanistic Target of Rapamycin Complex 2 (mTORC2) and Regulatory Effects in the Generation of Type II Interferon Biological Responses. *J Biol Chem* **291**, 2389–2396 (2016).

23. Imanishi, T. *et al.* mTORC1 signaling controls TLR2-mediated T-cell activation by inducing TIRAP expression. *Elsevier*.

24. Fulton, S. A. *et al.* Inhibition of Major Histocompatibility Complex II Expression and Antigen Processing in Murine Alveolar Macrophages by Mycobacterium bovis BCG and the 19-Kilodalton Mycobacterial Lipoprotein. *Infect Immun* **72**, 2101 (2004).

25. Huang, L., Nazarova, E. V., Tan, S., Liu, Y. & Russell, D. G. Growth of Mycobacterium tuberculosis in vivo segregates with host macrophage metabolism and ontogeny. *Journal of Experimental Medicine* **215**, 1135–1152 (2018).

26. De Nardo, D., Kalvakolanu, D. V. & Latz, E. Immortalization of murine bone marrow-derived macrophages. *Methods in Molecular Biology* **1784**, 35–49 (2018).

27. Braverman, J., Sogi, K. M., Benjamin, D., Nomura, D. K. & Stanley, S. A. HIF-1α Is an Essential Mediator of IFN-γ-Dependent Immunity to Mycobacterium tuberculosis. *J Immunol* **197**, 1287–1297 (2016).

28. Kiritsy, M. C. *et al.* Mitochondrial respiration contributes to the interferon gamma response in antigen-presenting cells. *Elife* **10**, (2021).

29. Thomas, S. T., Wierenga, K. A., Pestka, J. J. & Olive, A. J. Fetal Liver–Derived Alveolar-like Macrophages: A Self-Replicating Ex Vivo Model of Alveolar Macrophages for Functional Genetic Studies. *Immunohorizons* **6**, 156–169 (2022).

30. Gorki, A.-D. *et al.* Murine Ex Vivo Cultured Alveolar Macrophages Provide a Novel Tool to Study Tissue-Resident Macrophage Behavior and Function. (2022) doi:10.1165/rcmb.2021-0190OC.

31. Fejer, G. *et al.* Nontransformed, GM-CSF-dependent macrophage lines are a unique model to study tissue macrophage functions. *Proc Natl Acad Sci U S A* **110**, E2191 (2013).

32. Kendall, R. L., Ray, J. L., Hamilton, R. F. & Holian, A. Self-replicating murine ex vivo cultured alveolar macrophages as a model for toxicological studies of particle-induced inflammation. *Toxicol Appl Pharmacol* **461**, 116400 (2023).

33. Guilliams, M., Kleer, I. De, Henri, S., … S. P.-J. of E. & 2013, undefined. Alveolar macrophages develop from fetal monocytes that differentiate into long-lived cells in the first week of life via GM-CSF. *rupress.org*.

34. Baker, A. D. *et al.* PPARγ regulates the expression of cholesterol metabolism genes in alveolar macrophages. *Biochem Biophys Res Commun* **393**, 682–687 (2010).

35. Subramanian, S. *et al.* Long-term culture-expanded alveolar macrophages restore their full epigenetic identity after transfer in vivo. *Nature Immunology 2022 23:3* **23**, 458–468 (2022).

36. Mould, K. J., Jackson, N. D., Henson, P. M., Seibold, M. & Janssen, W. J. Single cell RNA sequencing identifies unique inflammatory airspace macrophage subsets. *JCI Insight* **4**, (2019).

37. Baker, A., Malur, A., Barna, B., … M. K.-B. and & 2010, undefined. PPARγ regulates the expression of cholesterol metabolism genes in alveolar macrophages. *Elsevier*.

38. Sun, F. *et al.* Alveolar Macrophages Inherently Express Programmed Death-1 Ligand 1 for Optimal Protective Immunity and Tolerance. *J Immunol* **207**, 110–114 (2021).

39. Nash2, T. W., Libby, D. M. & Horwitz3, M. A. IFN-gamma-activated human alveolar macrophages inhibit the intracellular multiplication of Legionella pneumophila. *The Journal of Immunology* **140**, 3978–3981 (1988).

40. Wu, C. *et al.* IFN-γ Primes Macrophage Activation by Increasing Phosphatase and Tensin Homolog via Downregulation of miR-3473b. *The Journal of Immunology* **193**, 3036–3044 (2014).

41. Zhang, F. *et al.* IFN-γ and TNF-α drive a CXCL10+ CCL2+ macrophage phenotype expanded in severe COVID-19 lungs and inflammatory diseases with tissue inflammation. *Genome Med* **13**, 1–17 (2021).

42. Buhtoiarov, I. N. *et al.* CD40 ligation activates murine macrophages via an IFN-gamma-dependent mechanism resulting in tumor cell destruction in vitro. *J Immunol* **174**, 6013–22 (2005).

43. Wijdeven, R. H. *et al.* Chemical and genetic control of IFNγ-induced MHCII expression. *EMBO Rep* **19**, e45553 (2018).

44. Zhou, F. Molecular mechanisms of IFN-γ to up-regulate MHC class i antigen processing and presentation. *Int Rev Immunol* **28**, 239–260 (2009).

45. Ono, T., Yanagawa, Y., Iwabuchi, K., Nonomura, K. & Onoé, K. Glycogen synthase kinase 3 activity during development of bone marrow-derived dendritic cells (DCs) essential for the DC function to induce T helper 2 polarization. *Immunology* **122**, 189–198 (2007).

46. Cortés-Vieyra, R. *et al.* Glycogen Synthase Kinase 3β Modulates the Inflammatory Response Activated by Bacteria, Viruses, and Parasites. *Front Immunol* **12**, (2021).

47. Marckmann, S. *et al.* Interferon-beta up-regulates the expression of co-stimulatory molecules CD80, CD86 and CD40 on monocytes: significance for treatment of multiple sclerosis. *Clin Exp Immunol* **138**, 499–506 (2004).

48. Chen, L. & Flies, D. B. Molecular mechanisms of T cell co-stimulation and co-inhibition. *Nature Reviews Immunology 2013 13:4* **13**, 227–242 (2013).

49. 011005 - P25 TCR-Tg Strain Details. https://www.jax.org/strain/011005

50. Tamura, T. *et al.* The role of antigenic peptide in CD4+ T helper phenotype development in a T cell receptor transgenic model. *Int Immunol* **16**, 1691–1699 (2004).

51. Wolf, A. J. *et al.* Initiation of the adaptive immune response to Mycobacterium tuberculosis depends on antigen production in the local lymph node, not the lungs. *J Exp Med* **205**, 105 (2008).

52. Dalrymple, H. *et al.* Alveolar macrophages of GM-CSF knockout mice exhibit mixed M1 and M2 phenotypes. *BMC Immunol* **14**, (2013).

53. Gautier, E., Chow, A., … R. S.-T. J. of & 2012, undefined. Systemic analysis of PPARγ in mouse macrophage populations reveals marked diversity in expression with critical roles in resolution of inflammation and airway. *journals.aai.org*.

54. Guilliams, M., Kleer, I. De, Henri, S., … S. P.-J. of E. & 2013, undefined. Alveolar macrophages develop from fetal monocytes that differentiate into long-lived cells in the first week of life via GM-CSF. *rupress.org*.

55. Gautier, E. *et al.* Gene-expression profiles and transcriptional regulatory pathways that underlie the identity and diversity of mouse tissue macrophages. *nature.com*.

56. Reddy, R. C. Immunomodulatory Role of PPAR-+ in Alveolar Macrophages. doi:10.2310/JIM.0b013e3181659972.

57. Rovetta, A. I. *et al.* IFNG-mediated immune responses enhance autophagy against Mycobacterium tuberculosis antigens in patients with active tuberculosis. *Autophagy* **10**, 2109–2121 (2014).

58. Bogunovic, D. *et al.* Mycobacterial disease and impaired IFN-γ immunity in humans with inherited ISG15 deficiency. *Science (1979)* **337**, 1684–1688 (2012).

59. Pai, R. K., Convery, M., Hamilton, T. A., Boom, W. H. & Harding, C. V. Inhibition of IFN-γ-Induced Class II Transactivator Expression by a 19-kDa Lipoprotein from Mycobacterium tuberculosis : A Potential Mechanism for Immune Evasion . *The Journal of Immunology* **171**, 175–184 (2003).

60. Bustamante, J., Boisson-Dupuis, S., Abel, L. & Casanova, J.-L. Mendelian susceptibility to mycobacterial disease: Genetic, immunological, and clinical features of inborn errors of IFN-γ immunity. *Semin Immunol* **26**, 454–470 (2014).

61. Ernst Preston J Hill, J. D. *et al.* Mycobacterium tuberculosis Inhibits Macrophage Responses to IFN-γ through Myeloid Differentiation Factor 88-Dependent and-Independent Mechanisms. *J Immunol References* **172**, 6272–6280 (2004).

62. Flynn, J. L. *et al. An Essential Role for Interferon Gamma in Resistance to Mycobacterium tuberculosis Infection*. http://rupress.org/jem/article-pdf/178/6/2249/1104362/2249.pdf (1993).

63. Schroder, K., Hertzog, P. J., Ravasi, T. & Hume, D. A. Interferon-γ: an overview of signals, mechanisms and functions. *J Leukoc Biol* **75**, 163–189 (2004).

64. Braverman, J., Sogi, K. M., Benjamin, D., Nomura, D. K. & Stanley, S. A. HIF-1α is an essential mediator of IFN-γ dependent immunity to Mycobacterium tuberculosis. *J Immunol* **197**, 1287 (2016).

65. Beurel, E. & Jope, R. S. Differential regulation of STAT family members by glycogen synthase kinase-3. *Journal of Biological Chemistry* **283**, 21934–21944 (2008).

66. Panagi, I. *et al.* Salmonella Effector SteE Converts the Mammalian Serine/Threonine Kinase GSK3 into a Tyrosine Kinase to Direct Macrophage Polarization. *Cell Host Microbe* **27**, 41-53.e6 (2020).

67. Martin, M., Rehani, K., Jope, R. S. & Michalek, S. M. Toll-like receptor–mediated cytokine production is differentially regulated by glycogen synthase kinase 3. *Nature Immunology 2005 6:8* **6**, 777–784 (2005).

68. He, H. *et al.* Characterization of a toxoplasma effector uncovers an alternative GSK3/β-catenin-regulatory pathway of inflammation. *Elife* **7**, (2018).

69. Kai, J. I. *et al.* Glycogen synthase kinase-3β indirectly facilitates interferon-γ-induced nuclear factor-κB activation and nitric oxide biosynthesis. *J Cell Biochem* **111**, 1522–1530 (2010).

70. Park, S. *et al.* Tumor necrosis factor induces GSK3 kinase–mediated cross-tolerance to endotoxin in macrophages. *nature.com* **12**, 607–615 (2011).

71. Beurel, E., Michalek, S. M. & Jope, R. S. Innate and adaptive immune responses regulated by glycogen synthase kinase-3 (GSK3). *Trends Immunol* **31**, 24–31 (2010).

72. Hermida, M. A., Dinesh Kumar, J. & Leslie, N. R. GSK3 and its interactions with the PI3K/AKT/mTOR signalling network. *Adv Biol Regul* **65**, 5–15 (2017).

73. Ko, R., Park, J. H., Ha, H., Choi, Y. & Lee, S. Y. Glycogen synthase kinase 3β ubiquitination by TRAF6 regulates TLR3-mediated pro-inflammatory cytokine production. *Nat Commun* **6**, (2015).

74. Wang, H. *et al.* IFN-β Production by TLR4-Stimulated Innate Immune Cells Is Negatively Regulated by GSK3-β. *J Immunol* **181**, 6797 (2008).

75. Hu, X. *et al.* IFN-gamma suppresses IL-10 production and synergizes with TLR2 by regulating GSK3 and CREB/AP-1 proteins. *Immunity* **24**, 563–574 (2006).

76. Ding, L. *et al.* Nrf2 exerts mixed inflammation and glucose metabolism regulatory effects on murine RAW264.7 macrophages. *Int Immunopharmacol* **71**, 198–204 (2019).

77. Riley, J. S. & Tait, S. W. Mitochondrial DNA in inflammation and immunity. *EMBO Rep* **21**, (2020).

78. Dhir, A. *et al.* Mitochondrial double-stranded RNA triggers antiviral signalling in humans. *Nature 2018 560:7717* **560**, 238–242 (2018).

79. York, A. G. *et al.* Limiting Cholesterol Biosynthetic Flux Spontaneously Engages Type I IFN Signaling. *Cell* **163**, 1716–1729 (2015).

80. Kiritsy, M. C. *et al.* A genetic screen in macrophages identifies new regulators of ifnγ-inducible mhcii that contribute to t cell activation. *Elife* **10**, (2021).

81. Busch, C., Favret, J., Geirsdóttir, L., … K. M.-B. & 2019, undefined. Isolation and long-term cultivation of mouse alveolar macrophages. *bio-protocol.org*.

82. Weischenfeldt: Bone marrow-derived macrophages (BMM):... - Google Scholar. https://scholar.google.com/scholar_lookup?title=Bone%20marrow-derived%20macrophages%20%28BMM%29%3A%20isolation%20and%20applications.&author=J.%20Weischenfeldt&author=B.%20Porse&publication_year=2008&journal=CSH%20Protoc&volume=2008&pages=prot5080.

83. Babraham Bioinformatics - FastQC A Quality Control tool for High Throughput Sequence Data. https://www.bioinformatics.babraham.ac.uk/projects/fastqc/.

84. Langmead, B. & Salzberg, S. L. Fast gapped-read alignment with Bowtie 2. *Nature Methods 2012 9:4* **9**, 357–359 (2012).

85. Liao, Y., Smyth, G. K. & Shi, W. featureCounts: an efficient general purpose program for assigning sequence reads to genomic features. *Bioinformatics* **30**, 923–930 (2014).

86. Love, M. I., Huber, W. & Anders, S. Moderated estimation of fold change and dispersion for RNA-seq data with DESeq2. *Genome Biol* **15**, 1–21 (2014).

CHAPTER 4: Concluding Remarks and Future Directions

CONCLUDING REMARKS

People have suffered from the vast effects of TB for millenia [1]. TB comes with economic hardships, long term illness, and ultimately fatality [2,3]. *Mtb* has evolved sophisticated strategies to evade host immune responses that make finding effective treatment strategies challenging [4,5]. Unfortunately, *Mtb* has evolved faster than the science has, and current treatments are poor, and we lack effective vaccines [6–9]. However, the World Health Organization's End TB Strategic Plan aims to reduce TB deaths and incidence by 90% and 80% respectively by 2030 [10]. My contribution to this mission is this body of work that aims to further define the role of IFNγ, a known critical factor for *Mtb* control needed to limit TB disease progression, in macrophage function as well as better define the regulation of AMs during host defense. [11]. This work acts as a foundation for future questions surrounding the complexities of macrophage inflammatory responses and how we can target such responses in specific macrophage populations to limit infection and disease.

FUTURE DIRECTIONS

In Chapter 2, I highlight two of the hundreds of genes we have identified as new regulators of IFNγ-dependent MHCII expression on iBMDMs, Med16 and GSK3β [12]. These two genes, when knocked out, independently limit IFNγ-dependent MHCII expression. This data was not only valuable on its own, but it also helped to validate a CRISPR Cas9 screen that we used to broadly identify macrophage genes important for IFNγ-dependent MHCII expression. I determined that both Med16 and GSK3β are upstream regulators of MHCII that impact the activation of Ciita, a crucial transcriptional complex for MHCII expression. Additionally, both Med16 and GSK3β individually impact CD4+ T cell activation because of their role in limiting MHCII surface expression on macrophages when knocked out. Together, these data suggested to

us the possibility that these two genes function through the same regulatory pathway. Using RNAseq and a combination of genetic KOs and chemical inhibition, we found that Med16 and GSK3β function independently of each other and control distinct subsets of IFNγ-mediated genes. Together indicating that we had identified and validated two distinct regulators of IFNγ-dependent MHCII.

What are the mechanisms of Med16-dependent Ciita regulation and how does Med16 modulate disease outcome?

As described in Chapter 3, I continued this work by further investigating the relationship of IFNγ and GSK3. However, Med16 is also an interesting candidate that requires additional study. There are two broad questions that I am particularly interested in regarding Med16; first, how does Med16 control Ciita and second, how does Med16 impact the immune response during *Mtb* infection? Med16 is a component of the mediator complex, an evolutionarily conserved co-activator that is central to gene transcription in all eukaryotes [13]. The specific function of the complex is highly context dependent, and the mechanisms used to transcribe most genes are unknown. I do not know how IFNγ effects the composition of the mediator complex, how such changes alter MHCII expression, or the specific role of Med16 in these changes. We have determined that our phenotype for MHCII limitation is specific to Med16 and that knocking out other subunits does not impact MHCII expression. We also found that treating cells with IFNγ does not alter the expression level of Med16. Together this suggests that IFNγ alters the entire complex in such a way that Med16 is required for transcription but does not directly target Med16 itself. To understand how Med16 regulates Ciita expression, it would first be important to understand the effect IFNγ has on the composition of the mediator complex. Using an HA-tagged Med16 we could conduct co-immunoprecipitation where we precipitate the entire complex from

untreated and IFNγ treated cells and then use quantitative mass spectrometry to identify Med16 interaction partners, or other subunits of the complex. This will demonstrate how IFNγ alters the composition of the complex, however it is also important to consider the chromatin accessibility of MHCII regulatory genes. The mediator complex is known to modify chromatin architecture [14,15]; however, I do not yet understand the specific role of Med16 or the effects IFNγ has on such modifications. Using ATAC-seq to compare chromatin accessibility between wildtype and Med16 KO macrophages that are both untreated and IFNγ treated would be telling of how chromatin architecture and gene accessibility is changed under these conditions. To fully understand the impact of chromatin architecture, we also must determine what specific MHCII regulatory genes require Med16 for transcription. To do this, we can explore the genome binding of Med16 and its transcription factors using chromatin immunoprecipitation and ChIP-seq for wildtype and Med16 Kos that are untreated and IFNγ treated. This paired with ATAC-seq will provide an in depth understanding of how Med16 controls the transcription of MHCII regulatory genes like Ciita.

The second major question that remains about Med16 is how does Med16 impact the immune response during *Mtb* infection? The role of Med16 in *Mtb* infection has yet to be directly tested. We have determined that cytokine profiles differ between Med16 KO and wildtype macrophages that are infected with *Mtb* indicating that Med16 will directly impact infection, but we have yet to determine the impact on infection broadly. To ask this question properly we must consider the state of the pathogen, the immune profile, and the disease state of the host under several conditions. First, we should investigate how *Mtb*'s growth is impacted by Med16. This could be a simple ex vivo experiment comparing growth between WT macrophages, Med16 KO macrophages, and RFX5 KO macrophages, a known MHCII regulator,

both with and without IFNγ. While ex vivo studies will answer a subset of questions, it is essential to also devise strategies in vivo to understand the impact of Med16 on *Mtb* growth, Immune cell profiles, cytokine profiles, and overall host disease state. Unfortunately, knocking out Med16 results in lethality of the mouse, however we could get around this using adoptive transfer techniques that are common in *Mtb* infection studies. Naïve CD45.2 TCR transgenic T cells would be transferred into a CD45.1 mouse. WT and KO macrophages would be treated with IFNγ or left untreated and then infected with YFP-*Mtb* and injected into the mouse using IT transfer. In this one experimental set-up we could determine *Mtb* growth levels, T-cell activation, and the recruitment of immune cells. This would be an informative study that would characterize the role of Med16 in controlling several aspects of TB disease progression in one model.

What are the distinct roles of GSK3α and GSK3β in the regulation of IFNγ responses in macrophages?

Beyond Med16, there remains significant questions about the shared and distinct functions of the GSK3 isoforms, GSK3α and GSK3β in terms of MHCII expression and macrophage function. GSK3α and β share 98% homology, but despite their similarities are not completely redundant [16]. In Chapter 2, we identified an interesting distinction between the function of GSK3α and GSK3β when comparing the results of a GSK3β KO with cells treated with CHIR99021, an inhibitor of both GSK3α/β. GSK3α did not appear in our CRISPR Cas9 screen but seems to partially compensate for the loss of GSK3β when it comes to MHCII expression. The differences between GSK3α and GSK3β in the regulation of MHCII expression remain unclear. We hypothesize that GSK3α compensates for the loss of GSK3β, however is this compensation enough to recover disease outcome? First, it would be interesting to compare global genetic profiles of GSK3α KO macrophages vs GSK3β KO macrophages with and

without IFNγ treatment. This would provide a clear understanding of the distinct roles between GSK3α and β in response to IFNγ in macrophages. Next, is the GSK3α compensation enough to influence disease state? We found that our MHCII expression data directly correlates with T cell activation meaning that KO GSK3α/β together causes more limitation that GSK3α or β alone and KO GSK3β alone causes more restriction that what was observed when GSK3α is KO. While there are differences, it is unclear exactly how much activation is needed to alter the disease state in vivo. Together, these findings will allow us to better understand the distinct roles between GSK3α and GSK3β in IFNγ responses thus helping us understand if they are both or individually better to target given their overlapping and distinct functions.

Dissecting novel regulators of MHCII expression

While Chapter 2 focuses on Med16 and GSK3β, we also identified several other genes and pathways that had yet to be associated with the regulation of IFNγ signaling. These genes and pathways would be interesting to continue validating individually but also in combination. We found that GSK3 and Med16 function independently in their role in MHCII but given their shared effects we had hypothesized that their roles could share the same pathway. While this was not the case for these two genes, this could be possible with others. There are 13 other positive regulatory genes from the screen that have been validated and found to limit MHCII expression after IFNγ stimulation that would be interesting to follow up on. These genes include: Arl8a, Hexim1, Ssaf, Sirt1, Strap, Ppmb1, RNF215, Leprotl, Senp1, Hspa13, Tax1bp1, Vim, and Tfap4. By following up on these other genes we would likely identify additional regulators, but also possible novel combinatory regulation mechanisms. In addition to the positive regulators, we also have a population of negative regulators that have yet to be validated or investigated. These are genes that increase MHCII when they are knocked out, or genes that potentially suppress

MHCII when active. It is important to investigate these genes to further understand MHCII regulation, IFNγ-dependent gene regulation, and potential targets for host directed therapies. We should follow up on these additional genes using similar methods to what was used for GSK3β and Med16. The role of these genes in MHCII and other macrophage surface molecules could be determined using flow cytometry and qRT-PCR. Next, we would want to quantify T-cell activation in response to macrophages with each distinct knockout. Lastly, we could broaden our understanding of each KO using additional techniques including cytokine profiling and RNAseq to explore additional regulators of MHCII. [17]

Defining the targeting potential of identified regulators by enhancing gene expression

All of the studies shared here have been inhibitory, but how would increasing the regulators that we have identified modulate MHCII expression, T cell activation, and eventually disease state? The long-term goal and reason to identify novel regulators is to find potential targets for host-directed therapy, whether that be to inhibit or augment their function. It is easy to say that removing GSK3 limits MHCII, so increasing GSK3 must drive MHCII, but that is not yet clear. We do not know if increasing GSK3 will sufficiently drive MHCII and T-cell activation at all, if it will drive them enough to alter disease state, or if it'll drive activation too much leading to T cell exhaustion and tissue damage. We can investigate this using a genetic tool recently optimized in our lab called the synergistic activation mediator, or SAM. The SAM system is a gain-of-function genetic tool that drives transcription using a catalytically inactive Cas9 that is coupled to transcriptional activation machinery [17]. Using SAM we can induce the expression of targeted genes that may otherwise be off or low. This allows us to investigate how increasing the expression of our identified regulators impacts the expression of MHCII, overall macrophage function, and more.

Defining IFNγ-dependent macrophage responses in vivo

In Chapter 3 I introduce the FLAM cells and provide further data that supports their use as an alveolar macrophage model [18]. Historically, AMs have been challenging to work with. Mice yield a very small quantity of cells requiring many sacked mice for big experiments and once isolated primary AMs are only viable for a short time [19]. FLAMs allow us to limit the number of mice and increase the length of time that we can work with a batch of isolated cells [18]. Though the impact of my dissertation work is really focused on the host response to *Mtb* infection, the majority of our findings are ex vivo models that identify key regulatory patterns without the involvement of a specific pathogen. This was done for the purpose of gaining a broad understanding of IFNγ function and allows us to use these findings in different infection models in the future and not be limited to one pathogen. That being said, I have several goals for this project regarding the models and infections that are used to study key IFNγ-dependent regulators important in different macrophage types. We have yet to determine how GSK3 impacts the critical role of IFNγ during *Mtb* infection. I would be interested in following up on GSK3α/β in a similar way to what I have proposed for Med16 in terms of infection. I'd first be curious how the loss of GSK3α, GSK3β, and GSK3α/β impact *Mtb* growth. This could be investigated first ex vivo to observe initial differences. In parallel, I am curious how the loss of GSK3 impacts the growth of other pathogens. We know that IFNγ is critical for the control of *Mtb* infection, but we also understand its importance in controlling other infections such as *Chlamydia* [20], *Salmonella* [21,22], and *Listeria* [23]. Salmonella actually targets GSK3 to direct macrophage polarization during infection suggesting that pathogens are able to manipulate this pathway directly [24]. Does GSK3-dependent IFNγ signaling serve the same purpose and cause the same phenotype regardless of pathogen or is it pathogen specific? I anticipate that initially the function of IFNγ is the same,

however diverse environments and varying evasion tactics of these pathogens will cause differential regulation and differential disease outcomes. Given the differences that we have seen between IFNγ and CHIR treated iBMDMs and FLAMs, it will also be important to consider the type of macrophage used to investigate each pathogen. I expect that after introducing a pathogen to these studies we will continue to see variation by macrophage type. To really understand the role of GSK3 in *Mtb* infection we would also need to study these conditions in vivo. Knocking out GSK3 is embryonically lethal, however we have a collaborator, Dr. Jim Woodgett, who has developed mice with floxed alleles for both GSK3α and GSK3β that are viable [25]. Additionally, these mice can be bred with promoter-specific Cre-recombinase mice for cell-specific deletions. Our lab is currently generating GSK3α, GSK3β, and GSK3α/β KO mice by breeding these mice with LysM-Cre specific mice that express Cre in macrophages. Once generated, these mice can be infected with *Mtb*, or other pathogens, to investigate the specific role of GSK3α, β, and α/β in *Mtb* infection and in the IFNγ-dependent control of infection. Important effects to consider in these experiments include *Mtb* growth, immune cell profiling, cytokine quantification, and overall disease state of the host.

How consistent are IFNγ response across a diverse population?

One last tool that would be interesting to use in the modeling of these experiments that would broaden the impact of our phenotypes and provide additional information about the specificity of IFNγ responses is to use collaborative cross murine cell lines [26–28]. Pathogenic infections differ from host to host, those infected with *Mtb* experience a range of disease outcomes. The reasons for such variability during infection are not clear. To understand the potential of our discovered targets, we must consider the heterogeneity within a population. This considered, it is important to think about the implications of our findings across a diverse

population rather than a couple of controlled cell lines. Models are often the Achilles heel of biological experiments, given the limitations of replicating the human population. Currently, the collaborative cross murine model system is the best model available to recapitulate genetic diversity across a population. CC strains are derived from eight founder mouse strains that include 5 inbred strains and 3 wild-derived strains using a funnel breeding strategy followed by inbreeding [27]. The CC line has proven useful for infection studies to look at immune responses [29–31]. These lines have also been shown to be representative of the vast T cell diversity found in humans [32]. Together, it would be interesting to complete the proposed in vivo studies using the heterogeneity of the CC mice to determine the consistency of IFNγ responses across a diverse population.

How does metabolism drive IFNγ responses?

Outside of model systems, there is one last arm of this work that I would have liked to advance further during my time at MSU, and that is how IFNγ impacts metabolism and the direct impact of those changes on the host immune response. When the CRISPR Cas9 screen from Chapter 2 was completed, there were 2 additional screens done in parallel looking at IFNγ induced CD40 and PDL1 [33]. This provided a broad understanding of the regulators important for IFNγ-inducible T cell stimulatory or inhibitory proteins. One shared finding from these screens was the importance of complex I of the mitochondrial respiratory chain for all 3 markers, thus its importance in the IFNγ signaling pathway [33]. But how does IFNγ modulate metabolism in different cell types, is that contributing to the phenotypes we have observed, and how does GSK3 impact this modulation? In FLAMs we have found that IFNγ stimulation increases oxygen consumption rate (OCR) and extracellular acidification rate (ECAR), but when cells are treated with both CHIR and IFNγ, OCR and ECAR are limited to nearly untreated levels. This suggests

that GSK3 directly modulates both oxidative phosphorylation (OXPHOS) and glycolysis of FLAMs. In iBMDMs, IFNγ also increases OCR and ECAR, however CHIR IFNγ treatment does not limit OCR in iBMDMs and minimally restricts ECAR. Together these data show that IFNγ increases both OXPHOS and glycolysis in both FLAMs and iBMDMs and that GSK3 differentially regulates metabolism depending on cell type. But the bigger question here is, are these metabolic differences the reason behind our differential phenotypes and what are the mechanisms. We investigated the possibility of the mTOR pathway, which appeared in our MHCII screen and has been shown to modulate GSK3 activity. However, we found that while mTOR is important for IFNγ-dependent MHCII expression, it acts independently of GSK3. Given that both GSK3 and IFNγ have been shown to be important in metabolism, but both with varying results that seem to be highly context dependent and complex, I think it would be best to follow up using LC/MS to quantify metabolites under several conditions and using both cell types. This would indicate which specific metabolites are active with IFNγ stimulation, GSK3 inhibition, and combined treatments providing a high-level view of the metabolic differences. From there we could investigate specific mechanisms to identify if metabolic shifts are responsible for the differences that we see between iBMDMs and FLAMs.

In this dissertation we dissect the complexities of macrophage responses during infection and disease. While this work stands alone in terms of further defining macrophage immune responses, this also serves as the foundation for several additional studies that will define macrophage defense strategies and how to effectively target these mechanisms for host directed therapy. The beauty of this work is that while *Mtb* drove our investigative reasoning, our findings can be applied to other intracellular pathogens, lung infections, and respiratory diseases. Here, we found that IFNγ responses differ between lung resident and recruited macrophage

populations, which prompts the question if IFNγ is a good target for host directed therapy and if so, how do we target specific responses in distinct macrophage types? We know that simply increasing IFNγ is suboptimal and can actually drive T-cell exhaustion and tissue damage, so additional understanding of specific IFNγ regulatory mechanisms is needed to target IFNγ with the finesse that will limit infection and halt disease progression. Additionally, we found that GSK3 has a very specific role in driving co-stimulatory molecules in IFNγ treated FLAMs. Broadly, this identifies major differences between AMs and BMDMs in terms of how their inflammatory responses are regulated; this really drives the importance of acknowledging distinctions between different macrophage populations when conducting host defense studies. Together, we have identified key distinctions in macrophage responses and functions during inflammation, driving the importance of distinct macrophage populations during infection and disease.

REFERENCES

1. Zink, A. R. *et al.* Characterization of Mycobacterium tuberculosis Complex DNAs from Egyptian Mummies by Spoligotyping. *J Clin Microbiol* **41**, 359 (2003).

2. Tanimura, T., Jaramillo, E., Weil, D., Raviglione, M. & Lönnroth, K. Financial burden for tuberculosis patients in low- And middle-income countries: A systematic review. *European Respiratory Journal* vol. 43 1763–1775 Preprint at https://doi.org/10.1183/09031936.00193413 (2014).

3. Lönnroth, K., Jaramillo, E., Williams, B. G., Dye, C. & Raviglione, M. Drivers of tuberculosis epidemics: The role of risk factors and social determinants. *Soc Sci Med* **68**, 2240–2246 (2009).

4. Storla, D. G., Yimer, S. & Bjune, G. A. A systematic review of delay in the diagnosis and treatment of tuberculosis. *BMC Public Health* vol. 8 Preprint at https://doi.org/10.1186/1471-2458-8-15 (2008).

5. Ankley, L., Thomas, S. & Olive, A. J. Fighting persistence: How chronic infections with mycobacterium tuberculosis evade T cell-mediated clearance and new strategies to defeat them. *Infect Immun* **88**, (2020).

6. Dockrell, H. M. & Smith, S. G. What have we learnt about BCG vaccination in the last 20 years? *Frontiers in Immunology* vol. 8 Preprint at https://doi.org/10.3389/fimmu.2017.01134 (2017).

7. Tostmann, A. *et al.* Isoniazid and its toxic metabolite hydrazine induce in vitro pyrazinamide toxicity. *Int J Antimicrob Agents* **31**, 577–580 (2008).

8. Girling, D. J. The hepatic toxicity of antituberculosis regimens containing isoniazid, rifampicin and pyrazinamide. *Tubercle* **59**, 13–32 (1977).

9. Singh, M. *et al.* Studies on toxicity of antitubercular drugs namely isoniazid, rifampicin, and pyrazinamide in an in vitro model of HepG2 cell line. *Medicinal Chemistry Research* **20**, 1611–1615 (2011).

10. Guidance for national strategic planning for tuberculosis. *World Health Organization* https://www.who.int/publications/i/item/9789240052055 (2022).

11. Flynn, J. L. *et al. An Essential Role for Interferon Gamma in Resistance to Mycobacterium tuberculosis Infection*. http://rupress.org/jem/article-pdf/178/6/2249/1104362/2249.pdf (1993).

12. Kiritsy, M. C. *et al.* A genetic screen in macrophages identifies new regulators of ifnγ-inducible mhcii that contribute to t cell activation. *Elife* **10**, (2021).

13. Soutourina, J. Transcription regulation by the Mediator complex. *Nature Reviews Molecular Cell Biology 2017 19:4* **19**, 262–274 (2017).

15. Kagey, M. H. *et al.* Mediator and cohesin connect gene expression and chromatin architecture. *Nature 2010 467:7314* **467**, 430–435 (2010).

16. Lai, F. *et al.* Activating RNAs associate with Mediator to enhance chromatin architecture and transcription. *Nature 2013 494:7438* **494**, 497–501 (2013).

17. Woodgett, J. R. & Waterfield, M. Molecular cloning and expression of glycogen synthase kinase-3/factor A. *EMBO J* **9**, 2431 (1990).

18. Konermann, S. *et al.* Genome-scale transcriptional activation by an engineered CRISPR-Cas9 complex. *Nature* **517**, 583–588 (2015).

19. Thomas, S. T., Wierenga, K. A., Pestka, J. J. & Olive, A. J. Fetal Liver–Derived Alveolar-like Macrophages: A Self-Replicating Ex Vivo Model of Alveolar Macrophages for Functional Genetic Studies. *Immunohorizons* **6**, 156–169 (2022).

20. Busch, C., Favret, J., Geirsdóttir, L., … K. M.-B. & 2019, undefined. Isolation and long-term cultivation of mouse alveolar macrophages. *bio-protocol.org*.

21. Naglak, E., Morrison, S., immunity, R. M.-I. and & 2016, undefined. Gamma interferon is required for optimal antibody-mediated immunity against genital Chlamydia infection. *Am Soc Microbiol* **84**, 3232–3242 (2016).

22. Muotiala, A. & Mäkelä, P. H. The role of IFN-γ in murine Salmonella typhimurium infection. *Microb Pathog* **8**, 135–141 (1990).

23. Bao, S., Beagley, K. W., France, M. P., Shen, J. & Husband, A. J. Interferon-γ plays a critical role in intestinal immunity against Salmonella typhimurium infection. *Immunology* **99**, 464–472 (2000).

23. Kernbauer, E. *et al.* Conditional Stat1 Ablation Reveals the Importance of Interferon Signaling for Immunity to Listeria monocytogenes Infection. *PLoS Pathog* **8**, e1002763 (2012).

24. Panagi, I. *et al.* Salmonella Effector SteE Converts the Mammalian Serine/Threonine Kinase GSK3 into a Tyrosine Kinase to Direct Macrophage Polarization. *Cell Host Microbe* **27**, 41-53.e6 (2020).

25. Kaidanovich-Beilin, O. & Woodgett, J. R. GSK-3: Functional Insights from Cell Biology and Animal Models. *Front Mol Neurosci* **4**, 40 (2011).

26. Valdar, W., Flint, J., Genetics, R. M.- & 2006, undefined. Simulating the collaborative cross: power of quantitative trait loci detection and mapping resolution in large sets of recombinant inbred strains of mice. *academic.oup.com*.

27. Roberts, A., Pardo-Manuel De Villena, F., Wang, W., McMillan, L. & Threadgill, D. W. The polymorphism architecture of mouse genetic resources elucidated using genome-wide resequencing data: Implications for QTL discovery and systems genetics. *Mammalian Genome* **18**, 473–481 (2007).

28. Churchill: The Collaborative Cross, a community resource... - Google Scholar. https://scholar.google.com/scholar_lookup?title=The%20Collaborative%20Cross%2C%20a%20community%20resource%20for%20the%20genetic%20analysis%20of%20complex%20traits&author=G%20A%20Churchill&author=D%20C%20Airey&author=H%20Allayee&author=J%20M%20Angel&author=A%20D%20Attie&publication_year=2004&journal=Nat.%20Genet.&volume=36&pages=1133-1137.

29. Noll, K. E., Ferris, M. T. & Heise, M. T. The Collaborative Cross: A Systems Genetics Resource for Studying Host-Pathogen Interactions. *Cell Host Microbe* **25**, 484–498 (2019).

30. Abu Toamih Atamni, H., Nashef, A. & Iraqi, F. A. The Collaborative Cross mouse model for dissecting genetic susceptibility to infectious diseases. *Mammalian Genome 2018 29:7* **29**, 471–487 (2018).

31. Phillippi, J. *et al.* Using the emerging Collaborative Cross to probe the immune system. *Genes Immun* **15**, 38 (2014).

32. Graham, J. B. *et al.* Extensive Homeostatic T Cell Phenotypic Variation within the Collaborative Cross. *Cell Rep* **21**, 2313–2325 (2017).

33. Kiritsy, M. C. *et al.* Mitochondrial respiration contributes to the interferon gamma response in antigen-presenting cells. *Elife* **10**, (2021).

APPENDIX A: TGFβ PRIMES ALVEOLAR-LIKE MACROPHAGES TO INDUCE TYPE I IFN FOLLOWING TLR2 ACTIVATION

DECLARATIONS

Authors

Sean Thomas*[1], Laurisa Ankley*[1], Kayla Conner[1], Alex Rapp[2], Chris Tanner[2], Abigail McGee[2], Joshua Obar[2], Andrew Olive[1]

[1]Michigan State University

[2]Dartmouth College

*Authors contributed equally

Contributions

The following chapter describes the role of TGFβ in the induction of type I IFN responses in alveolar macrophages. JO and AO conceptualized the idea to test the role of TGFβ in alveolar macrophages and how it contributes to IFN responses. LA completed qPCR to characterize FLAMs with and without TGFβ and the experiment for RNAseq. KC did all analysis and figure creation for the RNAseq data. ST conducted all Mtb experiments and KO characterization experiments. AR, CT, and AM completed antagonist experiments exploring CXCL10 phenotypes. AO, ST, and LA wrote the chapter together.

ABSTRACT

Alveolar macrophages (AMs) are key mediators of lung function and are potential targets for therapies during respiratory infections. The cytokine TGFβ is an important regulator of AM maintenance but, how TGFβ directly modulates the innate immune responses of AMs remains unclear. This shortcoming prevents effective targeting of AMs to improve lung function in health and disease. Here we leveraged an optimized *ex vivo* AM model system, fetal-liver derived alveolar-like macrophages (FLAMs), to dissect the role of TGFβ in AMs. Using transcriptional analysis, we globally defined how TGFβ regulates gene expression of resting FLAMs. We found that TGFβ maintains the baseline metabolic state of AMs by driving lipid metabolism and restricting inflammation. To better understand inflammatory regulation in FLAMs, we directly tested how TGFβ alters the response to the TLR2 agonist PAM3CSK4. While both TGFβ (+) and TGFβ (-) FLAMs robustly responded to TLR2 activation we found an unexpected activation of type I interferon (IFN) responses only in TGFβ (+) FLAMs. Follow up studies found that several TLR2 activators, including *Mycobacterium tuberculosis* infection, drive robust type I IFN responses in FLAMs and primary AMs in a TGFβ dependent manner. Further examination of the pathways driving this IFN response determined that the mitochondrial antiviral signaling protein and the interferon regulator factors 3 and 7 were required for IFN production. In contrast, we observed a limited role for aerobic glycolysis in driving IFNs. Together, these data suggest that TGFβ modulates AM metabolic networks and innate immune signaling cascades to control inflammatory pathways in AMs.

INTRODUCTION

The pulmonary space is a specialized environment evolved to facilitate gas exchange and maintain lung function (1, 2). To protect against exposures to airborne microorganisms and particulates, lung alveoli contain a specialized phagocyte population, alveolar macrophages (AMs) (2, 3). These AMs, like many other tissue-resident macrophages, seed the lungs from the fetal liver and serve two primary purposes: to preserve lung homeostasis by maintaining optimal surfactant levels in the lungs and to patrol the alveolar space for inhaled debris, initiating an inflammatory response when necessary (4-6). Given the importance of maintaining pulmonary function, AMs must strictly regulate their inflammatory responses to prevent unnecessary inflammation and tissue damage (7, 8). Compared to other inflammatory macrophages, including bone marrow-derived macrophages (BMDMs), AMs are more hypo-inflammatory against many pathogenic stimuli, a characteristic that is mediated by their distinct ontogeny and the lung environment (8-10). In fact, circulating monocytes that are recruited to the lungs following infection have been shown to adapt to the local environment and take on AM-like phenotypes (11). Two key cytokines, GM-CSF and TGFβ, are known to mediate AM functions in the lung environment (6, 12, 13). While the role of GM-CSF is better understood due to its importance in preventing pulmonary alveolar proteinosis, how TGFβ directly modulates the AM state and function remains unclear, limiting our ability to target AMs and improve lung function in health and disease.

TGFβ exists as three separate isoforms (TGFβ1-3) that all bind to the same TGFβ coreceptors (TGFβRI, TGFβRII) (14). TGFβ-1 is primarily produced by macrophages, but in an inactive form, conjugated with a latency-associated peptide (LAP) (15-17). Inactive TGFβ1 (referred to as TGFβ from here on) is activated following enzymatic, acidic, or receptor-

mediated cleavage of the LAP from TGFβ (17, 18). In the lungs, inactive TGFβ is primarily produced by AMs which is then activated by the alveolar epithelial type II cells (AECII) through the activity of the αvβ6 integrin on alveolar epithelial cells (6, 17). Thus, maintaining AMs requires unique interactions between the lung epithelium and disruptions of this environment results in dysregulated pulmonary responses.

In its active form, TGFβ is a versatile cytokine that triggers Smad complex translocation to the nucleus to drive a multitude of processes, including stem cell differentiation, chemotaxis, and immune regulation, depending on the context in which it is acting (19, 20). Much of this heterogeneity in cellular responses to TGFβ is thought to be due to crosstalk between other transcriptional regulators and epigenetic regulation (21). In the lungs, TGFβ plays critical roles both in lung development and disease. Mice lacking any of the three isoforms of TGFβ or either of the two receptors have varying degrees of deformed lung structure and alveologenesis due to dysregulated interactions between the lung epithelium and mesenchyme during development (22-25). TGFβ is also implicated in the development of idiopathic pulmonary fibrosis (IPF) through its induction of myofibroblast differentiation from lung fibroblasts and suppression of anti-fibrotic factors prostaglandin E2 and hepatocyte growth factor production (26-28). Given the importance of TGFβ to maintain AMs in the lungs it is essential to better understand how TGFβ modulates the inflammatory potential of AMs.

Fully dissecting the role of TGFβ in AM regulation requires *ex vivo* models that faithfully recapitulate key aspects of the lung environment. Recent work by several groups showed that growth of macrophages in both GM-CSF and TGFβ stabilizes the AM-like state for cells grown in culture (29-31). We recently optimized the fetal liver-derived alveolar-like macrophages (FLAMs) model which propagates fetal liver cells in both GM-CSF and TGFβ allowing for long-

term propagation and genetic manipulation of cells that recapitulate many aspects of AM functions (31). Removing TGFβ from these cells results in a loss of the AM-like state such as decreased expression of the key AM transcription factor peroxisome-proliferating activating receptor gamma (PPARγ) and increased expression of the LPS co-receptor CD14. These data suggest that TGFβ not only maintains the AM state but plays an important role in modulating the inflammatory response of AMs.

In this report we directly examine how TGFβ shapes AM function and inflammatory responses. Using transcriptional analysis, we globally defined how TGFβ regulates the gene expression of resting FLAMs, identifying a key role of TGFβ in maintaining the metabolic state of AMs. In parallel, we characterized how TGFβ shapes the inflammatory response of AMs following the activation of toll-like receptor 2 (TLR2), uncovering an unexpected link between TGFβ, TLR2, and type I interferon (IFN). We found that a range of TLR2 agonists, including *Mycobacterium tuberculosis*, drive exacerbated IFN responses in a TGFβ-dependent manner. Further mechanistic studies found this IFN response was not dependent on glycolysis and required the mitochondrial antiviral signaling adaptor (MAVS) as well as the transcription factors interferon regulatory factor 3 and 7 (IRF3/7). These data suggest that TGFβ rewires the metabolic networks in AMs and this activates unique innate immune signaling not observed in other macrophage populations.

RESULTS

TGFβ drives lipid metabolism, restrains cytokine expression, and maintains FLAMs in the AM-like state.

We previously developed FLAMs as an *ex vivo* model of AMs to understand the mechanistic signals and regulatory networks that maintain cells in the AM-like state (31). TGFβ is a key

cytokine needed to maintain AMs *in vivo* and to maintain FLAMs in the AM-like state, yet how TGFβ modulates AM functions and transcriptional networks remains unclear. As a first step, we confirmed that TGFβ is required to broadly maintain the AM-like state in FLAMs. Since PPARγ is a key transcription factor in AMs, and is expressed in AMs and FLAMs, we measured the effect of TGFβ on PPARγ expression (Figure 3.1A) (31). FLAMs were grown in GM-CSF in the presence or absence of TGFβ for two-weeks and the mRNA expression of the transcription factor PPARγ was quantified by quantitative RT-PCR. As expected, FLAMs with TGFβ maintained higher expression of PPARγ, while cells grown in the absence of TGFβ significantly decreased PPARγ expression (6, 31). These data confirm that TGFβ helps maintain FLAMs in an AM-like state long-term.

To better understand how TGFβ globally regulates FLAMs, we next conducted whole-transcriptome RNA sequencing analysis on FLAMs grown in the presence and absence of TGFβ. Differential expression analysis identified hundreds of genes that were significantly changed between FLAMs grown with or without TGFβ (Figure 3.1B). To globally identify pathways that were uniquely enriched in TGFβ (+) FLAMs, we employed gene set enrichment analysis (GSEA), using a ranked gene list generated from the differential expression analysis. Among the top KEGG pathways enriched in TGFβ (+) FLAMs were PPAR signaling, fatty acid synthesis, lipid metabolism, and lysosome pathways (Figure 3.1C). Given that AMs are known to drive PPARγ-dependent lipid metabolism, these data suggest the FLAM transcriptional profile is similar to primary AMs (32, 33). In contrast, pathways enriched in TGFβ (-) FLAMs were related to cytokine and chemokine expression and cell proliferation. We directly compared the expression of a subset of genes related to these pathways and AM signature genes (Figure 3.1C). We found high expression of PPARγ, MARCO, SiglecF in TGFβ (+) FLAMs in addition to lipid

metabolism genes including Acat2, Acat3, and FadS2 (Figure 3.1D). In TGFβ (-) FLAMs, we observed a significant increase in chemokines including CCL2, CCL3, CCL4 and CXCL3 (Figure 3.1D). Taken together these data show that TGFβ maintains metabolic functions of AMs while restraining inflammation in line with previous reports suggesting AMs are hypo-inflammatory (8).

TGFβ mediates a type 1 IFN in AMs following Pam3 Activation.

Since TGFβ (+) FLAMs did not express inflammatory genes as highly as TGFβ (-) FLAMs, we next directly tested the response of these cells to inflammatory stimuli. Many bacterial respiratory infections, including *Mycobacterium tuberculosis*, activate TLR2 signaling during infection (34, 35). Thus, we examined how the activation of TLR2 with the purified agonist Pam3CSK4 (referred to as Pam3) differentially alters the transcriptome of FLAMs in a TGFβ-dependent manner. TGFβ (+) and TGFβ (-) FLAMs were stimulated with Pam3 for 18 hours, then, RNA sequencing and differential expression analysis was used to identify changes in the transcriptional landscape. We identified hundreds of genes that were significantly altered following Pam3 activation of TGFβ (+) FLAMs compared to untreated TGFβ (+) FLAMs (Figure 3.2A) and Pam3 activated TGFβ (-) FLAMs (Figure 3.2B). We were curious as to what pathways were enriched in TGFβ (+) FLAMs compared to following PAM activation to identify TGFβ -dependent and perhaps, AM-specific immune signaling (Figure 3.2A). Using GSEA we found an unexpected enrichment in pathways related to IFN signaling (Figure 3.2C). When we examined the entire IFN hallmark pathway across all conditions we only observed robust induction of IFN-related genes in Pam3 activated TGFβ (+) FLAMs (Figure 3.2D). This finding suggests that while TGFβ restrains several inflammatory cytokines following Pam3 stimulation, TGFβ skews the macrophages response to drive the activation of IFN pathways.

To further understand the role of nucleotide sensing in the TLR2 response of TGFβ (+) FLAMs, we next directly examined the normalized reads of IFNβ and two other interferon-stimulated genes (ISGs) (Figure 3.3A). While we observed similar baseline expression of IFNβ1, CXCL10 and Rsad2 between conditions, TGFβ (+) FLAMs induced significantly higher expression of all three genes following Pam3 activation. To corroborate the RNA sequencing results, we compared the secretion of cytokines in resting and Pam3-activated TGFβ (+) and TGFβ (-) FLAMs using a multiplex Luminex assay (Figure 3.3B). In agreement with our transcriptional results, we observed a significant increase in IFNβ1 and CXCL10 in Pam3-activated TGFβ (+) FLAMs compared to TGFβ (-) FLAMs. We next confirmed this phenotype occurs in primary AMs by isolating cells from the lungs and activating them with Pam3 and examining the production of IFNβ by ELISA (Figure 3C). In line with our results in FLAMs, we observed a significant increase in IFNβ in AMs following activation with Pam3. These data confirm that TGFβ signaling in AMs drives the production of type I IFN following Pam3 stimulation.

TGFβ mediates TLR2-dependent type 1 IFN activation in AMs.

Pam3 is a potent TLR2 agonist, so we hypothesized that other TLR2 activators would similarly drive the production of type I IFNs in TGFβ (+) FLAMs. To test this, we stimulated TGFβ (-) and TGFβ (+) cells with the known TLR2 activators Peptidoglycan and Zymosan. Since Zymosan can activate cells through both TLR2 and Dectin1, we also tested depleted Zymosan and curdlan that will only activate cells through Dectin1. 18 hours after activation with each agonist, we measured the CXCL10 by ELISA as a marker for IFN production (Figure 3.4A). We observed that both Peptidoglycan and Zymosan stimulations of TGFβ (+) FLAMs resulted in a significant increase in CXCL10 production compared to TGFβ (-) FLAMs.

However, we observed no significant induction of CXCL10 following activation with depleted Zymosan or curdlan. We next infected TGFβ (-) and TGFβ (+) FLAMs with *Mycobacterium tuberculosis*, a known activator of TLR2, and quantified the production of IFNβ (Figure 3.4B) and CXCL10 (Figure 3.4C) using a multiplex Luminex assay the following day (35). We found that infection of TGFβ (+) FLAMs resulted in a significant increase in both IFNβ and CXCL10 compared to TGFβ (-) FLAMs.

Since our results suggested that TLR2-dependent activation drives the increased IFN response in TGFβ (+) FLAMs, we next directly tested this using TLR2-/- FLAMs. Wild type and TLR2-/- TGFβ (+) FLAMs were stimulated with Pam3 and the following day IFNβ was quantified in the supernatants by ELISA. While wild type TGFβ (+) FLAMs robustly induced IFNβ, this was lost in TLR2-/- FLAMs. Taken together these results suggest that TGFβ signaling in FLAMs drives a unique response to TLR2 activation that results in the production of type I IFN.

MAVS and IRF3/7 but not aerobic glycolysis contribute to TGFβ-dependent Type I IFN responses.

We next wanted to better understand the pathways driving the TGFβ-dependent type I IFN response. One key type I IFN production pathway is mediated by the mitochondrial antiviral-signaling protein (MAVS) which triggers the activation of the transcription factors interferon regulatory factors 3 and 7 (Irf3/Irf7) to mediate the transcription of IFNβ (36, 37). To test the role of these genes in controlling TGFβ-dependent IFN responses, we used our previously described CRISPR-Cas9 editing approaches in FLAMs to target *Mavs, Irf3* and *Irf7* with individual sgRNAs (Figure 3.5A) (31). We then left cells untreated or stimulated TGFβ (+) wild type, TLR2-/-, sgMAVs, sgIrf3, and sgIrf7 FLAMs with zymosan, depleted zymosan, or

LyoVec-complexed Poly I:C and quantified secreted IFNβ the following day. We observed that wildtype FLAMs induced IFNβ in all conditions, except following depleted zymosan stimulation. In contrast, for all stimulations, we found significantly reduced IFNβ from sgMAVs, sgIrf3, and sgIrf7 FLAMs. These data suggest that TGFβ-dependent, TLR2-mediated type I IFN responses are controlled by MAVS and Irf3/Irf7.

A previous report showed that MAVS signaling is regulated by lactate produced through glycolysis (38). Given the expression differences in key metabolic pathways we observed between TGFB- and TGFβ (+) FLAMs, we wondered whether differential metabolic regulation of MAVS may explain differences in the type I IFN response. As a first step, we tested whether direct activation of the MAVS pathway with poly I:C would result in differential type I IFN between TGFβ (+) and TGFβ (-) FLAMs (Figure 3.5B). We observed that TGFβ (+) FLAMs induced significantly more CXCL10 compared to TGFβ (-) FLAMs, suggesting increased activity of the RIG-I/MAVS signaling pathway. We next tested whether inhibiting lactate dehydrogenase and thus, reducing intracellular lactate levels would alter the TGFβ-dependent type I IFN response in FLAMs. FLAMs grown with and without TGFβ were transfected with poly I:C with increasing levels of Oxamate and the following day we quantified CXCL10 in the supernatants (Figure 3.5C). We observed a dose-dependent decrease in CXCL10 production in TGFβ (-) FLAMs suggesting the IFN response in these cells is dependent on aerobic glycolysis. In contrast, we observed no significant effect of oxamate on the high CXCL10 production found in TGFβ (+) FLAMs. Taken together these data suggest that TGFβ-dependent type I IFN responses in FLAMs is independent of changes in aerobic glycolysis.

FIGURES

Figure 3.1. TGFβ drives lipid metabolism, restrains cytokine expression, and maintains FLAMs in the AM-like state. (A) PPARγ transcription was quantified by qRT-PCR using $2^{(-DDCT)}$ relative to GAPDH in untreated (+) and (-) TGFβ FLAMS. Each point represents a technical replicate from one representative experiment of 3. **p<.01 by unpaired students t-test. **(B)** Differentially expressed genes were identified between untreated (+) and (-) TGFβ FLAMS. Red points represent significantly underexpressed genes and blue points represent significantly overexpressed genes between (+) and (-) TGFβ FLAMs. Each point represents the mean of three biological replicates from one experiment. DeSeq2 was used to determine significance using the adjusted p-value to account for multiple hypothesis testing. **(C)** Expression of genes from three pathways that are enriched between untreated (+) and (-)TGFβ FLAMs and a subset of AM-signature genes. Each column is representative of one technical replicate. **(D)** Gene expression was quantified from normalized counts for key genes important in lipid metabolism, inflammation, and TGFβ signaling. Each point represents a technical replicate from one experiment. *** adjusted p-value <.001 using DeSeq2 analysis.

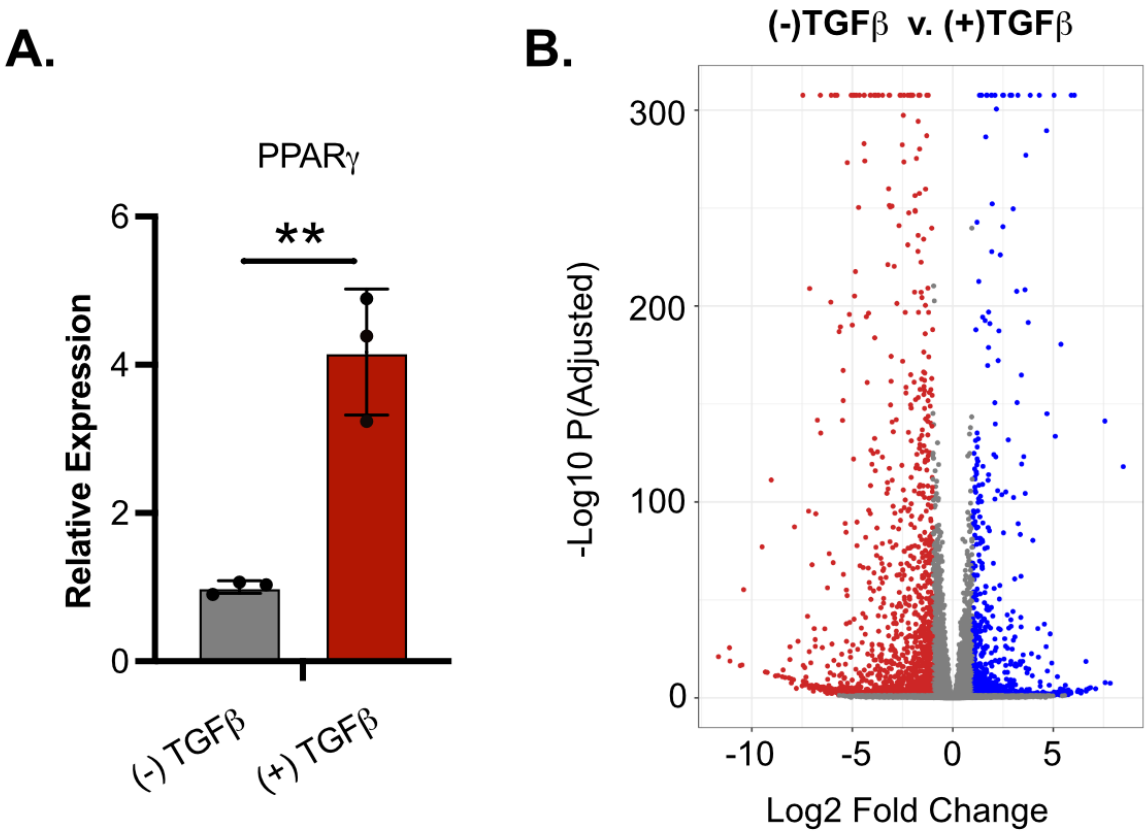

Figure 3.1 (cont'd)

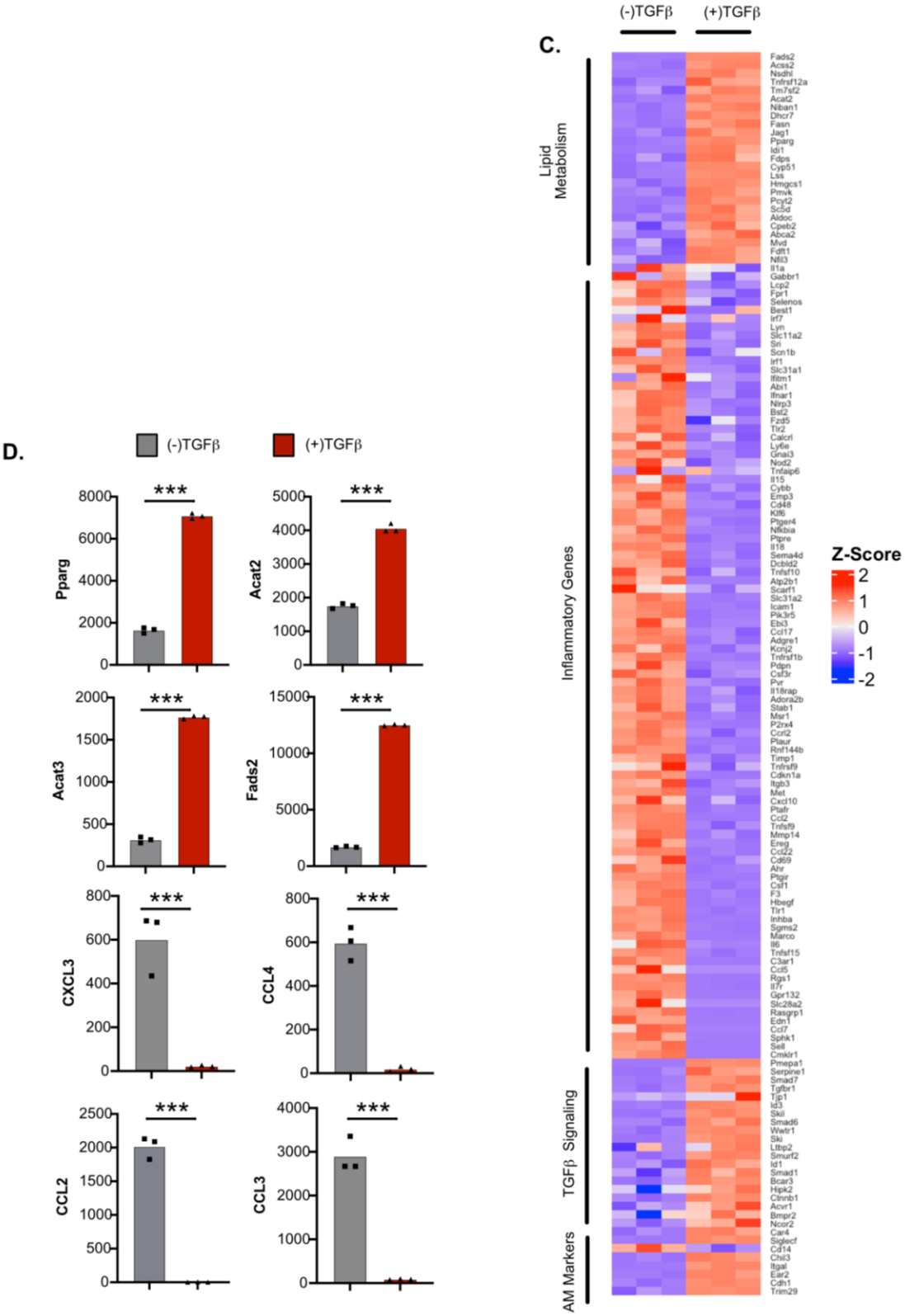

Figure 3.2. TGFβ mediates cytosolic DNA sensing and type 1 IFN responses during TLR2 activation. (A) Differentially expressed genes were identified between +TGFβ FLAMs (+) and (-) Pam3 treated for 6 hours. Red points represent underexpressed genes and blue points represent overexpressed genes between (+) and (-) TGFβ FLAMs. Each point represents the mean of three biological replicates from one experiment. **(B)** Differentially expressed genes were identified between (+) and (-) TGFβ FLAMs treated with Pam3 for 6 hours. Red points represent underexpressed genes and blue points represent overexpressed genes between (+) and (-) TGFβ FLAMs. Each point represents the mean of three technical replicates from one experiment. **(C)** Leading edge analysis of the IFN hallmark Pathway comparing Pam3 activation in (+) and (-) TGFβ FLAMs **(D)** Expression of genes representing the IFN hallmark pathway between (+) and (-) TGFβ FLAMs that have or have not been treated with Pam3. Each column represents a biological replicate from one experiment.

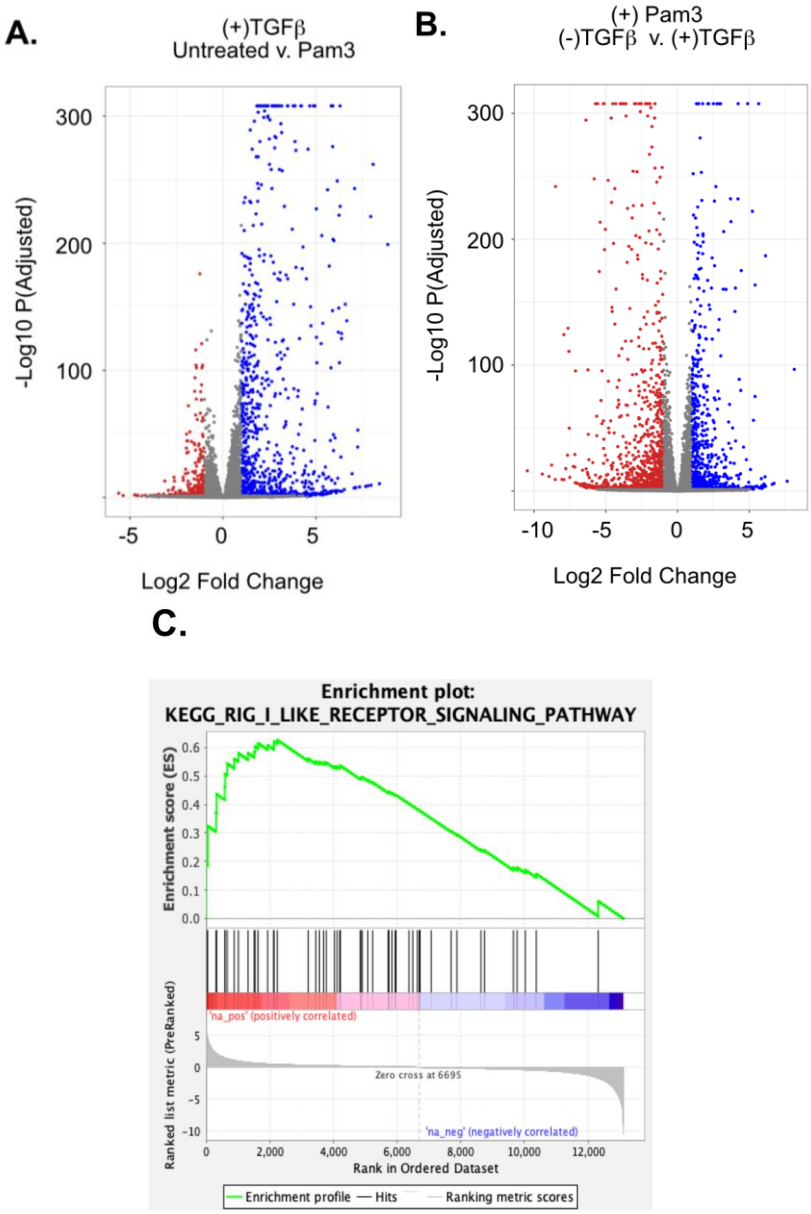

Figure 3.2 (cont'd)

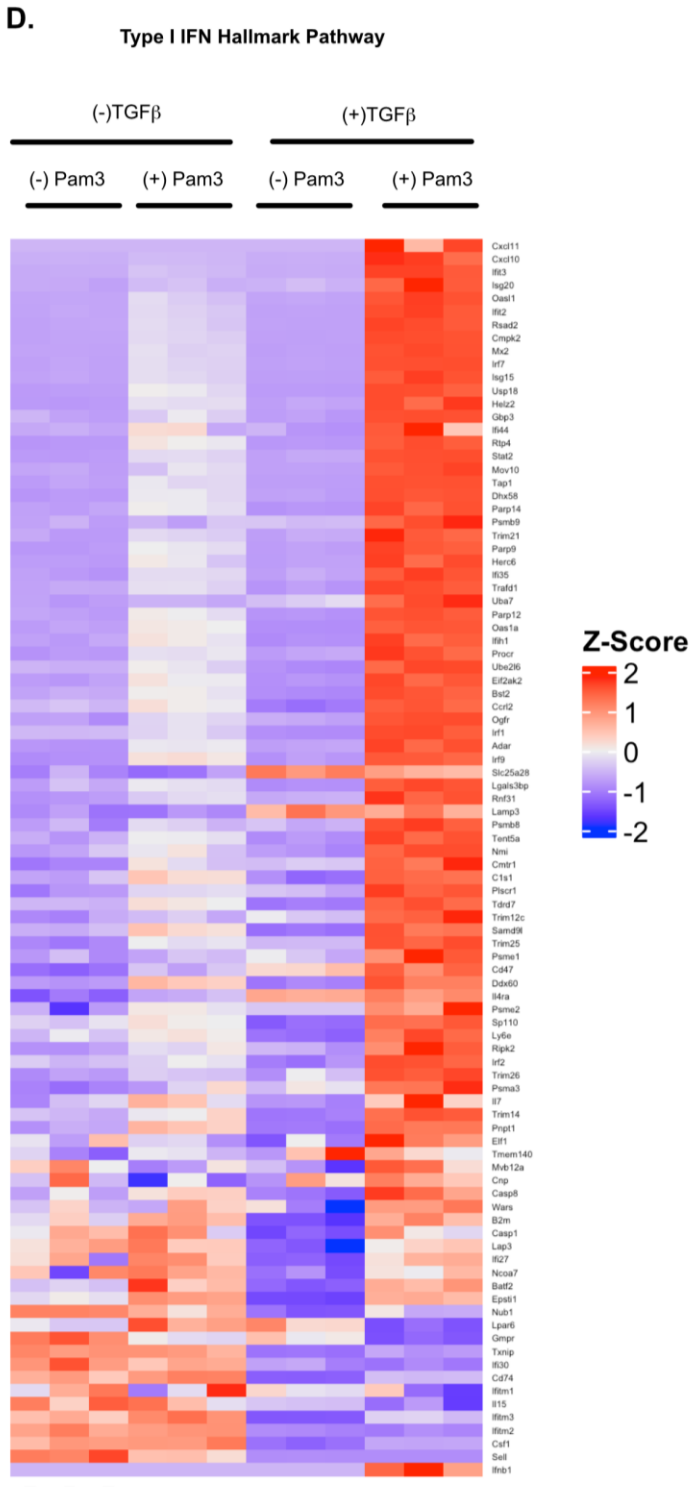

Figure 3.3. IFNβ and ISG transcription and secretion is heightened in Pam3-activated AMs and FLAMs cultured with TGFβ. (A) Normalized read counts from IFNβ, Rsad2 and CXCL10 from Pam3 RNA sequencing experiment. *** adjusted p-value <.001 using DeSeq2 analysis. **(B)** (+) and (-) TGFβ FLAMs were stimulated with Pam3 for 24hrs. Supernatants were collected and IFNβ, CXCL10 were quantified by Luminex cytokine assay. **(C)** Primary AMs were stimulated with Pam3 and IFNβ was quantified by bioluminescent ELISA the following day. Shown is one representative experiment of two with 3 replicates per experiment. **p<.01 by unpaired students t-test.

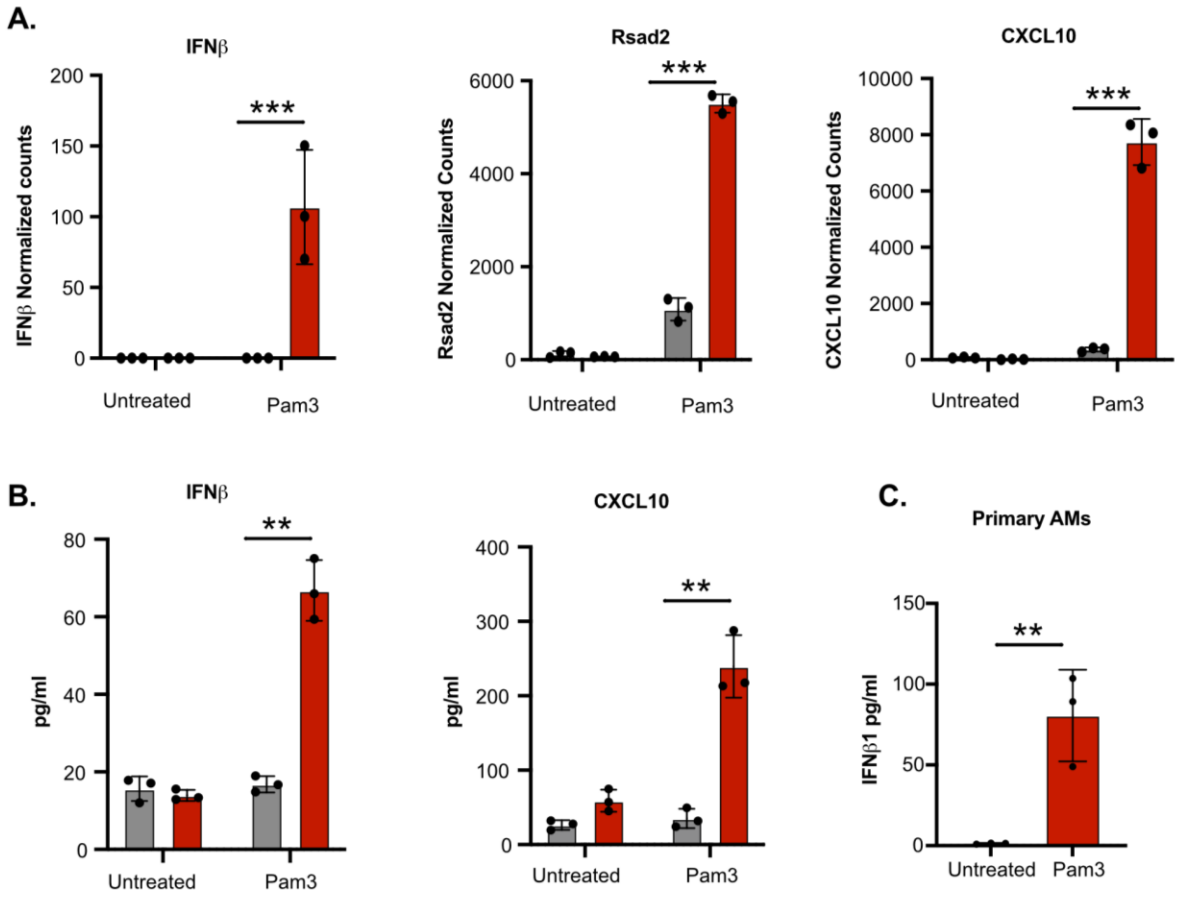

Figure 3.4. TLR2-dependent activation of type 1 IFN pathways in (+) TGFβ FLAMs is conserved among physiologically relevant TLR2 agonists. (A) (+) and (-) TGFβ FLAMs were stimulated with 50ug/ml Peptidoglycan, Zymosan, Zymosan Depleted, or Curdlan for 24hrs. CXCL10 was quantified by ELISA. **(B and C)** (+) and (-) TGFβ FLAMs were left uninfected or infected with Mtb H37Rv at an MOI of 5 for 24hrs. **(B)** IFNβ and **(C)** CXCL10 were quantified by Luminex multiplex assay. **(D)** WT FLAMs, TLR2-/- FLAMs, and Primary AMs were stimulated with Pam3 for 24hrs. Secreted IFNβ was quantified by bioluminescent ELISA. Each point represents data from a single well from one representative experiment of three. ****p<.0001 ** p<.01 by one-way ANOVA with a tukey test for multiple comparisons.

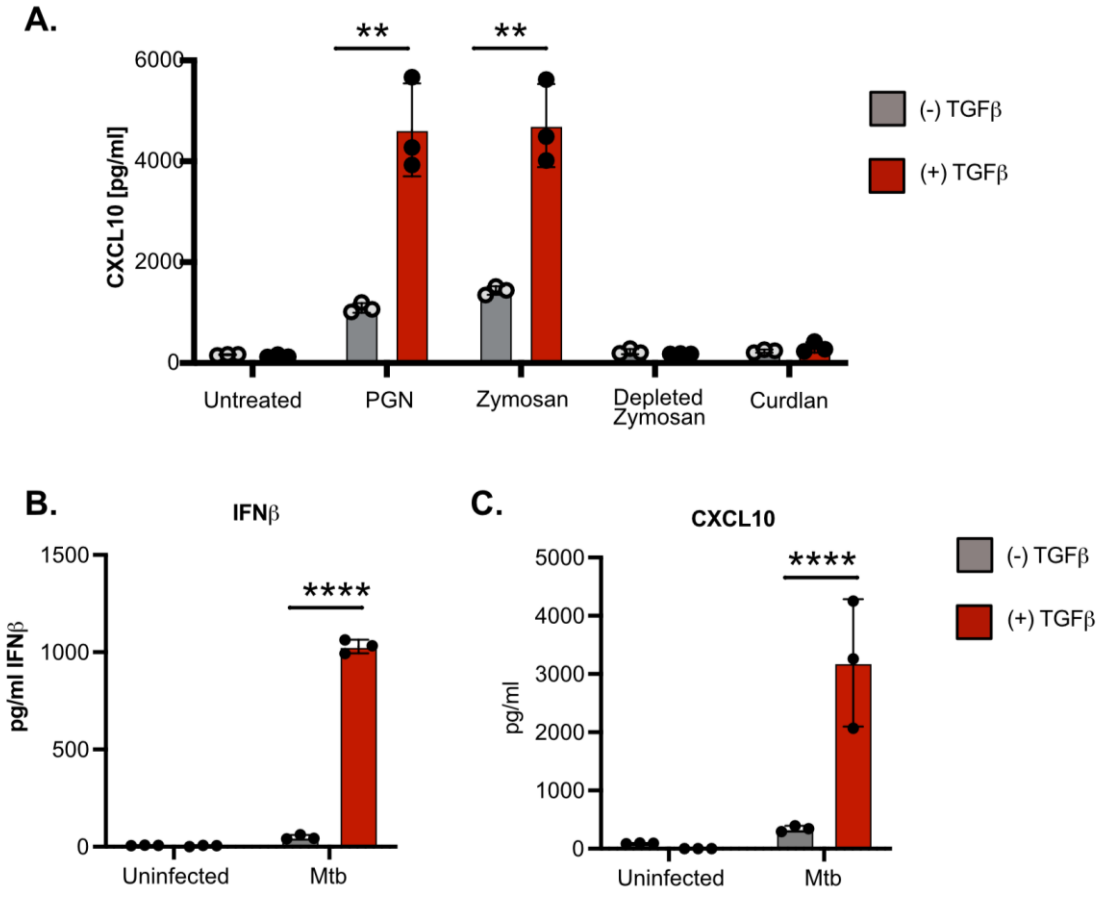

Figure 3.4 (cont'd)

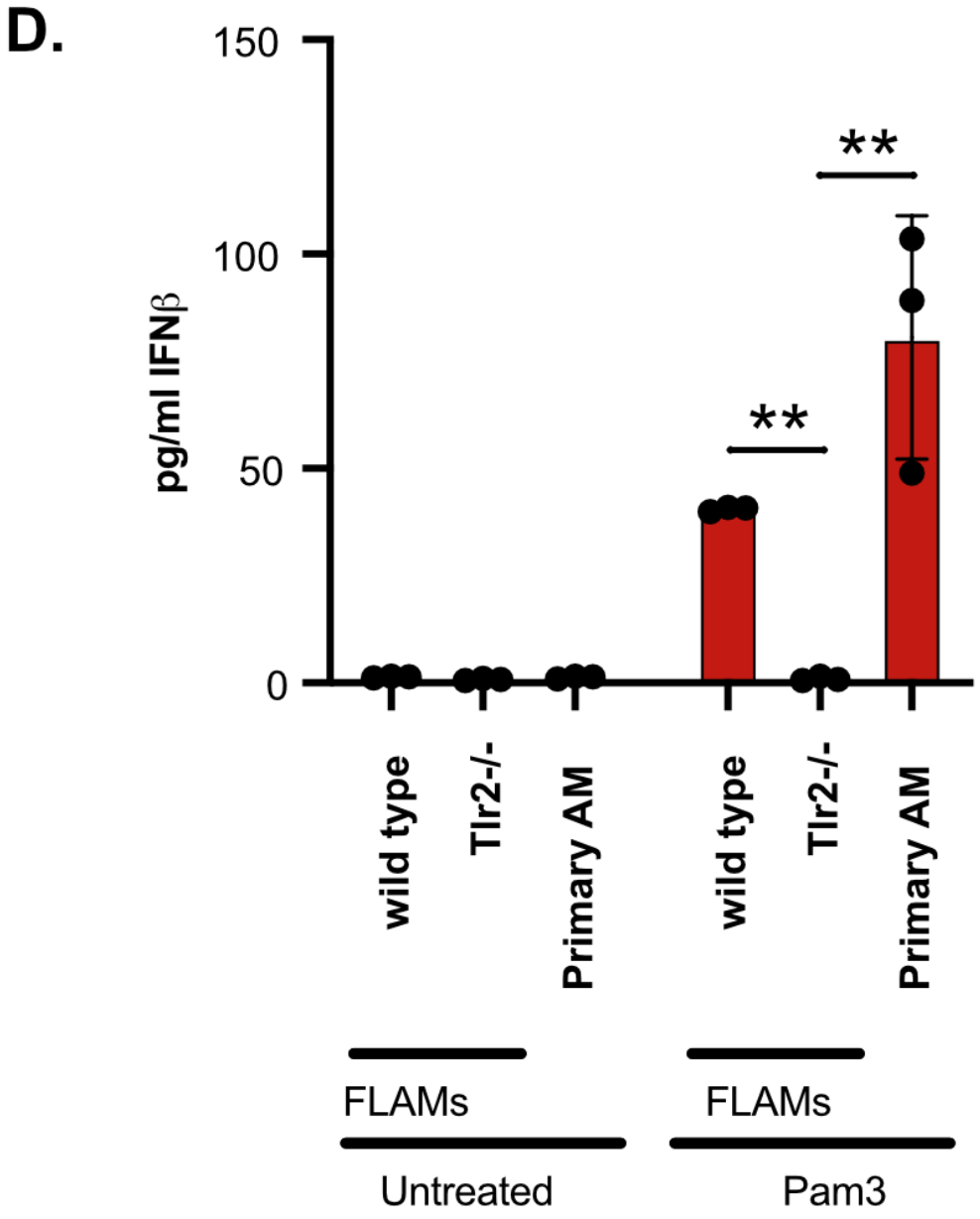

Figure 3.5. MAVS and IRF3/7, but not aerobic glycolysis, contribute to TGFβ-dependent Type I IFN responses. (A) Wild type, sgMAVS, sgIRF3, and sgIRF7 FLAMs were stimulated with Zymosan, Zymosan Depleted, and poly I:C for 24hrs. Secreted IFNβ was quantified by bioluminescent ELISA. **(B)** (+) and (-) TGFβ FLAMs were treated with poly I:C for 24hrs. Secreted CXCL10 was quantified by ELISA. **(C)** (+) and (-) TGFβ FLAMs were stimulated with complexed poly I:C and left untreated or treated with Oxamate. Secreted CXCL10 was quantified by ELISA. Each point represents data from a single well from one representative experiment of three. *** p<.001, ** p<.01 by one-way ANOVA with a tukey test for multiple comparisons.

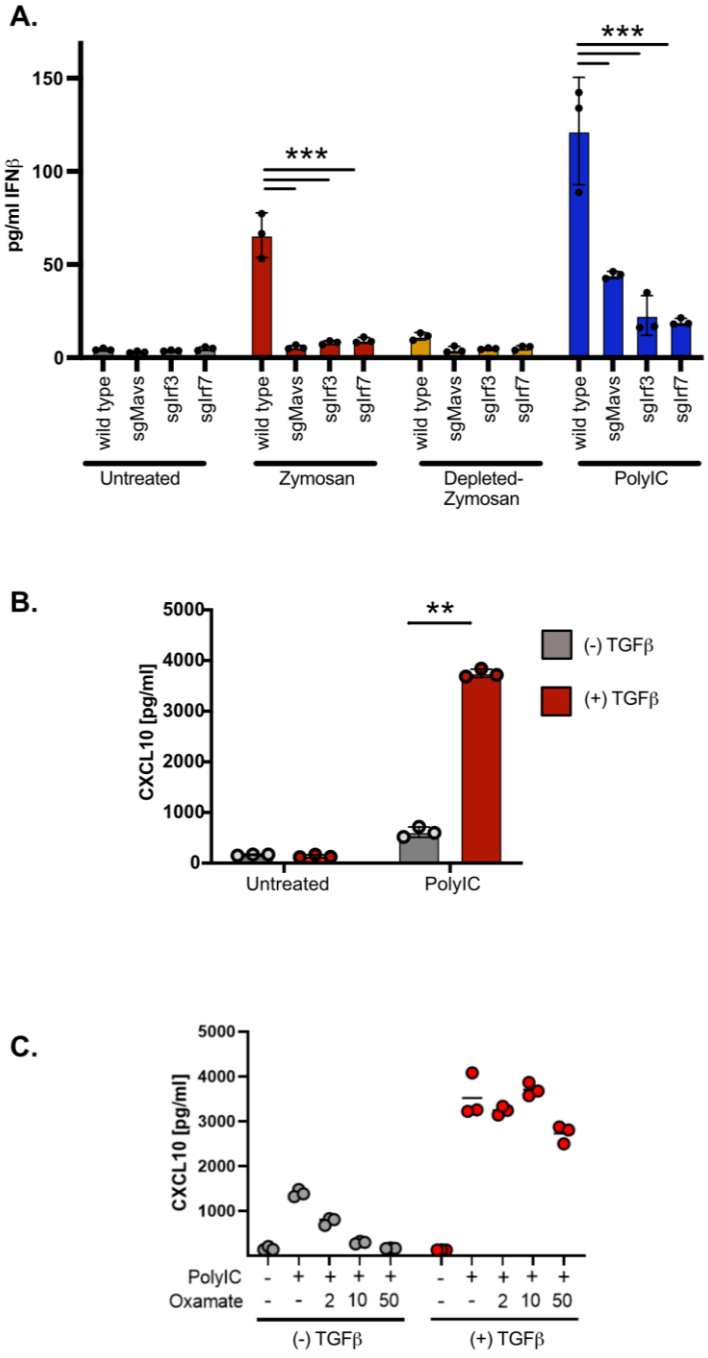

DISCUSSION

TGFβ signaling is essential for alveolar macrophage (AM) development and homeostasis in the lung environment (6). How TGFβ regulates distinct functions of AMs and their response to external stimuli remains unclear. Here, we leveraged an *ex vivo* model of AMs, known as FLAMs, to dissect transcriptional changes in AM-like cells that are mediated by TGFβ. We found that while TGFβ restrains a subset of inflammatory pathways, TGFβ also primes AMs for a type I IFN (IFN) response following TLR2 activation. These results suggest that distinct innate immune signaling networks in AMs are regulated by the tissue environment and directly alter the inflammatory response following the activation of TLR2.

While our findings suggest an unexpected link between TLR2 and IFN in AMs, how TLR2 activates IFN remains an open question. Several pattern recognition receptors (PRRs), including TLR3, TLR7 and TLR9 activate IFNs through the activation of IRF3 or IRF7, but these PRRs are localized to the endosome and generally respond to viral ligands (39, 40). In contrast, TLR2 is present on both the surface and in the endosome, similar to TLR4. Previous studies showed that TLR4 signaling through the plasma membrane drives Myd88-dependent NFkb activation while signaling through the endosome activates a TRIF dependent IFN response (41). Whether the localization of TLR2 drives the IFN response in TGFβ cultured AMs and the contribution of the adaptors, Myd88 and TRIF, to the response will need to be determined. While several previous studies suggest TLR2 can activate IFNs, the ligands and cell types capable of this response remain controversial (42-45). For example, Barbalat et al showed BMDMs can make IFN in response to viral ligands but not bacterial ligands, while Dietrich et al. showed BMDMs can make IFN following activation with bacterial ligands (43, 44). Our data support the role of bacterial and fungal TLR2 ligands in activating an IFN response in AMs that is dependent

on TGFβ signaling. FLAMs grown in the absence of TGFβ did not robustly induce IFNs following TLR2 activation. Our genetic studies found that IRF3, IRF7, and MAVS were all required for the TLR2-activated IFN response. This suggests TLR2-mediated IFN may activate parallel pathways, one dependent on direct signaling through MyD88/TRIF, and a second dependent on the cytosolic nucleotide sensing pathways dependent on MAVS. Given that we observed exacerbated IFN responses in TGFβ (+) FLAMs following direct activation of MAVS by poly I:C treatment, our data support a model where TGFβ primes AMs to enhance the activation of MAVS-dependent IFN production.

The mechanisms underlying TGFβ priming IFN responses remain unknown. TGFβ is known to activate PPARγ and fatty acid oxidation, which we confirmed through our transcriptional analysis (6). Previous studies have linked cellular metabolism and type I IFN production. Both cholesterol biosynthesis and glycolysis byproducts such as lactate are known to regulate the magnitude of the type I IFN response in BMDMs (38, 46). However, when lactate levels were modulated with the pyruvate dehydrogenase inhibitor oxamate, we observed no changes in the TGFβ-dependent IFN response. Thus, lactate is not directly modulating the IFN response in our model. Given the increased fatty acid oxidation and mitochondrial function in TGFβ cultured FLAMs, it is possible that TGFβ-dependent changes in lipid metabolism and mitochondrial function directly drive subsequent IFN responses following TLR2 activation. Since we observed increased activation of MAVS-dependent IFN production following TLR2 stimulation in the absence of exogenous cytosolic nucleotides, this suggests the possibility of endogenous cellular ligands such as mitochondrial DNA amplifying the TLR2 response in AMs (47). How changes in mitochondrial dynamics or possibly mitochondrial ROS generation contribute to the production of IFNβ remains unknown. Future studies will be needed to dissect

the role of fatty acid oxidation, oxidative respiration, and mitochondrial damage in driving TLR2-mediated TGFβ-dependent IFN responses in AMs.

Our finding that AMs are uniquely programmed by TGFβ to drive an IFN response suggests that these specialized resident macrophages differentially activate their inflammatory profiles in the lung environment compared to other macrophages. Understanding the consequences of an IFN-skewed response in the lungs is an important line of research for future studies. Type I IFNs are known to be potent regulators of antiviral immunity, suggesting the host response in the lungs is particularly tuned to respond to invading viral pathogens (37). However, IFNs also play a key role in controlling fungal pathogens like *Aspergillus fumigatus* in humans and in mice (48). In several disease states however, including Systemic Lupus Erythematosus (SLE) and tuberculosis, elevated type I IFNs are associated with worse disease, and blocking type I IFN has been shown to improve clinical outcomes (49-51). Our data support the role of type I IFNs as a key initial response to invading pathogens in the lungs and more broadly suggests the balance of type I IFNs can mediate protective or pathologic host responses.

Interestingly, TGFβ is produced in an inactive form by AMs in the lungs and it is processed into an active form by integrins on lung epithelial cells which then signal back to AMs to maintain their function (6, 17, 18). This interconnected signaling ensures that AMs are properly tuned to the airspace and suggests the lung environment is an important mediator of the enhanced type I response observed in AMs. Better understanding the underlying mechanisms driving TGFβ-dependent type I IFN may enable the development of therapeutics that modulate the balance of type I IFNs more effectively in the lungs to control infections and prevent autoinflammatory diseases.

MATERIALS AND METHODS

Animals

Experimental protocols were approved by the Institutional Animal Care and Use Committee at Michigan State University (animal use form [AUF] no. PROTO202200127). All protocols were strictly adhered to throughout the entire study. Six- to 8-wk-old C57BL/6 mice (catalog no. 000664), TLR2-/- mice (catalog no. 004650) and $Cas9^{(+)}$ mice (catalog no. 026179) were obtained from The Jackson Laboratory (Bar Harbor, ME). Mice were given free access to food and water under controlled conditions (humidity, 40–55%; lighting, 12-hour light/12-hour dark cycles; and temperature, 24 ± 2°C), as described previously (Bates 2002, 2015). Pregnant dams at 8–10 week of age and 14–18 gestational days were euthanized to obtain murine fetuses. AMs were isolated from male and female mice >10 week of age.

FLAM cell culture

Wild type and TLR2-/- FLAMs were isolated as previously described (31) cultured in complete RPMI (Thermo Fisher Scientific) containing 10% FBS (R&D Systems), 1% penicillin-streptomycin (Thermo Fisher Scientific), 30 ng/ml recombinant mouse GM-CSF (PeproTech), and 20 ng/ml recombinant human TGFβ1 (PeproTech) included where indicated. Media were refreshed every 2–3 d. When cells reached 70–90% confluency, they were lifted by incubating for 10 min with 37°C PBS containing 10 mM EDTA, followed by gentle scraping.

AM isolation and culture

Mice were euthanized by CO_2 exposure followed by exsanguination via the inferior vena cava. Lungs were lavaged as previously described (Busch, 2019). Cells were then resuspended in RPMI 1640 media containing 30 ng/ml GM-CSF and 20 ng/ml recombinant human TGFβ1 (PeproTech) and plated in untreated 48- or 24-well plates. AMs were lifted from plates using Accutase (BioLegend) and seeded for experiments.

TLR2 activation

Cells were seeded in 24-well treated culture plates at a density of 150,000 cells/well and allowed to settle overnight. Cells were treated with Pam3CSK4 25ng/ml (Invivogen, Cat no. tlrl-pms), peptidoglycan from *S. aureus* at 50ug/ml (Invivogen, cat no. tlrl-pgns2), zymosan at 50ug/ml (Invivogen, Cat no. tlrl-zyn), Zymosan Depleted at 50ug/ml (Invivogen, Cat no. tlrl-zyd), Curdlan at 50ug/ml (Invivogen, Cat no. tlrl-curd) or poly I:C at 20ug/mL (Invivogen, Cat no. tlrl-pic-5). Poly I:C was complexed with Lyovec for transfection prior to stimulation.

Cytokine analysis

Where indicated, supernatants were analyzed by a Luminex multiplex assay (Eve Technology). In addition, secreted CXCL10 was quantified using the R&D Duoset kit (R&D Sciences) per manufacturer's instructions. Secreted IFNβ was quantified with the LumiKine Xpress mIFN-B 2.0 kit (Invivogen, catalog no luex-mIFNβv2) per manufacturer's instructions. Luminescent signal was detected on a Spark® multimode microplate reader (Tecan).

Mtb culture and infection

FLAMs were seeded at 200,000 cells/well in a 6 well plate prior to infection. PDIM-positive H36Rv was grown in 7H9 medium containing 10% oleic albumin dextrose catalase growth supplement and 0.05% Tween 80 as done previously (52). To obtain a single cell suspension, samples were centrifuged at 200xg for 5 minutes to remove clumps. Culture density was determined by taking the supernatant from this centrifugation and determining the OD_{600}, with the assumption that OD_{600} = 1.0 is equivalent to $3x10^8$ bacteria per ml. Bacteria were added to macrophages for 4 hours then cells were washed with PBS and fresh media was added. 24 hours later, supernatant was removed and sterile filtered for analysis.

qRT PCR

RNA from FLAMs was extracted using the Directzol RNA Extraction Kit (Zymo Research, Cat no. R2072) according to the manufacturer's protocol. Quality was assessed using NANODROP. The One-step Syber Green RT-PCR Kit (Qiagen, Cat no. 210215) reagents were used to amplify the RNA and amplifications were monitored using the QuantStudio3 (ThermoFisher, Cat no. A28567).

PPARg FWD: 5'-CTC CAA GAA TAC CAA AGT GCG A -3'

PPARg REV: 5'-GTA ATC AGC AAC CAT TGG GTC A -3'

GAPDH FWD: 5'-AGG TCG GTG TGA ACG GAT TTG-3'

GAPDH REV: 5'-TGT AGA CCA TGT AGT TGA GGT CA- 3'

CRISPR-targeted knockouts

Single-guide RNA (sgRNA) cloning sgOpti was a gift from Eric Lander and David Sabatini (Addgene plasmid no. 85681) (53). Individual sgRNAs were cloned as previously described (54). In short, sgRNA targeting sequences were annealed and phosphorylated, then cloned into a dephosphorylated and BsmBI (New England Biolabs) digested sgOpti. sgRNA constructs were then packaged into lentivirus as previously described and used to transduce early passage $Cas9^{+}$ FLAMs. Two days later, transductants were selected with puromycin. After 1 week of selection, cells were validated for SiglecF/CD14 expression and used for experimentation.

sgIRF3-Fwd: CACCGGGCTGGACGAGAGCCGAACG
sgIRF3-Rev: AAACCGTTCGGCTCTCGTCCAGCCC

sgIRF7-Fwd: CACCGCTTGCGCCAAGACAATTCAG
sgIRF7-Rev: AAACCTGAATTGTCTTGGCGCAAGC

sgMAVS-Fwd: CACCGGAGGACAAACCTCTTGTCTG
sgMAVS-Rev: AAACCAGACAAGAGGTTTGTCCTCC

RNAseq

FLAMs with and without TGFβ were plated in 6-well plates at 1 x 10^6 cells/well and treated with Poly(I:C), or PAM as described above for 6 hours. We used the Direct-zol RNA Extraction Kit (Zymo Research, Cat no. R2072] to extract RNA according to the manufacturer's protocol. Quality was assessed by the MSU Genomics Core using an Agilent 4200 TapeStation System. The Illumina Stranded mRNA Library Prep kit (Illumina, Cat no. 20040534) with IDT for Illumina RNA Unique Dual Index adapters was used for library preparation following the manufacturer's recommendations but using half-volume reactions. Qubit™ dsDNA HS (ThermoFischer Scientific, Cat no. Q32851) and Agilent 4200 TapeStation HS DNA1000 assays (Agilent, Cat no. 5067-5584) were used to measure quality and quantity of the generated libraries. The libraries were pooled in equimolar amounts, and the Invitrogen Collibri Quantification qPCR kit (Invitrogen, Cat no. A38524100) was used to quantify the pooled library. The pool was loaded onto 2 lanes of a NovaSeq S4 flow cell, and sequencing was performed in a 2x150 bp paired end format using a NovaSeq 6000 v1.5 100-cycle reagent kit (Illumina, Cat no. 20028316). Base calling was performed with Illumina Real Time Analysis (RTA; Version 3.4.4), and the output of RTA was demultiplexed and converted to the FastQ format with Illumina Bcl2fastq (Version 2.20.0).

RNAseq analysis was completed using the MSU High Performance Computing Center (HPCC). FastQC (Version 0.11.7) was used to assess read quality. Bowtie2 (Version 2.4.1) (55) with default settings was used to map reads with the GRCm39 mouse reference genome. Aligned reads counts were assessed using FeatureCounts from the Subread package (Version 2.0.0) (56). Differential gene expression analysis was conducted using the DESeq2 package (Version 1.36.0) (57) in R (Version 4.2.1).

REFERENCES

1. Hsia CC, Hyde DM, Weibel ER. 2016. Lung Structure and the Intrinsic Challenges of Gas Exchange. Compr Physiol 6:827-95.

2. Kopf M, Schneider C, Nobs SP. 2015. The development and function of lung-resident macrophages and dendritic cells. Nat Immunol 16:36-44.

3. Branchett WJ, Lloyd CM. 2019. Regulatory cytokine function in the respiratory tract. Mucosal Immunol 12:589-600.

4. Wu Y, Hirschi KK. 2020. Tissue-Resident Macrophage Development and Function. Front Cell Dev Biol 8:617879.

5. van de Laar L, Saelens W, De Prijck S, Martens L, Scott CL, Van Isterdael G, Hoffmann E, Beyaert R, Saeys Y, Lambrecht BN, Guilliams M. 2016. Yolk Sac Macrophages, Fetal Liver, and Adult Monocytes Can Colonize an Empty Niche and Develop into Functional Tissue-Resident Macrophages. Immunity 44:755-68.

6. Yu X, Buttgereit A, Lelios I, Utz SG, Cansever D, Becher B, Greter M. 2017. The Cytokine TGF-beta Promotes the Development and Homeostasis of Alveolar Macrophages. Immunity 47:903-912 e4.

7. Ardain A, Marakalala MJ, Leslie A. 2020. Tissue-resident innate immunity in the lung. Immunology 159:245-256.

8. Rothchild AC, Olson GS, Nemeth J, Amon LM, Mai D, Gold ES, Diercks AH, Aderem A. 2019. Alveolar macrophages generate a noncanonical NRF2-driven transcriptional response to Mycobacterium tuberculosis in vivo. Sci Immunol 4.

9. Pisu D, Huang L, Grenier JK, Russell DG. 2020. Dual RNA-Seq of Mtb-Infected Macrophages In Vivo Reveals Ontologically Distinct Host-Pathogen Interactions. Cell Rep 30:335-350 e4.

10. Huang L, Nazarova EV, Tan S, Liu Y, Russell DG. 2018. Growth of Mycobacterium tuberculosis in vivo segregates with host macrophage metabolism and ontogeny. J Exp Med 215:1135-1152.

11. Aegerter H, Kulikauskaite J, Crotta S, Patel H, Kelly G, Hessel EM, Mack M, Beinke S, Wack A. 2020. Influenza-induced monocyte-derived alveolar macrophages confer prolonged antibacterial protection. Nat Immunol 21:145-157.

12. Suzuki T, Sakagami T, Rubin BK, Nogee LM, Wood RE, Zimmerman SL, Smolarek T, Dishop MK, Wert SE, Whitsett JA, Grabowski G, Carey BC, Stevens C, van der Loo JC, Trapnell BC. 2008. Familial pulmonary alveolar proteinosis caused by mutations in CSF2RA. J Exp Med 205:2703-10.

13. Schneider C, Nobs SP, Kurrer M, Rehrauer H, Thiele C, Kopf M. 2014. Induction of the nuclear receptor PPAR-gamma by the cytokine GM-CSF is critical for the differentiation of fetal monocytes into alveolar macrophages. Nat Immunol 15:1026-37.

14. Tzavlaki K, Moustakas A. 2020. TGF-beta Signaling. Biomolecules 10.

15. Nunes I, Shapiro RL, Rifkin DB. 1995. Characterization of latent TGF-beta activation by murine peritoneal macrophages. J Immunol 155:1450-9.

16. Dennis PA, Rifkin DB. 1991. Cellular activation of latent transforming growth factor beta requires binding to the cation-independent mannose 6-phosphate/insulin-like growth factor type II receptor. Proc Natl Acad Sci U S A 88:580-4.

17. Annes JP, Rifkin DB, Munger JS. 2002. The integrin alphaVbeta6 binds and activates latent TGFbeta3. FEBS Lett 511:65-8.

18. Gleizes PE, Munger JS, Nunes I, Harpel JG, Mazzieri R, Noguera I, Rifkin DB. 1997. TGF-beta latency: biological significance and mechanisms of activation. Stem Cells 15:190-7.

19. Gong D, Shi W, Yi SJ, Chen H, Groffen J, Heisterkamp N. 2012. TGFbeta signaling plays a critical role in promoting alternative macrophage activation. BMC Immunol 13:31.

20. Gratchev A. 2017. TGF-beta signalling in tumour associated macrophages. Immunobiology 222:75-81.

21. Chung JY, Chan MK, Li JS, Chan AS, Tang PC, Leung KT, To KF, Lan HY, Tang PM. 2021. TGF-beta Signaling: From Tissue Fibrosis to Tumor Microenvironment. Int J Mol Sci 22.

22. Chen H, Zhuang F, Liu YH, Xu B, Del Moral P, Deng W, Chai Y, Kolb M, Gauldie J, Warburton D, Moses HL, Shi W. 2008. TGF-beta receptor II in epithelia versus mesenchyme plays distinct roles in the developing lung. Eur Respir J 32:285-95.

23. Sanford LP, Ormsby I, Gittenberger-de Groot AC, Sariola H, Friedman R, Boivin GP, Cardell EL, Doetschman T. 1997. TGFbeta2 knockout mice have multiple developmental defects that are non-overlapping with other TGFbeta knockout phenotypes. Development 124:2659-70.

24. Kulkarni AB, Huh CG, Becker D, Geiser A, Lyght M, Flanders KC, Roberts AB, Sporn MB, Ward JM, Karlsson S. 1993. Transforming growth factor beta 1 null mutation in mice causes excessive inflammatory response and early death. Proc Natl Acad Sci U S A 90:770-4.

25. Shull MM, Ormsby I, Kier AB, Pawlowski S, Diebold RJ, Yin M, Allen R, Sidman C, Proetzel G, Calvin D, et al. 1992. Targeted disruption of the mouse transforming growth factor-beta 1 gene results in multifocal inflammatory disease. Nature 359:693-9.

26. Willis BC, Liebler JM, Luby-Phelps K, Nicholson AG, Crandall ED, du Bois RM, Borok Z. 2005. Induction of epithelial-mesenchymal transition in alveolar epithelial cells by transforming growth factor-beta1: potential role in idiopathic pulmonary fibrosis. Am J Pathol 166:1321-32.

27. Frangogiannis N. 2020. Transforming growth factor-beta in tissue fibrosis. J Exp Med 217:e20190103.

28. Garrison G, Huang SK, Okunishi K, Scott JP, Kumar Penke LR, Scruggs AM, Peters-Golden M. 2013. Reversal of myofibroblast differentiation by prostaglandin E(2). Am J Respir Cell Mol Biol 48:550-8.

29. Gorki AD, Symmank D, Zahalka S, Lakovits K, Hladik A, Langer B, Maurer B, Sexl V, Kain R, Knapp S. 2022. Murine Ex Vivo Cultured Alveolar Macrophages Provide a Novel Tool to Study Tissue-Resident Macrophage Behavior and Function. Am J Respir Cell Mol Biol 66:64-75.

30. Luo M, Lai W, He Z, Wu L. 2021. Development of an Optimized Culture System for Generating Mouse Alveolar Macrophage-like Cells. J Immunol 207:1683-1693.

31. Thomas ST, Wierenga KA, Pestka JJ, Olive AJ. 2022. Fetal Liver-Derived Alveolar-like Macrophages: A Self-Replicating Ex Vivo Model of Alveolar Macrophages for Functional Genetic Studies. Immunohorizons 6:156-169.

32. Baker AD, Malur A, Barna BP, Ghosh S, Kavuru MS, Malur AG, Thomassen MJ. 2010. Targeted PPARgamma deficiency in alveolar macrophages disrupts surfactant catabolism. J Lipid Res 51:1325-31.

33. Remmerie A, Scott CL. 2018. Macrophages and lipid metabolism. Cell Immunol 330:27-42.

34. Oliveira-Nascimento L, Massari P, Wetzler LM. 2012. The Role of TLR2 in Infection and Immunity. Front Immunol 3:79.

35. Gopalakrishnan A, Salgame P. 2016. Toll-like receptor 2 in host defense against Mycobacterium tuberculosis: to be or not to be-that is the question. Curr Opin Immunol 42:76-82.

36. Ivashkiv LB, Donlin LT. 2014. Regulation of type I interferon responses. Nat Rev Immunol 14:36-49.

37. McNab F, Mayer-Barber K, Sher A, Wack A, O'Garra A. 2015. Type I interferons in infectious disease. Nat Rev Immunol 15:87-103.

38. Zhang W, Wang G, Xu ZG, Tu H, Hu F, Dai J, Chang Y, Chen Y, Lu Y, Zeng H, Cai Z, Han F, Xu C, Jin G, Sun L, Pan BS, Lai SW, Hsu CC, Xu J, Chen ZZ, Li HY, Seth P, Hu J, Zhang X, Li H, Lin HK. 2019. Lactate Is a Natural Suppressor of RLR Signaling by Targeting MAVS. Cell 178:176-189 e15.

39. Thompson MR, Kaminski JJ, Kurt-Jones EA, Fitzgerald KA. 2011. Pattern recognition receptors and the innate immune response to viral infection. Viruses 3:920-40.

40. Li D, Wu M. 2021. Pattern recognition receptors in health and diseases. Signal Transduct Target Ther 6:291.

41. Toshchakov V, Jones BW, Perera PY, Thomas K, Cody MJ, Zhang S, Williams BR, Major J, Hamilton TA, Fenton MJ, Vogel SN. 2002. TLR4, but not TLR2, mediates IFN-beta-induced STAT1alpha/beta-dependent gene expression in macrophages. Nat Immunol 3:392-8.

42. Stack J, Doyle SL, Connolly DJ, Reinert LS, O'Keeffe KM, McLoughlin RM, Paludan SR, Bowie AG. 2014. TRAM is required for TLR2 endosomal signaling to type I IFN induction. J Immunol 193:6090-102.

43. Dietrich N, Lienenklaus S, Weiss S, Gekara NO. 2010. Murine toll-like receptor 2 activation induces type I interferon responses from endolysosomal compartments. PLoS One 5:e10250.

44. Barbalat R, Lau L, Locksley RM, Barton GM. 2009. Toll-like receptor 2 on inflammatory monocytes induces type I interferon in response to viral but not bacterial ligands. Nat Immunol 10:1200-7.

45. Oosenbrug T, van de Graaff MJ, Haks MC, van Kasteren S, Ressing ME. 2020. An alternative model for type I interferon induction downstream of human TLR2. J Biol Chem 295:14325-14342.

46. York AG, Williams KJ, Argus JP, Zhou QD, Brar G, Vergnes L, Gray EE, Zhen A, Wu NC, Yamada DH, Cunningham CR, Tarling EJ, Wilks MQ, Casero D, Gray DH, Yu AK, Wang ES, Brooks DG, Sun R, Kitchen SG, Wu TT, Reue K, Stetson DB, Bensinger SJ. 2015. Limiting Cholesterol Biosynthetic Flux Spontaneously Engages Type I IFN Signaling. Cell 163:1716-29.

47. West AP, Shadel GS. 2017. Mitochondrial DNA in innate immune responses and inflammatory pathology. Nat Rev Immunol 17:363-375.

48. Wang X, Cunha C, Grau MS, Robertson SJ, Lacerda JF, Campos A, Jr., Lagrou K, Maertens J, Best SM, Carvalho A, Obar JJ. 2022. MAVS Expression in Alveolar Macrophages Is Essential for Host Resistance against Aspergillus fumigatus. J Immunol 209:346-353.

49. Mayer-Barber KD, Andrade BB, Oland SD, Amaral EP, Barber DL, Gonzales J, Derrick SC, Shi R, Kumar NP, Wei W, Yuan X, Zhang G, Cai Y, Babu S, Catalfamo M, Salazar AM, Via LE, Barry CE, 3rd, Sher A. 2014. Host-directed therapy of tuberculosis based on interleukin-1 and type I interferon crosstalk. Nature 511:99-103.

50. Ji DX, Witt KC, Kotov DI, Margolis SR, Louie A, Chevee V, Chen KJ, Gaidt MM, Dhaliwal HS, Lee AY, Nishimura SL, Zamboni DS, Kramnik I, Portnoy DA, Darwin KH, Vance RE. 2021. Role of the transcriptional regulator SP140 in resistance to bacterial infections via repression of type I interferons. Elife 10.

51. Postal M, Vivaldo JF, Fernandez-Ruiz R, Paredes JL, Appenzeller S, Niewold TB. 2020. Type I interferon in the pathogenesis of systemic lupus erythematosus. Curr Opin Immunol 67:87-94.

52. Olive AJ, Smith CM, Kiritsy MC, Sassetti CM. 2018. The Phagocyte Oxidase Controls Tolerance to Mycobacterium tuberculosis Infection. J Immunol doi:10.4049/jimmunol.1800202.

53. Fulco CP, Munschauer M, Anyoha R, Munson G, Grossman SR, Perez EM, Kane M, Cleary B, Lander ES, Engreitz JM. 2016. Systematic mapping of functional enhancer-promoter connections with CRISPR interference. Science 354:769-773.

54. Shalem O, Sanjana NE, Hartenian E, Shi X, Scott DA, Mikkelson T, Heckl D, Ebert BL, Root DE, Doench JG, Zhang F. 2014. Genome-scale CRISPR-Cas9 knockout screening in human cells. Science 343:84-87.

55. Langmead B, Salzberg SL. 2012. Fast gapped-read alignment with Bowtie 2. Nat Methods 9:357-9.

56. Liao Y, Smyth GK, Shi W. 2014. featureCounts: an efficient general purpose program for assigning sequence reads to genomic features. Bioinformatics 30:923-30.

57. Love MI, Huber W, Anders S. 2014. Moderated estimation of fold change and dispersion for RNA-seq data with DESeq2. Genome Biol 15:550.

APPENDIX B: THE GRIT STORY: PROMOTING EQUITY AND INCLUSION IN STEM PHD PROGRAMS

INTRODUCTION

In addition to my research, I have used my scientific training combined with my lived experience to ask questions, strategize methods, and develop solutions for problems associated with equity and inclusion in higher education. As a first-generation student with low-income status myself, I recognize the systemic barriers that keep STEM graduate programs homogenous. Students from historically marginalized populations must often outwork their peers to overcome challenges that not all students face. It is these challenges that are shared between myself, and my colleagues that have motivated me to make changes to graduate education that will ensure equitable opportunities for all. As a graduate student, I aimed to provide necessary support that promoted retention of students from all backgrounds. In the future I aim to drive successful recruitment strategies that give students the opportunity to thrive in an established environment that supports them throughout their PhDs.

In October of 2020 I founded the MSU Graduate Recruitment Initiative Team (GRIT) and have continued to serve as the director. GRIT is a grassroots graduate student organization focused on the recruitment and retention of historically excluded populations in STEM. GRIT is unique given that it is fully graduate student driven, thus addressing the issues that impact students most. We have worked closely with the Biomolecular Science Gateway program (BMS), the umbrella program responsible for recruiting students to six different biomolecular based departments, to implement strategies that promote equity and inclusion. In just a few years' time, GRIT has expanded from a one-person operation to a program with over 100+ participants and a ten-person leadership team that spans six departments, has multiple programs, and is supported by students, faculty, and administration. GRIT serves as a platform where

students can propose changes and develop initiatives that serve the graduate student community. This collaborative structure is what led to the creation of our peer mentorship program, a wellness series focused on graduate student mental health, and our merge with Voices of Color, a student driven initiative that offers support and community among graduate students on color.

Here, I highlight many of the accomplishments and successes of GRIT. These accomplishments are possible due to the hard work of several graduate students, whether it be initiating programs, organizing events, or sending emails, GRIT is what it is because of all of them. Additionally, I discuss potential future directions because while GRIT has made systemic changes to the BMS Ph.D. Program and has had lasting effects in all involved departments, there is still more work to be done. I have learned a lot through the creation of GRIT and have proven that I can successfully build an impactful organization that creates solutions to systemic problems in academia. GRIT is just the beginning; I will continue to create solutions that improve the equity and inclusion of STEM programs in higher education.

PROGRAMS AND ACCOMPLISHMENTS

Peer Mentorship

(Initiated through GRIT by Kaylee Wilburn and Natasha George)

First year students are paired with more senior graduate students during the first year of their PhD program. This pairing is made with department interests, schedules, and career goals in mind. All mentors are trained by POE on the issues of relationship violence and sexual misconduct, Title IX, and reporting protocols and are required to sign a formal pledge prior to being paired with a mentee. The mentor/mentee pair determines a regular schedule to meet and discuss weekly conversation topics provided by the program coordinators. The duration of this program is one academic year however we anticipate that relationships will be formed that go beyond the one-year length of the program. The program concludes with a celebratory social event that includes food, prizes, and a peer mentor of the year award given to one exceptional mentor.

Selected Weekly Conversation Topics Include:

- What to expect from grad level classes, how to navigate D2L
- Rotations 101
- Adjusting to Lansing/MSU
- Time Management Strategies
- Graduate Student Organizations and other opportunities
- Dealing with Imposter Syndrome
- Wellness Resources on Campus
- Networking
- Exploring Career Goals

The GRIT Peer Mentorship Program was developed and has been maintained exclusively by graduate students. In a short two-years this program has become a quintessential part of the PhD

first year experience for BMS students. While the program is fully optional, we have had 70% and 67% participation from first year BMS students in 2021 and 2022, respectively.

2021-2022 Student Testimonials:

"I think the program has been great, I've learnt as a mentor and I think is actually a great experience to help others to navigate in this everyday struggle called grad school, I am really thankful with GRIT for organizing this"

"I think having a mentor [with the] same interest academically helped me a lot. His advice shaped my path in a good way. Pairing people from [the] same program works pretty well, I think."

Comparable Efforts: The BMS Faculty Mentorship program in BMS (developed from GRIT suggestions) is similar to the peer mentorship program, but instead pairs students with faculty outside of their research interest to provide academic support.

Application Feedback Program:

(Initiated through GRIT by Laurisa Ankley)

Applicants interested in the BMS PhD program apply to the feedback program in early October by submitting their personal statement, academic statement, CV, and brief description of why they need our services. Once accepted, the applicants' materials are sent to a current graduate student for review. After completing orientation with the program director, the grad student reviews both statements and uses the CV to help the applicant focus on different aspects of their education/career in their statements. Once the review is complete, the applicant and graduate

student meet for 1 hour via zoom to discuss the feedback. Graduate students are provided a fellowship that equals $75 per applicant they review. The applicant receives the feedback and an application fee waiver for completing the program.

The GRIT Application Feedback Program was developed and has been maintained exclusively by graduate students. Since starting the program, we have accepted approximately 30 applicants per year with graduate reviewers from all six BMS departments.

2021-2022 Student Testimonials

"My reviewer was awesome and she gave great feedback I could tell she really took the time and care to review my statements thoroughly and even helped me with my CV even though that wasn't officially part of the program! 10/10"

"My reviewer is an extremely kind person and I loved all feedbacks she had on my essays. I liked her manner of pointing the aspects I could improve in my essays. It seemed she has a really good experience in giving feedbacks to prospective graduate students. I am sure her comments will be very useful not only to the actual application but for future ones as well."

"This is program has really been helpful. It needs to be continued."

"I'm not sure if MSU has this program in other departments but if not you should share the idea"

"My academic and personal statements were greatly improved by my reviewer. He took great time, effort, and patience to explain where I needed to improve and why. He also gave insights on where I should build my strengths, explain my deficiencies, and make my statements more cohesive."

"The feedback program is a very useful tool for prospective applicants to improve their essays. I would like to congrats the graduate students for the initiative. It was my first time seeing a program like that."

"It's a great idea to have this program and I really appreciated it!"

Comparable Efforts: The Graduate Student Mentorship Initiative by Cientifico Latino pairs mentors with applicants to guide them through the application process.

FUTURE DIRECTIONS

Candidate Selection Rubric: Creating a standard in NatSci acceptance across all programs and providing the resources for those programs to select students in an equitable manner based on course work, research experience, and leadership (can change these/add more). By creating a rubric, we also anticipate better feedback to be provided by the Application feedback program given that there is a specific standard for how students are selected. (Why not share this…? It would set clear expectations and demonstrate our standard of students). (What about blinding

reviewers to the applicants, home institution and personal contact info like name, birthday, email, also ask for number of research hours)

Comparable Efforts: I will need to get an understanding of the acceptance process for each program in NatSci, but here is a great document from UChicago GRIT on how to have an equitable holistic review process.

Example:

	1	2	3	4	Total Score
Scientific Coursework	The applicant has limited science coursework and did not demonstrate proficiency (<C)	The applicant has limited science coursework and demonstrated proficiency (A/B)	The applicant has a wide range of science coursework but did not demonstrate proficiency (<C)	The applicant has had a wide range of scientific coursework and demonstrated proficiency (A/B)	
Understanding of Research Experience	Research experience was mentioned without any detail	Research experience was mentioned with minimal description	Applicant has demonstrated a clear understanding of their work by noting the hypothesis and/or major conclusions	Applicant has demonstrated a clear understanding of their work by noting the hypothesis and/or major conclusions and discussed future directions and implications of the work	
Leadership	The applicant has not demonstrated any leadership experience	The applicant does not have any leadership experience but has indicated plans for future leadership	The applicant has demonstrated leadership experience.	The applicant has leadership experience and has indicated plans for future leadership	

Contribution to Society (Broader Impacts)	The applicant has not made any indication of broader goals that contribute to society, nor have they had contributions in the past	The applicant has indicated broader goals that contribute to society	The applicant has indicated broader goals that contribute to society and has indicated how they will do so	The applicant has indicated broader goals that contribute to society and has demonstrated contributions in the past	
Interest in MSU	The applicant has not made any indication of specific interest in MSU, its faculty, or its research programs.	The applicant has specifically indicated interest in MSU.	The applicant indicated specifics about MSU faculty, research, the area, etc. that demonstrates interest	The applicant has indicated specific about MSU and has made connections with relevant faculty and/or administration	
Would you let this student rotate in your lab based on the materials provided? (Not included in final score)	No			Yes	

List of Faculty Accepting Students: Faculty will be surveyed every summer to determine who is accepting rotation students and how many, their funding status, and a brief description of the research that they are recruiting for. This will increase visibility of less popular labs, save time of graduate students searching for labs, and prevent students from applying that are interested in faculty with inactive research programs.

Comparable Efforts: The GRIT August Newsletter shows all faculty accepting rotations students. NYU offers an interesting faculty search tool that could be adapted for faculty accepting rotation students here at MSU.

Effective Conference Recruitment: Conference recruitment is one of if not the most common ways to recruit students for PhD programs. Conferences provide a unique opportunity to build connections with exceptional students that is too often missed due to the fast-paced environment of conference recruiting. As assistant dean I propose that I attend 1-2 conferences per year, per program accompanied by 2 graduate students in said program each year. Prospective students will be sought out before attending the conference using conference award announcements, and relevant experience of faculty accepting students that year. Once a list of potential candidates has been made (prior to the conference) we (myself of the attending graduate students) will engage with the candidate by viewing their research talk/poster and directly chatting about opportunities at MSU. We will continue to broadly recruit at an exhibitor booth (breadth) but will also introduce this new targeted approach in parallel (depth). We will also revamp the advertising materials that are shared at conferences by focusing on the support available for research, career exploration, and more here at MSU.

Comparable efforts: UChicago welcomes graduate students to participate in their conference recruitment, providing a unique experience for potential applicants to comfortably have discussions and ask questions of current graduate students.

Recruitment from Underrepresented Undergraduate Groups: There are several exceptional groups working with undergraduate students from historically marginalized populations. Most of these programs are application based and therefore have students that meet a specific caliber. By connecting with these organizations (both here at MSU and at other universities across the

country) we can target an excellent pool of highly qualified students to recruit for our various graduate programs.

Comparable Efforts: In the past, BMS has offered a public forum for McNair scholars that highlights the BMS program, MSU, and the area.

Application Fee Waiver Program:

The application fee waiver is a burden for many applying to graduate school. Alleviating this stress from some, can be as simple as broadly sharing resources for fee waivers including the Big10 Freeapp and participating in the GRIT application feedback program.

Comparable Efforts: Some NatSci programs are already sharing this information, including Physics and Astronomy.

CONCLUDING REMARKS

GRIT was built to initiate solutions for inequities found in STEM higher education. We aim to foster an inclusive environment that supports all students to thrive and maximize their successes while embracing their uniqueness, rather than despite it. We have successfully done this by creating several sustainable programs that provide support to 100+ participating students annually from six different graduate programs. In just a few short years, GRIT has become a pillar in the BMS program and its affiliated departments. Thank you to those that have supported our mission and to those that continue to fight for it. Progress is progress and we are making it happen.